ALLOSTERIC INHIBITORS OF DIHYDRODIPICOLINATE SYNTHASE

A Thesis Submitted to the

College of Graduate Studies and Research

In Partial fulfillment of the Requirements for the Degree of

Master of Science in the Department of Chemistry

University of Saskatchewan, Saskatoon, SK

By

Aarti Bhagwat

PERMISSION TO USE

In presenting this thesis in partial fulfillment of the requirements for a postgraduate degree from the University of Saskatchewan, I agree that the Libraries of this University may make it freely available for inspection. I further agree that permission for copying of this thesis in any manner, in whole or in part, for scholarly purposes may be granted by the professors who supervised my thesis work or, in their absence, by the Head of Department or the Dean of the College in which my thesis work was done. It is understood that any copying or publication or use of this thesis or parts thereof for financial gain shall not be allowed without my written permission. It is also understood that due recognition shall be given to me and to the University of Saskatchewan in any scholarly use which may be made of any material in my thesis. Requests for permission to copy to make other use of material in this thesis in whole or part should be addressed to:

Head of the Department of Chemistry

University of Saskatchewan

Saskatoon, Saskatchewan (S7N 5C9)

ABSTRACT

Dihydrodipicolinate synthase (DHDPS) is an enzyme which catalyzes the first step of the lysine biosynthesis pathway in bacteria and plants. Deletion of the gene encoding DHDPS results in non-viable bacteria, therefore DHDPS is considered a validated drug target. The enzyme is feedback-regulated by lysine, and structural studies have shown that the tetrameric enzyme contains two allosteric sites, each of which bind two lysine molecules. The Palmer laboratory has previously developed a potent inhibitor "bislysine" that mimics the structure of two bound lysine molecules. Previous work showed that *S*-aminoethylcysteine ("thialysine") was a much poorer inhibitor than lysine, despite the structural similarity of the two compounds. This thesis describes the synthesis of new allosteric inhibitors of DHDPS, with the goal of defining their structural and chemical properties, such as inhibitor side chain length and pK_a, that lead to inhibition.

Racemic analogs of lysine were generated using the amidomalonic ester synthesis. Analogs of bislysine were generated from dimethyl 2,5-bis([(tertbutoxy)carbonyl]amino) hexanedioate by treatment with lithium diisopropylamide followed by alkylation using various electrophiles. This alkylation step hampers the overall process because it proceeds in low yield (typically near 10%). Studies were undertaken in an attempt to understand the factors influencing this reaction; however, variations in the reaction times, solvent composition, and additives did not improve the yield appreciably.

All the inhibitors were tested using the established DHDPS-DHDPR coupled assay to estimate the IC_{50} values. The lysine analogue ($\pm$)-(*E*)-2,6-diaminohex-4-enoic acid, which has a double bond in the side chain as the only modification, showed weaker inhibition ($IC_{50} = 3.7$ mM) compared to racemic lysine ($IC_{50} = 0.2$ mM). The altered pK_a of the ε-amino group, which makes a hydrogen bond with His59 when bound to the allosteric site, is proposed to account for the loss of activity. Triazolylmethylglycine, which is predicted to have a pK_a value closer to lysine, but contains a shorter side chain, was an even weaker inhibitor. Bis-amino acid versions of these compounds were much stronger inhibitors. A bis-analog of *para*-aminobenzylglycine showed weak inhibition as well, suggesting this bulkier compound, with a much lower side chain pK_a, could still bind to the allosteric cavity.

ACKNOWLEDGEMENTS

TABLE OF CONTENTS

TABLE OF FIGURES

LIST OF TABLES

LIST OF ABBREVIATIONS

ASA, (*S*)-Aspartate-β-semialdehyde

DEAM, diethyl acetamidomalonate

DHDPS, Dihydrodipicolinate Synthase

DHDPR, Dihydrodipicolinate Reductase

DHDP, 2,3-Dihydrodipicolinate

DTT, Dithiothreitol

DCM, Dichloromethane

DIBOC, Di-*tert*-butyl dicarbonate

DMF, *N,N*-Dimethylformamide

EDTA, Ethylenediaminetetraacetic acid

FCC, Flash column chromatography

GlcNAc, *N*-acetylglucosamine

HMPA, Hexamethylphosphoramide

HTPA, (4*S*)-Hydroxy-2,3,4,5-tetrahydro-(2*S*)-dipicolinic acid

HPLC, High performance liquid chromatography

HEPES, 4-(2-Hydroxyethyl)-1-piperazineethanesulfonic acid

ITC, Isothermal titration calorimetry

IC$_{50}$, Half maximal inhibitory concentration

IPTG, Isopropyl β-D-1-thiogalactopyranoside

iPr, isopropyl

LDA, Lithium diisopropylamide

NADH, Nicotinamide adenine dinucleotide, reduced form

NAD$^+$ Nicotinamide adenine dinucleotide, oxidized form

NADPH, Nicotinamide adenine dinucleotide phosphate, reduced form

NADP$^+$, Nicotinamide adenine dinucleotide phosphate, oxidized form

MurNAc, *N*-acetylmuramic acid

*m*DAP, *meso*-diaminopimelate

PDB, Protein Data Bank

PBP, Penicillin-binding proteins

PG, Peptidoglycan monomer

SDS-PAGE, Sodium dodecyl sulfate polyacrylamide gel electrophoresis

TEA, Triethylamine

TFA, Trifluoroacetic acid

THF, Tetrahydrofuran

TIM, Triosephosphate isomerase

TLC, Thin layer chromatography

Tris, 2-Amino-2-hydroxymethyl-propane-1,3-diol

1 INTRODUCTION

1.1 Need for new antibacterial agents

Antibiotic resistance in bacteria is a rapidly growing problem in the treatment of infectious diseases.[1] Since the introduction of penicillin in the 1940s to cure infections, several other antibiotics were discovered and were used extensively to cure previously untreatable pathogenic diseases.[2] However, such rampant use of antibiotics over a prolonged period led to the evolution of resistant strains of bacteria. Such bacteria have resulted in a relapse of infections which are now more difficult to control. The emergence of resistance in bacteria has reached an alarming level today rendering many antibiotics ineffective. According to a report by WHO in 2014, a survey conducted on the most common infection-causing bacteria such as *Escherichia coli, Klebsiella pneumoniae, Neisseria gonorrhoeae, Staphylococcus aureus, Mycobacterium tubercul*osis and *Shigella* species showed that they are rapidly showing resistance to the antibiotics which were previously used successfully to treat these infections.[3] Evolution of resistance mechanisms in bacteria is a continuous process, which means that the effectiveness of every new drug developed will decrease over time. Even though there are many synthetic and natural antibiotics in clinical trial at present, it's only a matter of time before they will be ineffective due to bacterial resistance. Hence, there will always be a need to find new antibacterial agents and drug targets, and to have a good understanding of the mechanism involved in drug resistance and drug action.[2,4]

Antibiotics act by inhibiting various cellular processes, for example cell division and DNA replication, RNA and nucleotide synthesis, protein synthesis and cell wall biosynthesis, which are vital to the survival of the pathogen.[5] This dissertation describes the synthesis and study of inhibitors of dihydrodipicolinate synthase (DHDPS), an enzyme in the lysine biosynthesis pathway of most bacteria that has been validated as a drug target.[6]

1.2 Peptidoglycan assembly in bacteria

A Gram-negative bacterial cell wall consists of a cell membrane, a peptidoglycan layer and an outer membrane. Peptidoglycan is a complex structure formed by polysaccharide chains which

are cross-linked by pentapeptide chains.[7] The process of peptidoglycan construction is shown schematically in Figure 1.1.
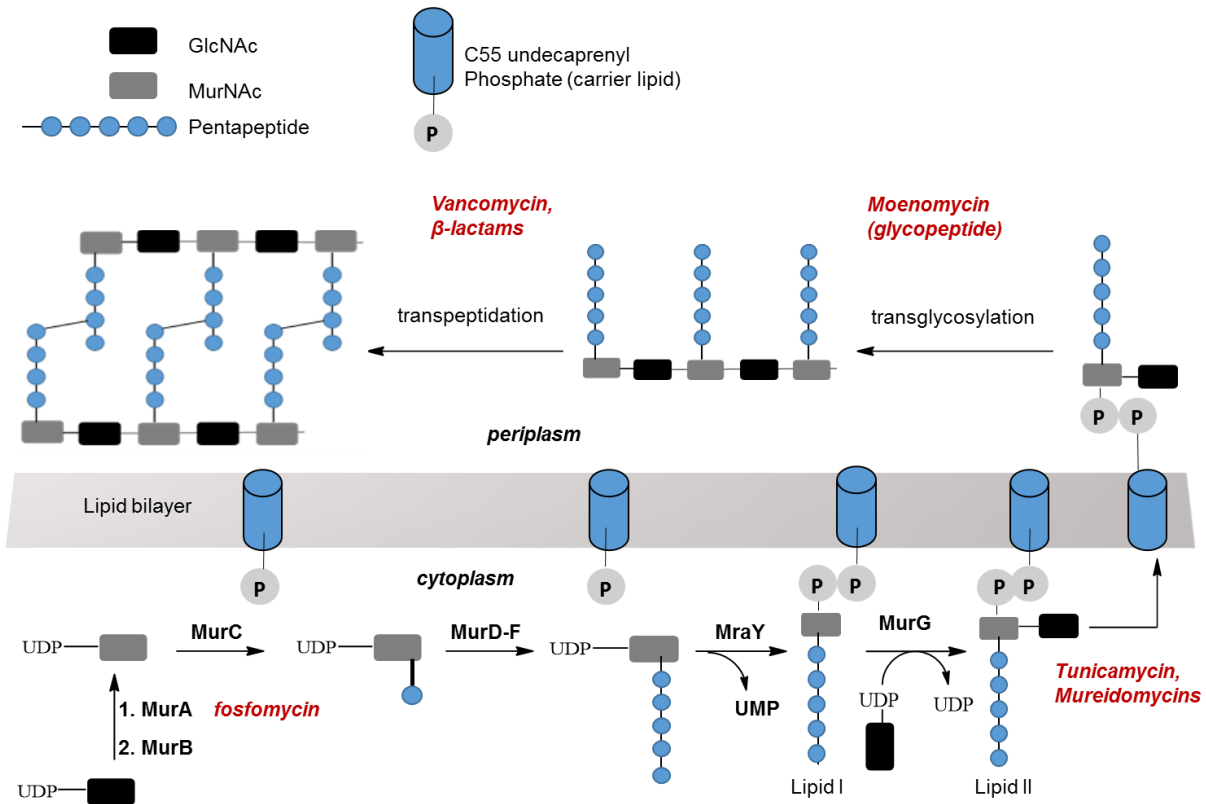
Figure 1.1. Peptidoglycan synthesis and prevalent antibiotics (red), targeting various enzymatic steps. Figure adapted from C. Walsh.[8]

The polysaccharide is made up of alternating units of *N*-acetylmuramic acid (MurNAc) and *N*-acetyl glucosamine (GlcNAc). The peptidoglycan assembly starts in the cytoplasm with the conversion of uridyl diphosphate-linked GlcNAc (UDP-GlcNAc) to UDP-MurNAc, both of which are the components of peptidoglycan (PG) monomer.[9] A peptide chain is then attached to UDP-MurNAc in a stepwise manner following the sequence L-Ala-D-Glu-*m*-DAP-D-Ala-D-Ala for Gram-negative bacteria (Figure 1.2). In Gram-positive bacteria, *m*-DAP (*meso*-diaminopimelate) is replaced by a lysine residue.[10] The resulting muramyl dipeptide is then anchored to the cell membrane via a C55 undecaprenyl phosphate, which is a carrier lipid and performs the function of transporting the muramyl peptide across the hydrophobic membrane.[11] The last cytoplasmic step is the attachment of a GlcNAc unit to the muramyl pentapeptide to complete the PG monomer. The monomer is then transferred to the periplasm via the C55 transporter where it is assimilated into the nascent peptidoglycan by transglycosylation and transpeptidation reactions. These

reactions are responsible for linking the PG monomers and crosslinking of peptide chains.[10,12] The resulting mesh-like structure around the cell provides it with structural rigidity. Peptidoglycan maintains the shape of the cell and is known to participate in cell division.[13] Therefore, the peptidoglycan layer is critical for the survival of bacteria and any form of disruption in its formation can result in cell lysis.[9]
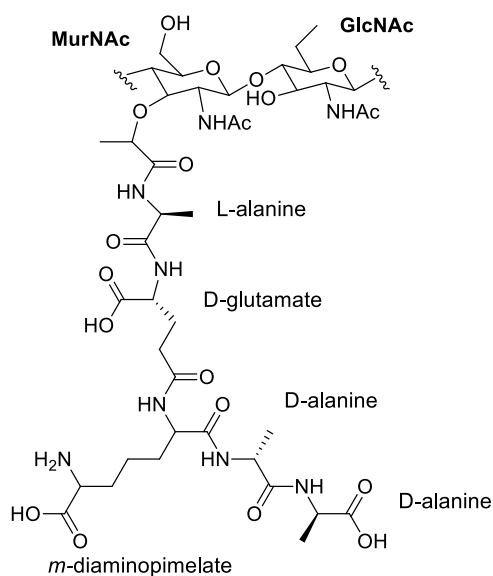
Figure 1.2. GlcNAc-MurNAc-pentapeptide, an uncrosslinked peptidoglycan monomer

1.3   Antibiotics targeting the peptidoglycan synthesis

1.3.1   β-Lactam antibiotics

β-Lactams are broad-spectrum antibiotics which include penicillins, carbapenemes, cephalosporin and monobactams.[8] As the name suggests, this group of antibiotics possess a β-lactam ring which is crucial for their inhibitory activity. β-Lactams act by inhibiting transpeptidation reaction in PG synthesis, which is catalyzed by the enzyme transpeptidase, a type of penicillin binding proteins (PBP).[14] Transpeptidation is the process of crosslinking the pentapeptides from the nascent PG to form a mesh-like structure. Transpeptidase possess a serine residue in the active site which acts as a nucleophile and attacks the amide bond between the last two D-Ala residues, forming an acyl-enzyme intermediate with the loss of the terminal D-Ala. In the second half of the reaction, the amine of a DAP residue from an adjacent pentapeptide attacks

the acyl intermediate to form a new peptide bond, which gives rise to a crosslinked structure strengthening the peptidoglycan.[9,10]
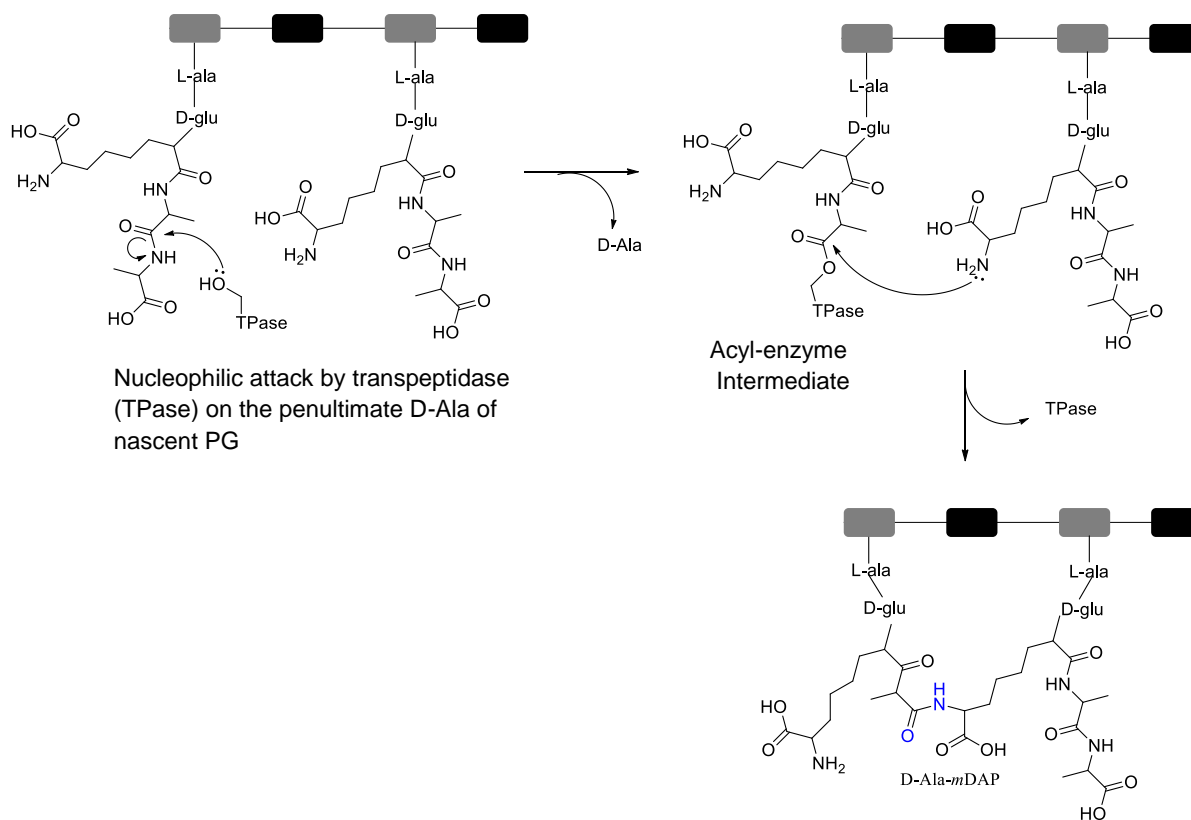
Figure 1.3. Reaction catalyzed by transpeptidase enzyme in the peptidoglycan synthesis to form the D-Ala-*m*-DAP bond.[8]

The β-lactam antibiotics possess a strained β-lactam ring which competes with D-Ala-D-Ala and acts as a substrate for transpeptidase.[14] The enzyme generates the acyl-enzyme intermediate with the β-lactam ring instead of the pentapeptide D-Ala-D-Ala bond (Figure 1.4).[15] These penicillinoyl adducts then start to accumulate because the active site lacks water to hydrolyze them. The site is thus blocked for its substrates, the PG monomers, which are no longer utilized.[14,15] The construction of peptidoglycan slows down drastically, eventually resulting in weakening of cell wall and cell lysis.[16]
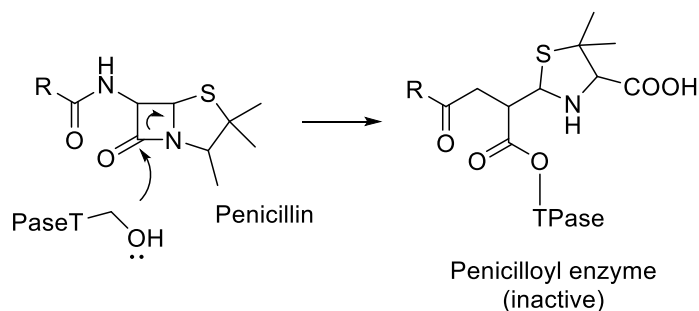
Figure 1.4. Deactivation of transpeptidase by penicillin by forming a penicillinoyl adduct.[14]

1.3.2 Glycopeptides

Vancomycin and teicoplanin are the most successfully employed antibiotics of this class. Glycopeptides also inhibit the transglycosylation and transpeptidation reaction in the PG assembly process.[17] Both vancomycin and teicoplanin are large molecules with a common cyclic heptapeptide scaffold. A molecule of vancomycin fits perfectly around the D-alanyl-D-alanine (D-Ala^4-D-Ala^5) unit of the muramyl-pentapeptide and gets anchored via hydrogen bonds (Figure 1.5). The peptide crosslinking is thus prevented because the substrate is sterically hindered from the transpeptidase enzyme. The vancomycin-bound pentapeptide has been identified by X-ray and NMR.[18] A drawback of glycopeptides is that because of their large structures, the antibiotics have poor oral absorptivity and are only effective against Gram-positive bacteria, which lacks the outer cell membrane.[19]
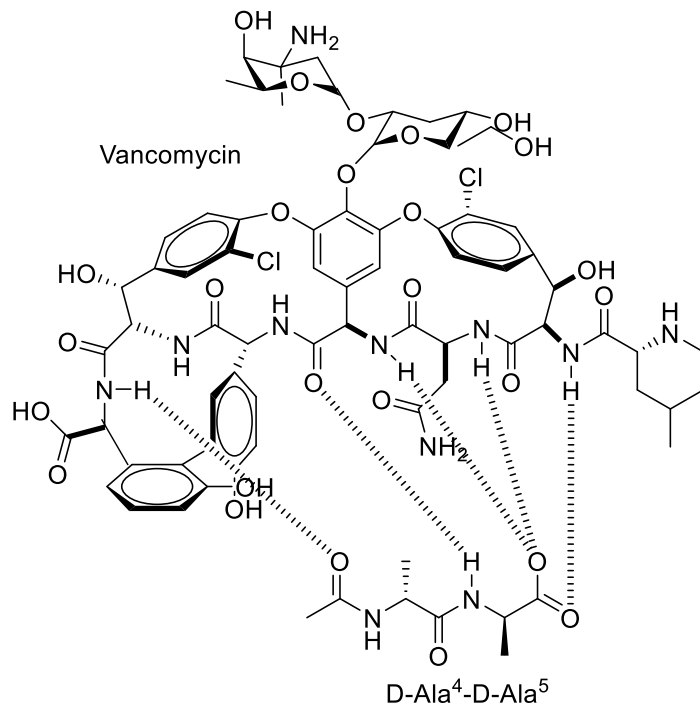
Figure 1.5. Prevention of transpeptidation by glycopeptide antibiotics: Interaction of the D-Ala⁴-D-Ala⁵ residues from peptidoglycan with vancomycin through five hydrogen bonds.[17]

1.3.3 Fosfomycin

Fosfomycin is the only antibiotic in clinical use that targets one of the muramyl (Mur) enzymes.[20] Muramyl A-F are a group of enzymes in the peptidoglycan assembly process which catalyze the cytoplasmic steps. MurC, MurD MurE and MurF catalyze the stepwise addition of amino acids to form muramyl pentapeptide while MurA and B catalyze the conversion of UDP-GlcNAc to UDP-MurNAc.[10] Inhibition of this reaction stops the supply of MurNAc, which is one of the two glycan units forming peptidoglycan. Fosfomycin is a simple epoxypropyl phosphonate compound which inactivates MurA. The cysteine residue in the active site of MurA attacks the epoxide ring of fosfomycin resulting in a covalent adduct, thus blocking the active site of the enzyme (Figure 1.6).[21] As a result, the conversion UDP-GlcNAc is inhibited, exhausting the pool of PG monomers required to build the peptidoglycan.
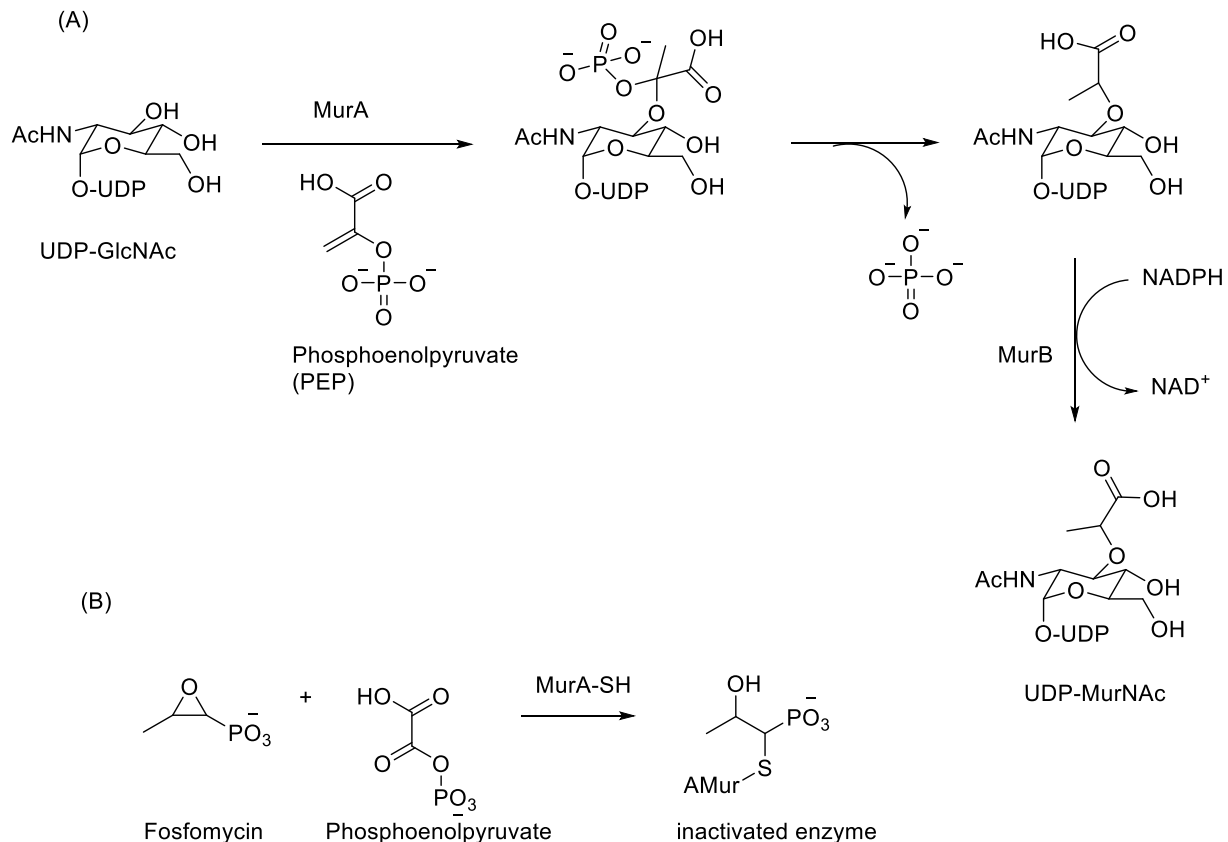
Figure 1.6. Conversion of UDP-GlcNAc to UDP-MurNAc by MurA and MurB enyzmes. (B) Inactivation of MurA by fosfomycin[8,21]

1.3.4 Resistance to antibiotics targeting the cell wall synthesis

Bacteria can adopt various resistance mechanisms against antibiotics such as modifying the target enzyme to reduce its affinity for the antibiotic, decreasing cell permeability, destroying the antibiotic before it reaches the target and evolving alternate biochemical routes with enzymes that are not recognized by the antibiotic.[4] In Gram-negative bacteria, resistance to β-lactams is offered primarily by enzymes called β-lactamases, which destroy the antibiotic by hydrolyzing the β-lactam ring before it reaches the target enzyme.[22] In *S. pneumoniae* and *S. aureus,* mutations result into modified PBPs which have low affinity for β-lactam antibiotics. Bacteria such as species of *Mycobacterium* and *Enterococcus* have mechanisms which do not employ transpeptidase, the target enzyme for penicillins. Instead, L,D-transpeptidase carries out the function of cross-linking the peptides using a mechanism different from transpeptidase, rendering the antibiotic ineffective in blocking this step.[5]

Different mechanisms of fosfomycin resistance have also emerged. The antibiotics-degradation mechanism has been observed to operate in fosfomycin-resistant bacteria. Three types of fosfomycin-inactivating enzymes, fosA, fosB and fosX, have been observed. These enzymes open the fosfomycin ring by adding glutathione (fosA), L-cysteine (fosB) or H_2O (fosX) to it before the antibiotic reaches the target.[23] In another mechanism, mutation in the genes encoding the fosfomycin transporters across the cell was observed, resulting in reduced uptake of the drug.[21] In *E. coli* and *M. tuberculosis*, modification of the active site of the target enzyme MurA offers the resistance.[24]

Resistance to glycopeptides antibiotics is offered by mutation in the target enzyme. The five hydrogen bonds formed between D-Ala^4-D-Ala^5 and vancomycin is responsible for its antibiotic action. In vancomycin-resistant enterococci (VRE), the D-Ala^5 residue is replaced by D-lactate, which eliminates the amide linkage forming the H-bond with vancomycin. The PG monomer with D-Ala-D-Lac does not interfere with the function of transpeptidase, but the affinity of transpeptidase towards vancomycin decreases 1000-fold, allowing the bacteria to survive. In some *Enterococci*, D-Ala^5 is replaced by a serine residue, which also results in decreased affinity for vancomycin.[25] The effectiveness of vancomycin against *S. aureus* is also decreasing gradually owing to resistance mechanism and poor bioavailiblity.[19]

The cell wall synthesis machinery is being reviewed for new targets and the efforts to develop drugs have met with mixed success. The lysine biosynthesis pathway is one of the biochemical routes which supplies the cell wall with *m*DAP and lysine, the components of a PG monomer. This pathway is therefore considered as a target for developing new antibacterial agents since no drugs targeting this pathway are currently in clinical use.[6,26]

1.4   The diaminopimelate pathway of lysine biosynthesis

The lysine biosynthesis pathway in bacteria is known as the diaminopimelate (DAP) pathway and leads to the production of lysine and *meso*-diaminopimelate.[6] Lysine and its biosynthetic precursor DAP are the key components of bacterial cell walls, cross-linking the PG monomers.[7,27] Lysine also plays an important role in many cellular processes, the ε-amino group being important for interaction with other proteins and nucleic acids. Inhibition of enzymes in this pathway would result in insufficient production of these components and eventually hinder

peptidoglycan synthesis. Since the DAP pathway is absent in mammals, drugs targeting this pathway would have minimum toxicity effects on mammalian cells.

The pathway begins with the conversion of aspartic acid to (*S*)-aspartate-β-semialdehyde (ASA) (Figure 1.7). At this point, it branches out into syntheses of leucine, isoleucine, threonine and lysine, also known as the aspartate family of amino acids.[28] For lysine synthesis the first step is the reaction between ASA and pyruvate which is catalyzed by dihydrodipicolinate synthase (DHDPS) to form dihydrodipicolinate (DHDP).[29] DHDP undergoes reduction in the presence of NADH to form tetrahydrodipicolinate (THDP) catalyzed by dihydrodipicolinate reductase DHDPR.[30] The cyclic product is then converted to *meso*-DAP via 3 steps: *N*-acylation, a transimination reaction and epimerization. All the enzymes in this pathway have been extensively studied and efforts have been made to design inhibitors of DHDPS, DHDPR, DAP epimerase, *N*-acyl transferase and DAP decarboxylase. So far, no inhibitors with high potency have been reported for these enzymes.[6,31,32]
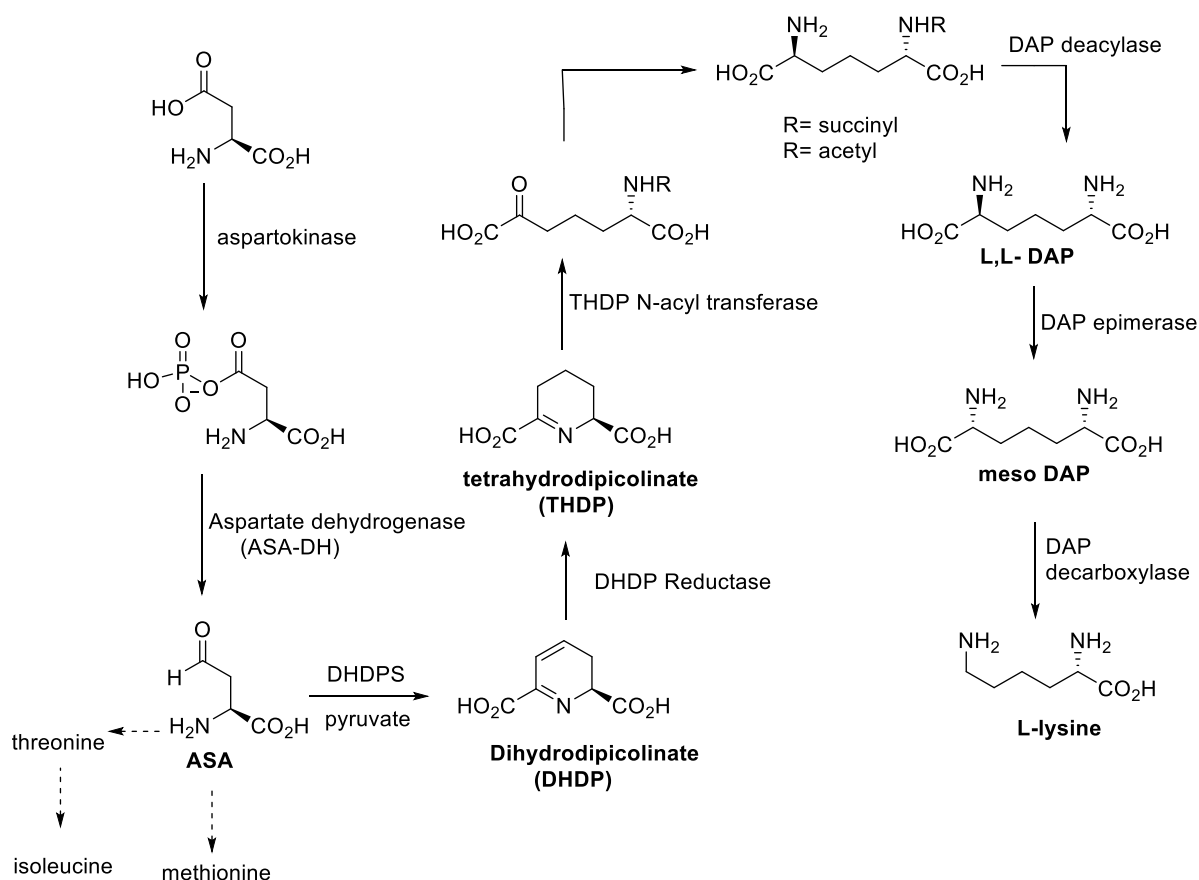
Figure 1.7. Diaminopimelate pathway in bacteria[26]

1.5 Dihydrodipicolinate synthase: A validated drug target

Dihydrodipicolinate synthase (DHDPS, E.C. 4.2.1.52) is an enzyme belonging to the DAP pathway which catalyzes the formation of dihydrodipicolinate from (*S*)-aspartate-β-semialdehyde and pyruvate. DHDPS has been validated as a drug target by gene knockout experiment. It was observed that deletion of the *dapA* gene in *E. coli* which encodes DHDPS resulted in cell death.[33] In *Mycobacterium smegmatis*, the gene encoding aspartokinase, the first enzyme in DAP pathway was deleted. The resulting mutant was not viable when deprived of DAP in the culture indicating that this pathway and its product DAP are essential for bacterial survival.[34] Since then, attempts have been made to design new antibacterial agents targeting bacterial DHDPS. This thesis focuses on DHDPS from *Campylobacter jejuni*, a Gram-negative pathogen, which causes gastroenteritis in humans. If left untreated, it can lead to more severe conditions such as Guillain-Barré syndrome, meningitis and chronic colitis.[35]

1.5.1   DHDPS mechanism

The mechanism has been well studied in DHDPS obtained from *E. coli*. DHDPS follows a substituted-enzyme, or ping pong, kinetic mechanism where pyruvate and (*S*)-aspartate-*β*-semialdehyde (ASA) are the two substrates.[36] In this type of enzyme mechanism, the enzyme and the first substrate bind to form a complex accompanied by the release of the first product. The second substrate then binds to this enzyme-substrate complex to release the second product. At the end of the reaction, the enzyme is regenerated for another catalytic cycle.[37] The mechanism with DHDPS is shown in (Figure 1.8)

Pyruvate H_2O ASA   HTPA

E   E:Pyruvate   ⇌   F   F:ASA   ⇌   E:DHDP   E

E- Enzyme
F- Enzyme-enamine intermediate
ASA- Aspartate semialdehyde
HTPA- (4*S*)-3-hydroxy-2,3,4,5-
          tetrahydro-(2*S*)-dipicolinic acid
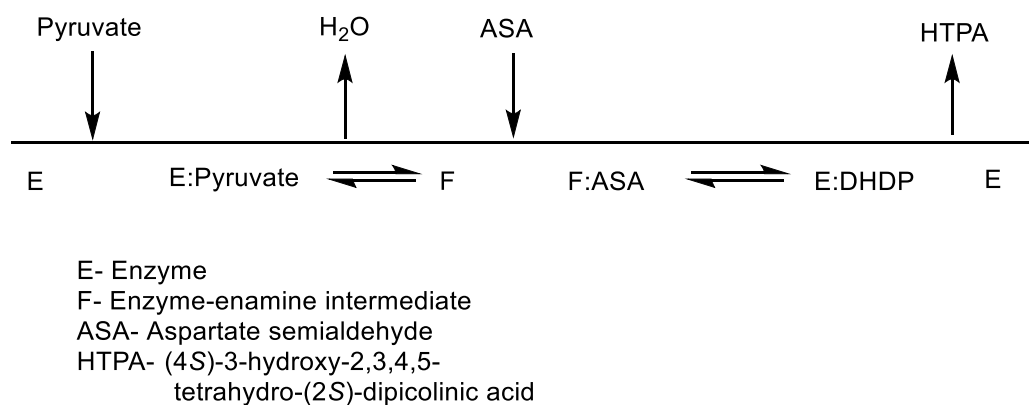
Figure 1.8. Substituted-enzyme mechanism of dihydrodipicolinate synthase

A catalytic triad consisting of two tyrosine residues and one threonine residue are proposed to facilitate the proton exchange required for the mechanism.[38] Mutagenesis of any of these three residues greatly reduces enzymatic activity. Pyruvate condenses with an active site lysine residue forming a Schiff base with the release of a water molecule as the first product.[29] The Schiff-base is converted to enamine by general base catalysis. Binding of the second substrate ASA to this enamine leads to a condensation reaction after which the second product, which was believed to be (4*S*)-3-hydroxy-2,3,4,5-tetrahydro-(2*S*)-dipicolinnic acid is expelled. This unstable cyclized product was shown to undergo dehydration spontaneously in solution.[39,40] The role of the catalytic triad and a detailed molecular mechanism is discussed in the next section.
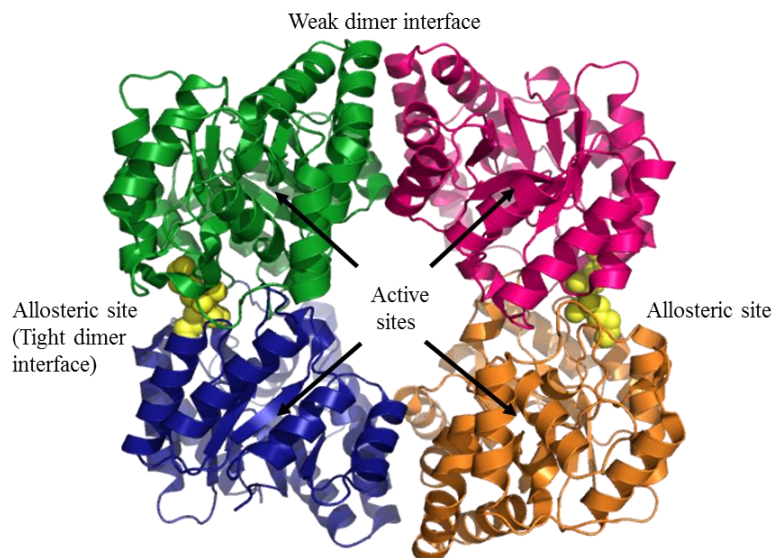
Figure 1.9. Homotetramer of DHDPS from *C. jejuni* with lysine (yellow spheres) in the allosteric site. (PDB: 4M19).

DHDPS exists as a homotetramer in most bacterial species examined (including *C. jejuni*) with the exception of *S. aureus* where the enzyme has a dimeric form.[41–44] The homotetramer can be described as a loose dimer of two tightly-bound dimers. The significance of the tetrameric structure towards enzyme activity has been explored before by disrupting the enzyme at the loose interface and comparing the activity of the resulting dimer with wild-type enzyme. The dimeric form of *E. coli* DHDPS showed decreased catalytic efficiency whereas the dimer from *M. tuberculosis* was as active as its tetramer.[45,46]

Each subunit of the tetramer consists of a $(\beta/\alpha)_8$ barrel in which eight β-strands are arranged in a circular structure to form a barrel which is surrounded by 8 helices. The active site is harbored within these folds.[44] The allosteric site of the enzyme is present at the tight dimer interface.[47]

1.5.3 Active site
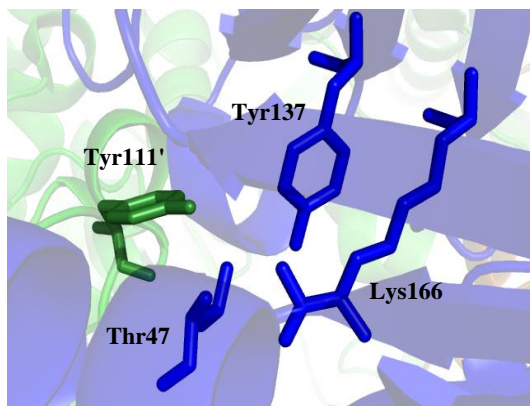
Figure 1.10. The catalytic triad (Tyr111', Tyr137 and Thr47) and the lysine residue (Lys166) from the active site of *C. jejuni* DHDPS (PDB: 3LER). Tyr111' (green, primed) belong to the adjacent monomer.

The active site in DHDPS from *C. jejuni* is similar to that from *E. coli*. The two species share 37% sequence identity, and all the important residues from active site and allosteric sites are conserved.[48] The enzyme mechanism has been studied in detail in *E. coli* using site directed mutagenesis and crystallography.[44] The structural alignment of DHDPS tetramers from *E. coli* and *C. jejuni* also highlights the similarities in the placement of the conserved residues active site and allosteric site.[49] The reaction is initiated by condensation of an active site lysine residue, which is K166 in *C. jejuni*, with pyruvate to form a Schiff base which tautomerizes to enamine. The proton transfer during the course of the reaction is proposed to be facilitated by a catalytic triad made up of highly conserved tyrosine (Y137 and Y111') and a threonine (T47).[38] For each active site, the Y111' residue from the neighboring monomer completes the triad (Figure 1.10). [41] The second substrate ASA condenses with the enamine, the product of which cyclizes into (4*S*)-hydroxy-2,3,4,5-tetrahydro-(2*S*)-dipicolinic acid (HTPA) via transamination.[40] This unstable heterocyclic product then spontaneously dehydrates to (*S*)-2,3-dihydropyridine-2,6-dicarboxylate (DHDP) (Figure 1.11).
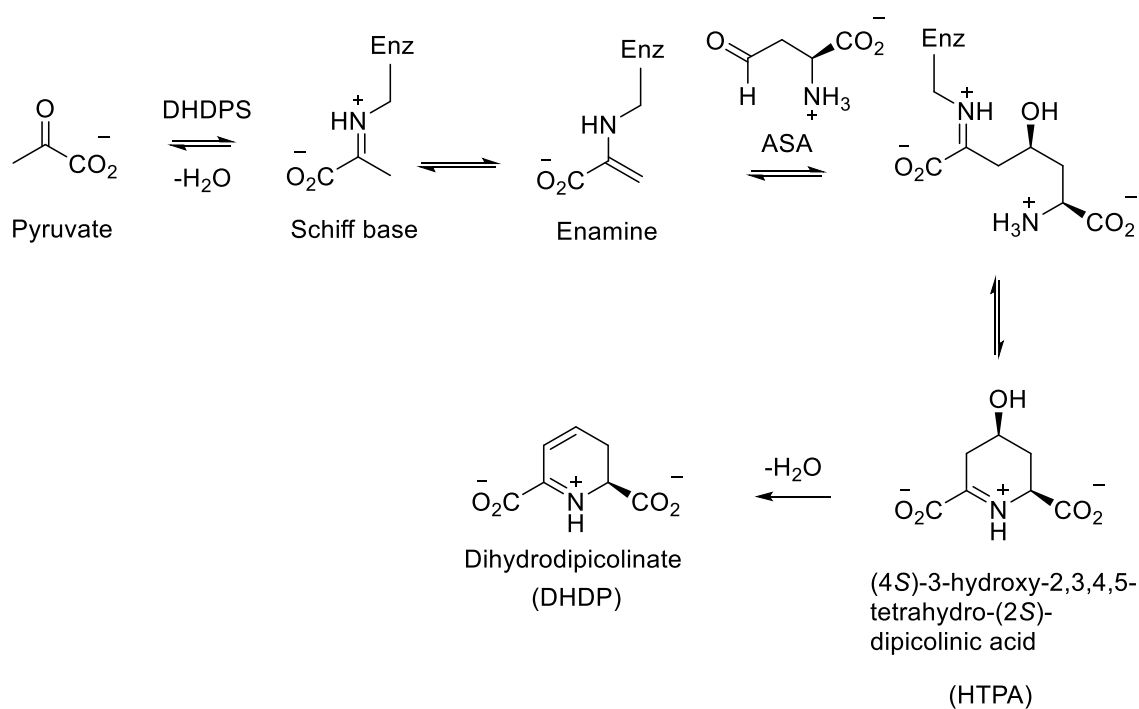
Figure 1.11. Reaction catalyzed by DHDPS

1.5.4 Allosteric site and lysine inhibition

Lysine is a feedback inhibitor of DHDPS in Gram-negative bacteria and plants while Gram-positive bacteria are weakly inhibited or completely insensitive to lysine.[42–44,50] Within the lysine-sensitive species, there is a variation in the degree of inhibition as well as the reported inhibitory mechanism. *C. jejuni* DHDPS is more sensitive to lysine ($IC_{50} = 65$ µM) compared to *E. coli* DHDPS ($IC_{50} = 200$ µM).[48] Inhibition by lysine was cooperative in nature where the binding of the second lysine molecule was 10^5 times stronger than the first.[51] The cooperativity of lysine binding was, however, only taken into account in recent DHDPS kinetic studies with *Vitis vinifera*[50] and *C. jejuni*[48] DHDPS. The degree of cooperativity in ligand binding is measured by calculating the Hill (cooperativity) coefficient. A value greater than 1 indicates positive cooperativity, meaning binding of one ligand increases the binding affinity of enzyme for the next ligand. The Hill coefficient for *C. jejuni* DHDPS was greater than 2, indicating that binding of lysine across the two allosteric sites was cooperative.[49] However, the crystallographic data provided no evidence of any major structural changes after lysine binding.[41] The mechanism of cooperativity is still not completely deduced and probably more than one subtle change in the enzyme is responsible for the communication from the allosteric site. The results obtained after incorporating the cooperativity coefficient in the kinetic equation showed that lysine was an

14

uncompetitive partial inhibitor with respect to pyruvate and *mixed partial* inhibitor with respect to ASA.[48] These models of inhibition implied that lysine preferentially binds to the enzyme-pyruvate complex over the ASA bound form.[41,48]

Across all the lysine-sensitive species, the allosteric site is located at the tight dimer interface of the homotetramer. Residues from both monomers of the tight dimer make up the allosteric site where two lysine molecules are bound. Crystal structures of DHDPS from different plant and bacterial species and site-directed mutagenesis studies helped to reveal important residues in the allosteric site. Studies of *E. coli* DHDPS showed that the two highly conserved tyrosine residues Tyr106-Tyr107 were possible links between the active site and the allosteric site. Conly et al.[41] recently reported the crystal structure of lysine-bound DHDPS from *C. jejuni* which did not reveal any changes in the architecture of the active site. However, lysine binding introduced domain movements in each monomer as well as changes in the cavity volumes of both the sites which could be a contributing factor to the allostery. A comparison of the lysine-bound tetramer to the free enzyme helped to show the importance of Tyr110 and Tyr111 as a linker between the active and allosteric site. Tyr110 forms a hydrogen bond with the carboxylate group of lysine inhibitor while the catalytic triad of the adjacent monomer is completed by Tyr111. These residues were therefore established as potential links between the active and allosteric sites.

The importance of Tyr110 was demonstrated by the mutant Y110F where the tyrosine110 was replaced by phenylalanine, which could not make a hydrogen bond with the carboxyl group of lysine. This mutant was drastically less sensitive to lysine (IC_{50} = 40 mM) compared to wild type (IC_{50} = 65 µM).[49] Apart from Tyr110, His56 and His59 also play important roles in the allosteric site. The binding of lysine to the pyruvate-bound enzyme results in a change in the positions of His56 and His59. Site-directed mutagenesis of these residues demonstrated the significance of these residues. The crystal structure showed that His59 is in a position to form a hydrogen bond with the ε-amino group of lysine (Figure 1.12). Mutants of His59 were designed to disrupt this hydrogen bond and observe its effects on the strength of lysine inhibition. Mutation of His59 to asparagine and alanine decreased the binding affinity of lysine 10-fold and 40-fold respectively, supporting the hypothesis that polar contacts with this histidine residue are important for allosteric inhibition. Mutation of His56 to asparagine and alanine resulted in three and five fold decrease in the binding affinity, which was consistent with the fact that His56 does not form any polar contacts directly with the lysine inhibitor.
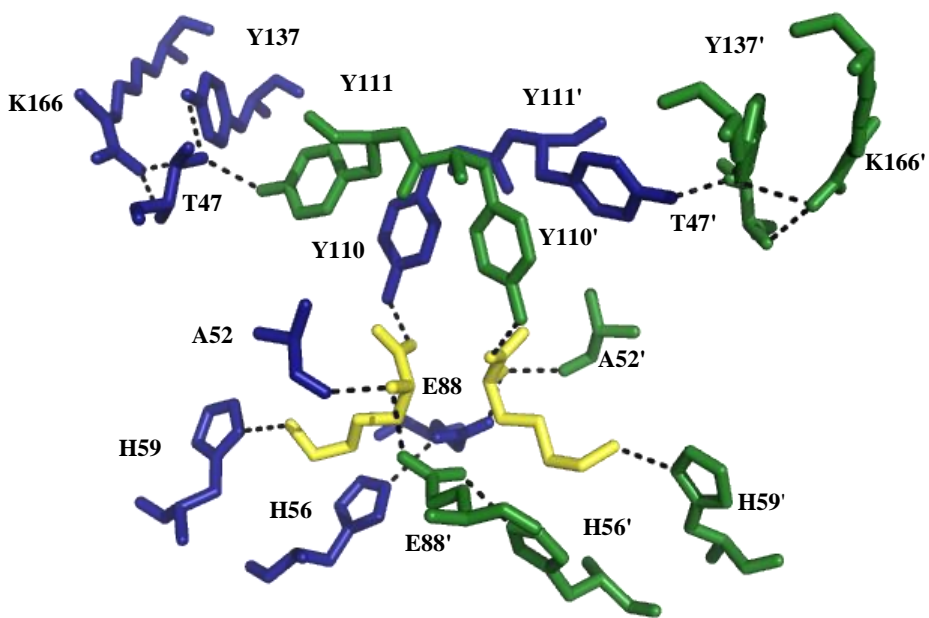
Figure 1.12. Allosteric site of *C. jejuni* DHDPS with two lysine molecules bound (yellow). Green (primed) and blue represent two adjacent monomers and black dashed bonds represent polar contacts. (PDB: 4M19).[41]

1.6 Inhibitors of DHDPS

1.6.1 Inhibitors targeting the active site

a) Substrate analogues

Pyruvate
$K_m = 194 \pm 33$ μM

$K_i = 0.22 \pm 0.02$ mM
1.1

$K_i = 0.83 \pm 0.06$ mM
1.2

$K_i = 16 \pm 2$ μM
1.3
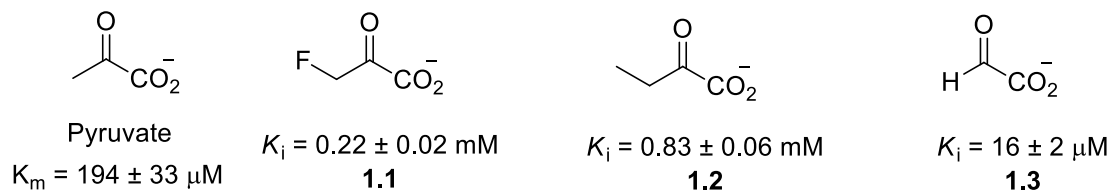
Figure 1.13. Pyruvate analogues as inhibitors of DHDPS.[39]

The pyruvate analogues in Figure 1.13 were shown to be competitive inhibitors with respect to pyruvate, for *E. coli* DHDPS.[39] The analogues varied in the chain length and their inhibition constants (K_i) were useful to gain more knowledge about the active site geometry. The compound 3-fluoropyruvate (**1.1**) had a K_i similar to the K_m of pyruvate suggesting that the substitution by fluorine was accommodated in the active site. Increasing the chain length resulted in weaker binding. The K_i for 2-ketobutyrate (**1.2**) was 4-fold higher than that of pyruvate. The K_i for glyoxalate (**1.3**) which is a smaller compound was also 10-fold lower than that of pyruvate, but no further data or explanation could be found in the literature.[39]

ASA analogues were synthesized based on the structure of the aldehyde form and the hydrate form, the latter of which is believed to be predominant in aqueous solution. It was also proposed that the hydrate may cyclize and exist in the form of a cyclic lactol.[52] All these forms were considered for synthesizing DHDPS inhibitors. Glutamic acid (**1.5**) was found to be uncompetitive inhibitor and aspartic acid (**1.4**) was a mixed inhibitor. These patterns indicate that these acid analogues bind in the allosteric site instead of the active site. Homoserine lactone (**1.7**) and 2-aminocyclopentanone (**1.8**) both displayed non-competitive inhibition, indicating that they are not a substrate analogue.[53] Another substrate analogue succinic semialdehyde (**1.6**) in which the amine from ASA was replaced by hydrogen also showed weak inhibition indicating that this strategy is not very promising for synthesizing DHDPS inhibitors.[6,39]
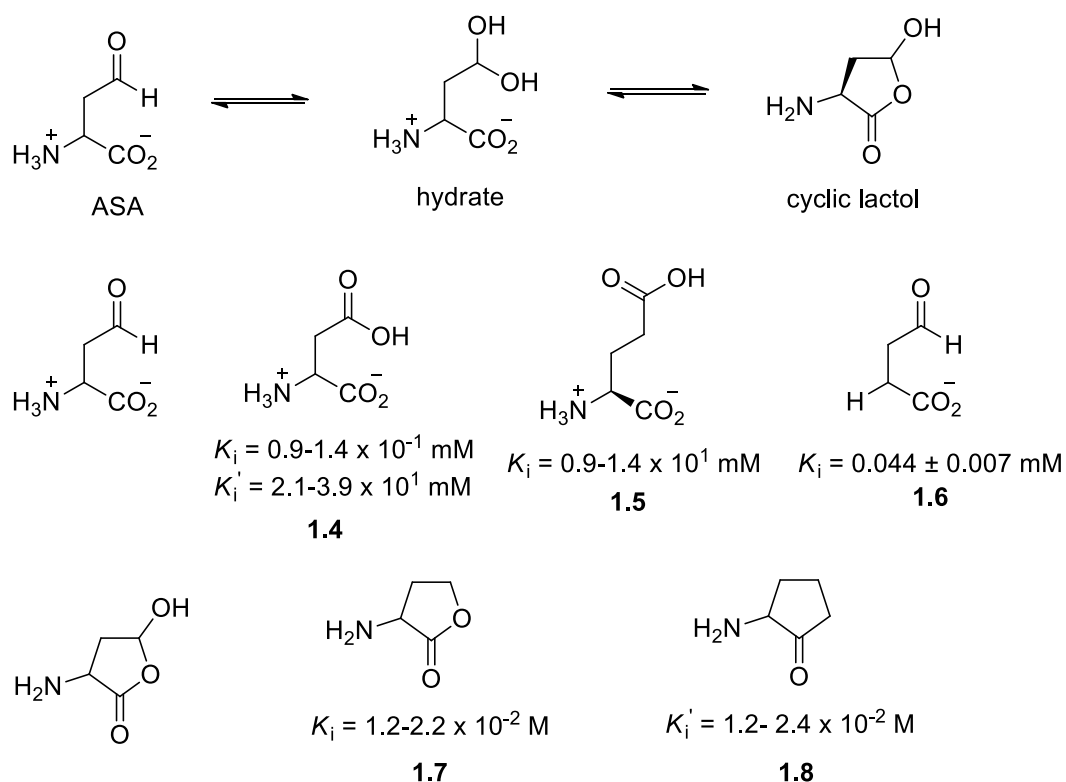
Figure 1.14. Analogues of ASA as inhibitors of DHDPS.[53]

b) Product analogues
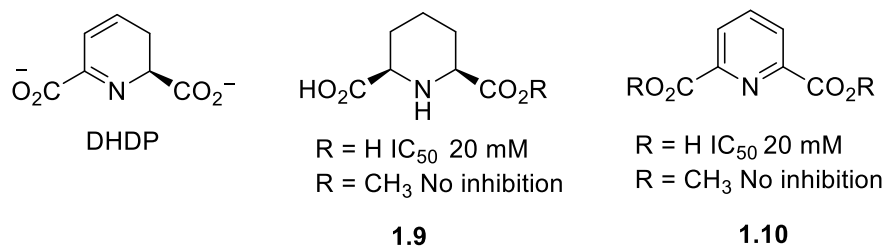
Figure 1.15. Analogues of DHDP as weak inhibitors of DHDPS.[54]

Based on the structure of DHDP, heterocyclic inhibitors such as **1.9** and **1.10** were synthesized and found to be weak inhibitors of *E.coli* DHDPS.[54] However, since DHDP is formed by dehydration of HTPA[40], it was proposed that analogues of HTPA might prove to be better inhibitors. Analogous heterocycles with an oxygen substituent at carbon 4 were synthesized. Dimethyl chelidamate and chelidamic acid (**1.13**) both were moderate uncompetitive inhibitors of DHDPS.[54] Both these compounds were also tested against other bacterial species and found to be

18

potent against *E. coli*, MRSA and *M. tuberculosis*.[55] The sulfur-containing analogues **1.11** and **1.12** were all weak inhibitors.[54]

THDP

50 mM, 14% inhibition
1.11

9 mM, 48% inhibition
1.12

R = H IC$_{50}$ 22 mM
R = Me IC$_{50}$ 14 mM
1.13

No inhibition
1.14
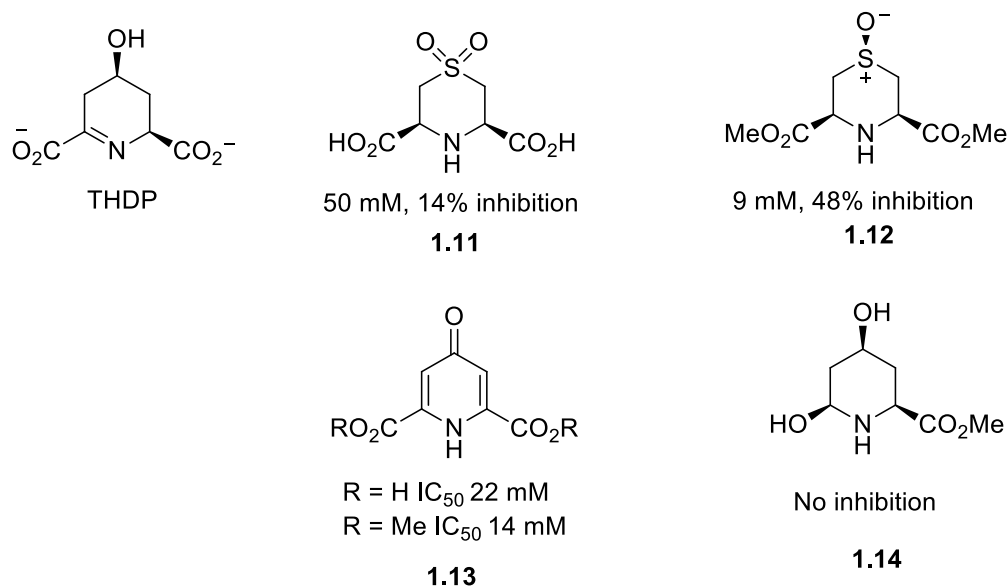
Figure 1.16. Tetrahydrodipicolinate analogues as moderate inhibitors of DHDPS.[54]

c) Enzyme-bound intermediate analogues

Recently, the acyclic enzyme-bound intermediate from the DHDPS catalyzed reaction was used as a template for analogous compounds as inhibitors (Figure 1.17). The first two compounds synthesized in this series were 4-oxo-heptenedioic acid and the corresponding ester (**1.8**) which showed irreversible inhibition.[56] The bis(oxime-ester) (**1.16**), bis(keto-ester) (**1.17**) and bis(keto-acid) (**1.19**) were synthesized as conformationally constrained analogues.[57] These compounds performed better than the product analogues and showed time dependent irreversible inhibition. The bis(keto-acid) (**1.18**) and **1.16** were selected as lead compounds and await further studies.[57]
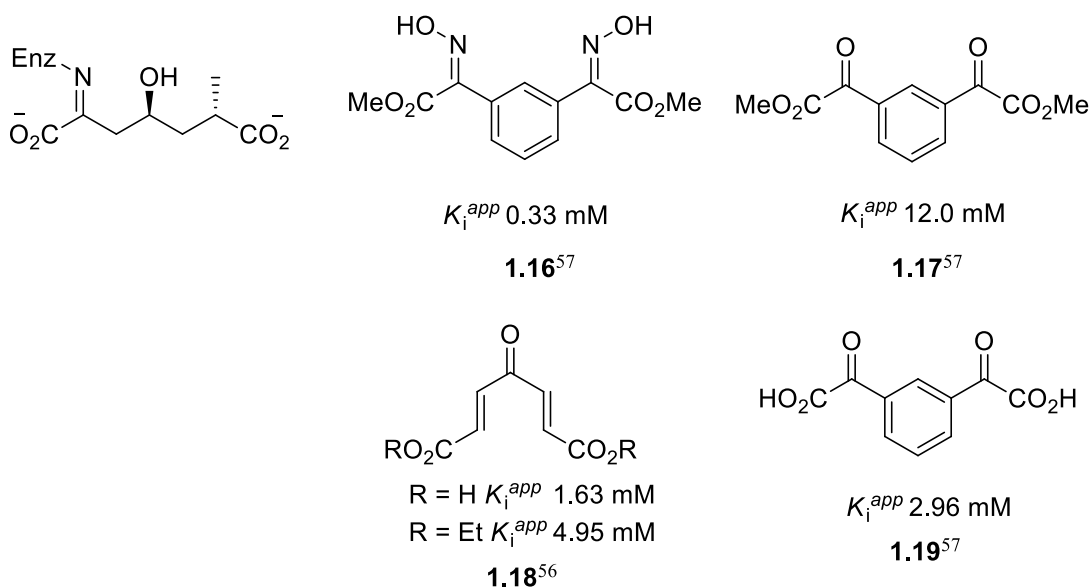
Figure 1.17. Moderately active DHDPS inhibitors based on the structure of enzyme-bound intermediate.

To summarize, the active site-directed inhibition is not a very promising strategy to synthesize potent inhibitors of DHDPS. The pyruvate and ASA analogues were weak inhibitors of DHDPS. The chelidamic acid and enzyme intermediate analogues did show moderate activity but no further data has been reported.

1.6.2 Allosteric inhibitors

Since the validation of DHDPS as a drug target, attempts have been made to design inhibitors of this enzyme, targeting the active site. These compounds showed only moderate to weak inhibition, suggesting a need to adopt a different strategy for designing inhibitors.[43] The kinetic studies of mutants of DHDPS gave information about the allosteric site and lysine binding. As a step toward synthesizing new inhibitors, lysine analogues were tested to see the effect of small structural changes on allosteric inhibition. Interestingly, the two analogues, α-methyl-DL-lysine and L-thialysine performed poorly as inhibitors compared to lysine.[49] This result indicated that the allosteric site is very specific to lysine. It was proposed that having a methyl substituent at the α-carbon hinders the binding of second lysine molecule thereby decreasing the inhibitory effect. But even simple heteroatom substitutions seem to affect the inhibition as observed with L-thialysine inhibitor. Substituting one of the carbons with sulfur lowered the pK_a of the ε -amino group which seems to affect the degree of inhibition. These results gave some insight on the requirements for a good inhibitor. First, the binding of both the lysine molecules is important for

achieving maximum inhibitory effect and second, the pK_a of lysine side chain is crucial. This amino group forms hydrogen bond with His59 but the exact role of this residue in allosteric inhibition is yet to be understood completely.
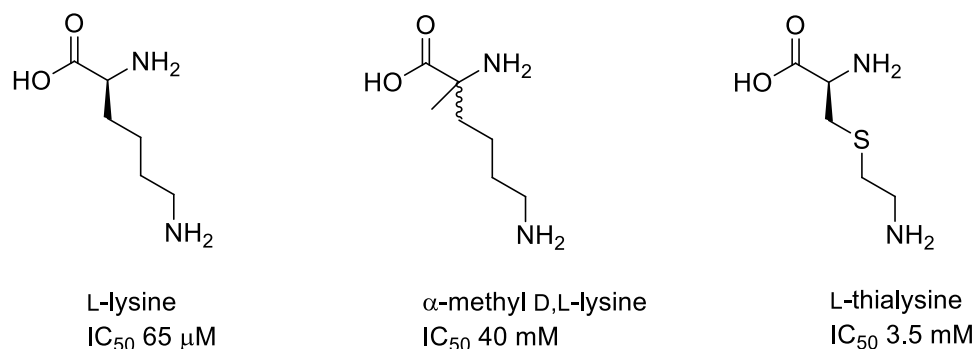
Figure 1.18. Lysine analogues as allosteric inhibitors of DHDPS

Based on these hypotheses, a ligand which could mimic the binding of lysine in allosteric site could be an inhibitor. There were no leads on building an inhibitor better than lysine until Phenix and Palmer[51] reported their findings from ITC studies that binding of the first lysine molecule induces favorable changes in enthalpy and entropy of binding, which results in tighter and almost simultaneous binding of the second lysine molecule. This result formed the basis of designing an inhibitor which would mimic the synchronous binding of a pair of lysine molecules in the allosteric site. The new inhibitor, (*R,R*)-bislysine was thus formed by joining two (*S*)-lysine molecules with a two carbon bridge separating the α-carbon atoms.[49]

1.7   Bislysine synthesis and activity

Synthesis of (±)-bislysine was achieved by bisalkylation of dimethyl 2,5 bis([(tertbutoxy)carbonyl]amino)hexanedioate **10** (Scheme 1.1). Adipic acid was converted to **10** using reported procedures by Sheehan.[58] It was then alkylated using 1-bromo-4-chlorobutane as the electrophile. The reaction proceeds with 19% yield generating a mixture of stereoisomers of the bisalkylated product. The *meso*:racemate ratio was 1:5 and the two were separated using flash column chromatography. The racemic mixture was transformed into corresponding phthalimides,

separated using chiral HPLC and deprotected to give (*R,R*)- and (*S,S*)-bislysine. (*R,R*)-bislysine, as predicted, proved to be the most potent inhibitor for DHDPS with $K_i = 0.2$ µM.[59]
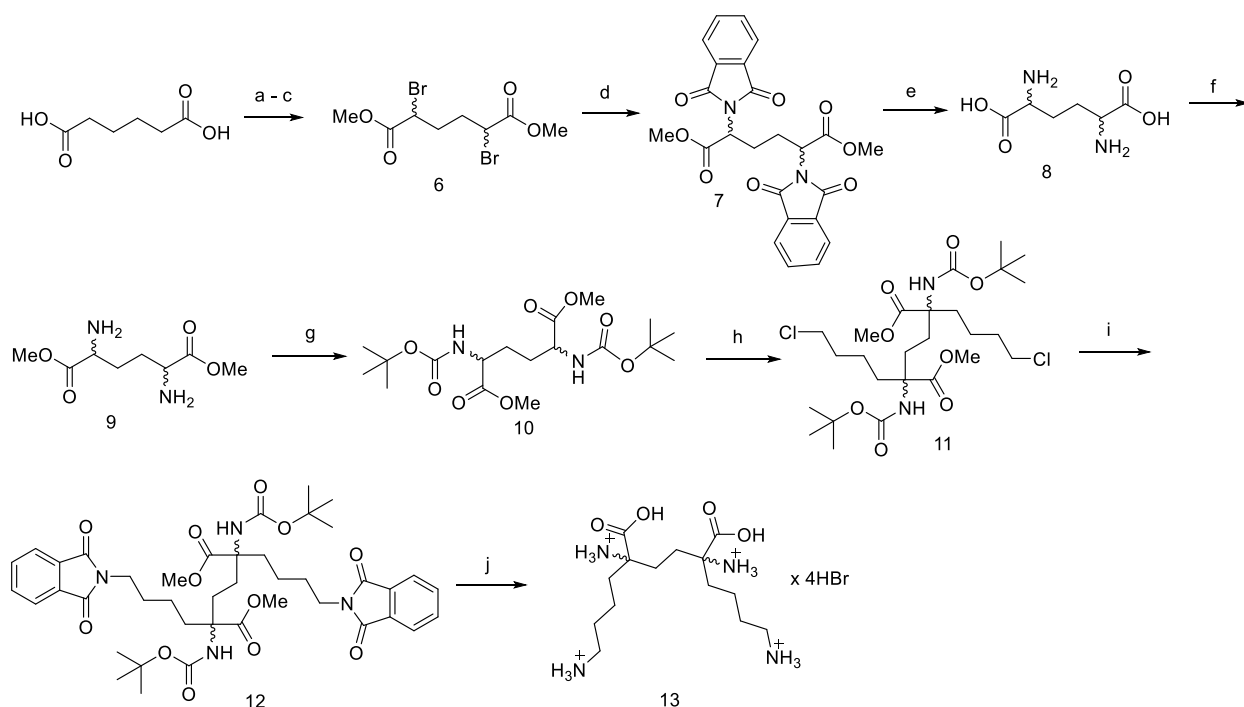
Scheme 1.1

Reagents: (a) SOCl$_2$, 80 °C, 3 h; (b) Br$_2$, 500 Watt, 12 h, 80 °C; (c) MeOH, 14 h, rt; a-c yield 87%; (d) potassium phthalimide, DMF, 90 °C, 2 h, 90%; (e) 1:1 48% HBr:AcOH, 14 d, 115 °C, 96%; (f) AcCl, MeOH, 2 h, 65 °C, quant. yield; (g) DIBOC, TEA, THF, 14 h rt, 3 h 50 °C, 72%; (h) 1-bromo-4-chlorobutane, LDA, THF/10% HMPA, 1 h, -78 °C, 19%; (i) potassium phthalimide, DMF, 90 °C, 2 h, 50%; (j) 1:1 48% HBr:AcOH, 3 d, 115 °C, AG 50W-X2, 88%.

A crystal structure of (*R,R*)-bislysine bound to DHDPS was also obtained, confirming the conformation of the compound in the allosteric site (Figure 1.19). Bislysine binds to the enzyme similar to lysine exactly as predicted, restoring all the essential polar contacts with the surrounding residues. However, kinetics studies with site-directed mutants showed major differences. The mutants Y110F, H59N, H59A showed comparable activity to wild type with bislysine with IC$_{50}$ values ranging from 0.2-0.6 µM for all the mutants whereas they were insensitive to lysine inhibition. This indicates that the absence of hydrogen bonds does not affect the inhibitory activity as strongly as it does for lysine and that the allosteric site can probably tolerate modifications in the structure of the inhibitor. Whether these residues are important for inhibition as predicted based

on crystallography data or only assist binding of an inhibitor is not clear. Also, the partial inhibition showed by lysine and bislysine is not yet explained. These results from mutagenesis studies suggest that a lot is unknown about the mechanism of allosteric inhibition in DHDPS.
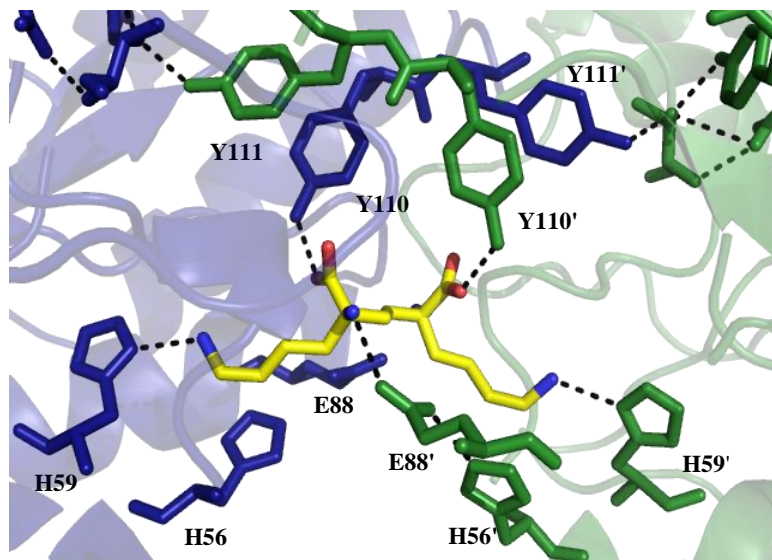
Figure 1.19. Allosteric site of *C. jejuni* DHDPS with (*R,R*)-bislysine (yellow stick) (PDB: 5F1V). Green (primed) and blue represent two adjacent monomers. Black dashed bonds represent polar contacts.[59]

Even though *R,R*-bislysine is an excellent inhibitor of DHDPS, it only represents the ideal inhibitor design. The results obtained from lysine analogues suggest that any modification introduced in this structure will have a negative effect on its activity. It is important to test a range of diverse compounds as inhibitors with minor to major structural modifications. With four positively charged amino groups and two carboxylic groups, the compound is not very lipophilic which can prevent it from crossing the cell membrane. Therefore, the compound does need certain modifications in order to overcome the structural drawbacks and evolve as a drug-like molecule. The bislysine structure, however successfully proved the hypothesis put forth by Phenix and Palmer[51], as described above and can be used as a core structure to synthesize other allosteric inhibitors for this enzyme.

2   RESEARCH OBJECTIVES

During previous studies on allosteric inhibition of DHDPS, some important information relevant to the strength of inhibitors was revealed,[49,59] which is summarized below:

- L-Thialysine was less effective in inhibiting the enzyme compared to its natural inhibitor L-lysine, putatively because of the lower pK_a of thialysine.
- The synthetic inhibitor *R,R*-bislysine was established as the most potent inhibitor of DHDPS yet studied.
- X-ray crystallography and site-directed mutagenesis studies showed that the hydrogen-bond between His59 and the inhibitor is crucial for inhibition.

Therefore, an important objective of this research was to synthesize a group of inhibitors which would demonstrate the effects of varying structural features such as the side chain, the pK_a of the side chain amine, and its ability to form a hydrogen-bond with His59. This information could be used to synthesize more potent and efficacious allosteric inhibitors.

Lysine is the natural allosteric inhibitor of DHDPS. Therefore, other amino acids could also be used to study the effects of modifications in the side chains. Since bislysine mimics the lysine pair bound in the allosteric site, the polar contacts made by lysine are retained in the bislysine-bound enzyme as proven by the crystal structure.[59] Thus, the implications of structural modifications would be similar on both 'monomeric' analogues and bislysine analogues. Some lysine analogues could be purchased, but others can be synthesized in well-established methods. Bislysine analogues could be obtained using a synthetic approach similar to that used for bislysine, and involving bisalkylation of a protected 2,5-diaminoadipate using different electrophiles. Since this reaction was common to the synthesis of all the inhibitors, its optimization was important to obtain maximum yield of bislysine and other inhibitors. Therefore, the factors affecting the bisalkylation reaction were also examined.

3 RESULTS AND DISCUSSION

3.1 Alkylation reactions of α-amino esters.

The alkylation of protected 2,5-diaminoadipate was a crucial step in the bislysine synthesis because of its outcome - the bisalkylated product which can be separated into diastereomers. This alkylation is the point where the synthesis can be diverted into varying target intermediates by using different electrophiles, which can be elaborated further into bislysine analogues. Therefore, the low yield of this reaction was of great concern and required a detailed study. For any reaction involving a stereogenic center, the stereoselectivity, along with the yield, needs to be optimized to get the desired isomer in adequate quantity. In the reported bislysine synthesis, the reaction favored formation of the desired racemic mixture as the major product; therefore improving the bisalkylation yield was prioritized over optimizing the stereochemical outcome of the reaction.

The bisalkylation proceeds via enolate formation from an α-amino ester which attacks the alkyl halide to form the *C*-alkylated product. Reactions involving α-amino ester enolates have been known to proceed in good yield. For example, Bartlett and Barstow[60] presented a study on the ester-enolate Claisen rearrangement of allylic esters derivatives where the influence of various factors such as additives, protecting groups, and α-substituents was investigated. The first step in this reaction is the formation of an α-amino ester enolate followed by silylation. The silyl enolate then rearranges at elevated temperature (55 °C) to give the rearranged product. The enolate formation was carried out in different conditions as described in Table 3.1. It was concluded from this study that the best condition for the deprotonation step was the 'standard condition', in which LDA was used as a base in tetrahydrofuran (THF) as solvent at −75 °C (entry 1).

Use of hexamethylphosphoric triamide (HMPT) as a cosolvent or tetramethylethylenediamine (TMEDA) as an additive lowered the yield and stereoselectivity (Entry 3 and 4). Reaction in diethyl ether instead of THF gave a low yield with no effect on the stereoselectivity (entry 2). Adding magnesium chloride also did not offer any advantage in yield or stereoselectivity (entry 6).
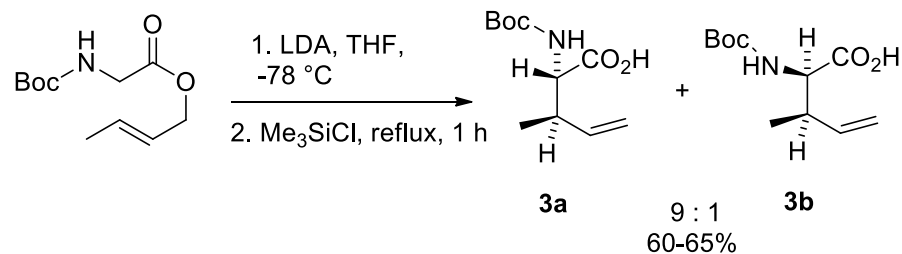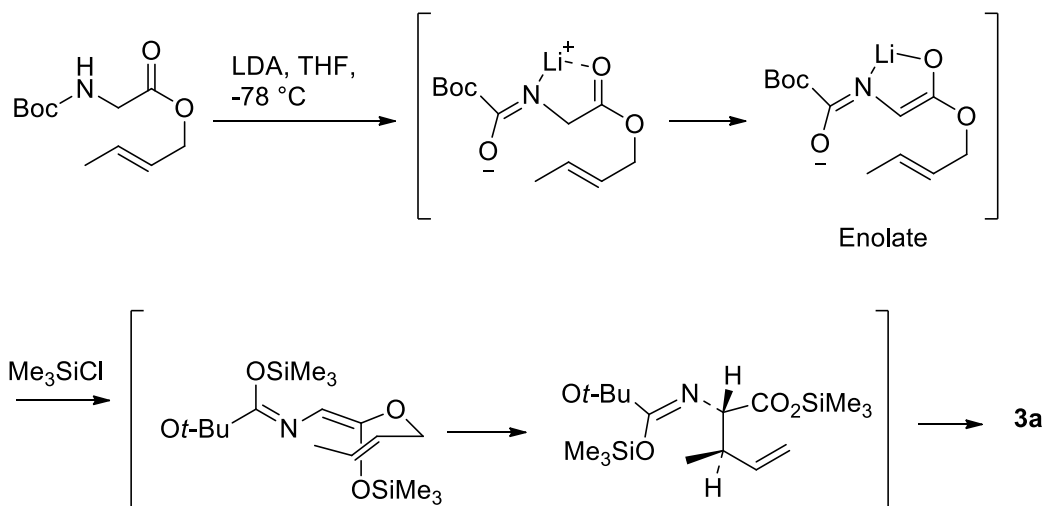
Scheme 3.1

Table 3.1. Influence of varying reaction conditions on Claisen rearrangement described in Scheme 3.1[60]

Entry	conditions	Yield %	3a:3b
1	2.1 eq. LDA in THF, 10 min. followed by silylation (standard)	60-65	9
2	Ether solvent	45	10
3	20% HMPT/THF solvent	51	4
4	2.2 equiv. TMEDA included with base	36	Not determined
5	KDA as base	0	-
6	1.1 equiv. MgCl$_2$ included with ester	42	10
7	Bromomagnesium isopropylcyclohexylamide as base	29	2

An elaborate study on *C*-alkylation of peptides was also carried out by Seebach[61] where deprotonation was achieved using LDA as base. Alkylation of dipeptides, polypeptides as well as large cyclic peptides was successfully performed with high yield and diastereoselectivity. It was observed that adding lithium salts such as LiCl or LiBr after deprotonation with LDA enhanced the yield without any epimerization at the stereogenic centers. The α-methylation of a β-aminobutyric acid derivative in THF proceeded with 73% yield; while in presence of LiCl, the yield increased to 87% (Scheme 3.2). In the absence of LiCl, the reaction mixture was heterogeneous and required warming to 0 °C to complete the methylation. Adding LiCl resulted in increased solubility of the deprotonated peptide by forming mixed aggregates, allowing the reaction to proceed at −78 °C. Methylation at multiple sites in large cyclic peptides was also achieved in high yield using lithium chloride.
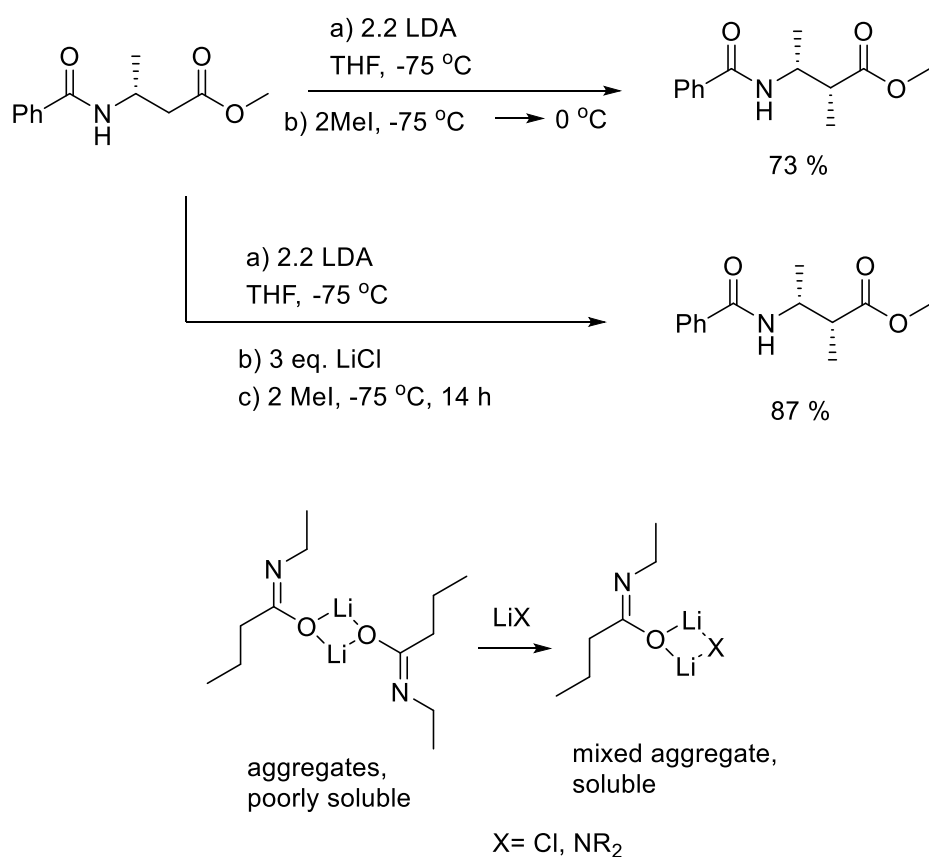
Scheme 3.2

Another strategy used to synthesize α-amino acids was using Scholkopf's alkylation method where stereoselective alkylation of a 2,5-dihydro-3,6-dimethoxy-2-isopropylpyrazine

(bis-lactim ether) was achieved using *n*BuLi. The alkylated bis-lactim ether was then subjected to a mild acid hydrolysis to obtain α- substituted amino acids. This method was exploited to synthesize α,α' substituted bridged amino acids For example, bisalkylation of Scholkopf's bis-lactim ethers where the two lactim rings were separated by a 5-carbon bridge with the two stereogenic centers α and α' was achieved using *n*BuLi as base (Scheme 3.3).[62] The alkylated product was obtained in 73% yield when allyl bromide was used as alkylating reagent. This strategy was used to synthesize α-amino acids.
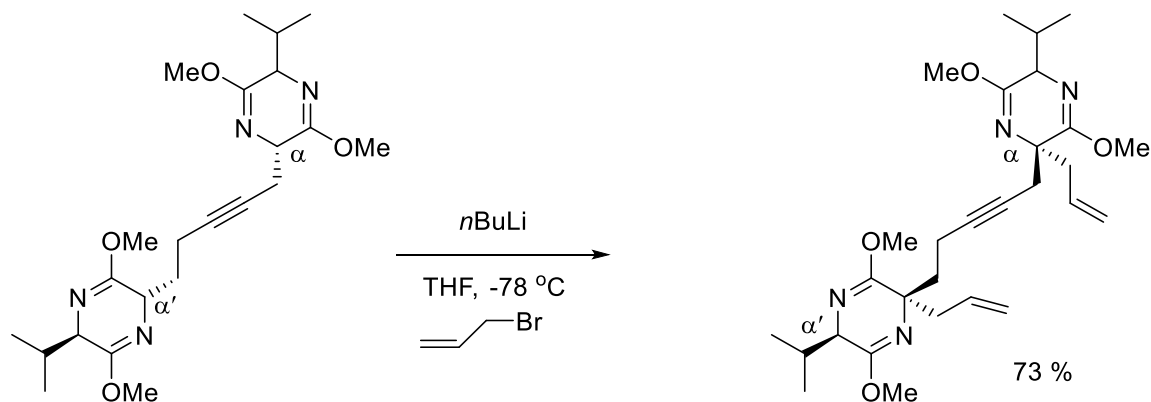
Scheme 3.3

To summarize, enolates of α-amino ester have previously been shown to be alkylated using LDA as the base and THF as the solvent. The Scholkopf's alkylation method was appealing since it could allow us to synthesize more bridged inhibitors. However, the choice of electrophiles in all these reactions was restricted to reactive species such as methyl iodide and allyl halides. The effect of lithium salts on the alkylation yield was also noteworthy and thought to be a promising strategy for improving the yield of bislysine synthesis.

3.2   Examination of conditions for the bisalkylation reaction

According to the reported procedure of the bisalkylation of the protected 2,5-diaminopimelate **10**,[59] an enolate was generated using LDA as the base in THF with HMPA as a cosolvent at −78 °C (Scheme 1.1). After 1 hour, an additional 2 eq. *n*BuLi was added followed by 1-bromo-4-chlorobutane. The reaction mixture was stirred at the same temperature for 2 hours and then quenched with aqueous ammonium chloride solution. With this reaction condition, 30% of the starting material was recovered with 19% bisalkylation yield. When this procedure was used for alkylation with propargyl bromide and (2*E*)-1,4-dibromo-2-butene, the crude was obtained as a complex mixture of impurities. The pure product was isolated by column chromatography with

great difficulty. Therefore, the existing reaction conditions were reexamined using the electrophile propargyl bromide (Table 3.2). The racemate:*meso* ratio was calculated based on the isolated yield for all the bisalkylation reactions. The enolate was formed at −78 °C in THF for all the entries. The use of reported conditions gave 23% yield with 2.8:1.0 ratio of racemate:*meso* (entry 1). Only 15% of the starting material could be recovered. In the following steps (entry 2 and 3), HMPA and the extra equivalent of *n*BuLi was excluded respectively. The exclusion of HMPA increased the yield to 30% and also led to a higher recovery of starting material. It was clear that HMPA and the extra *n*BuLi was not required to obtained the best possible yield and a simplified procedure could be used. In another attempt to improve bisalkylation yield, the reaction mixture was stirred for 10 hours at −78 °C (entry 4) after the addition of the electrophile but the extended time did not have any effect on the reaction yield. For the following alkylations with different electrophiles, the modified procedure, with 4.5 equivalents of LDA, without HMPA was used.

Table 3.2. Bisalkylation: Scope of the reaction with propargyl bromide as the electrophile

Entry	Reaction condition	Bisalkylation yield	Racemate:*meso*	Starting material recovered
1	4.5 + 2 eq. LDA, HMPA −78 ºC, 2 h	23%	2.8:1.0	15%
2	4.5 + 2 eq. LDA, −78 ºC, 2 h	30%	2.5:1.0	22%
3	4.5 eq. LDA, −78 ºC, 2 h	32 %	2.5:1.0	25%
4	4.5 eq. LDA, −78 ºC, 10 h after alkylation	32%	2.4 :1.0	22%

3.2.1 *Reactions with different electrophiles*

Since it was important to synthesize lysine-dimer analogues, the bisalkylation was carried out with different electrophiles which were strategically selected so that they could be further transformed into inhibitors. The electrophiles chosen were allyl bromide, propargyl bromide and

(2*E*)-1,4-dibromo-2-butene, all of which are more reactive than aliphatic halides. The adjacent π-electrons in these halides stabilize the transition state of the S_N2 reaction by conjugation, increasing the rate of the reaction. The electrophile (2*E*)-1,4-dibromo-2-butene was important because replacing the bromides of the bisalkylated compound with phthalimide moieties followed by hydrolysis would result in the formation of bislysine with a higher yield than the existing route.

Table 3.3. Comparison of bisalkylation reaction yields using various electrophiles

10
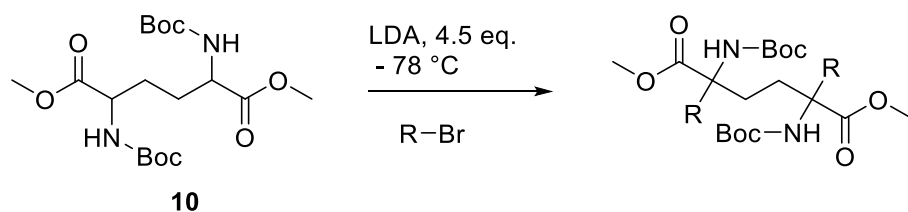
Entry	Electrophile, R-Br	Bisalkylation yield (%),	Racemate: *meso*	Monoalkylation Yield (%)	Starting material recovered (%)
1	Br⌒⌒⌒Cl	12	4.6:1.0	none	39
2	Br⌒⌒⌒Br	11	6.3:1.0	18	39
3	⌒⌒Br	28	5.2:1.0	22	28
4	⌒⌒Br	32	2.5:1.0	17	25
5	O₂N-⌬-CH₂Br	< 5		none	22

As expected, the reaction proceeded with higher yield with propargyl bromide and allyl bromide as electrophiles. However, a considerable amount of starting material was recovered along with monoalkylated product. The reaction with 1-bromo-4-chlorobutane as electrophile gave the bisalkylated product in 12% yield (Entry 1). The electrophile (2*E*)-1,4-dibromo-2-butene, which was expected to perform better than 1-bromo-4-chlorobutane did not show any improvement in the reaction yield. The reaction gave 11% yield, again with a high amount of starting material recovery as well as 18% monoalkylated product (entry 2). However the

racemate:*meso* ratio was slightly higher (6.3:1.0) compared to entry 1. Allyl bromide and propargyl bromide gave 28% and 32% yield; however, more than 20% starting material was recovered. For all the reactions, the products showed the same pattern on TLC and eluted in the same sequence, starting with the minor *meso*-isomer, then the racemate, followed by the monoalkylation product. The starting material was eluted at the end. The racemate and *meso* were confirmed by HPLC for 1-bromo-4-chlorobutane and (2*E*)-1,4-dibromo-2-butene. The reaction with 4-nitrobenzyl bromide (entry 5) proceeded with the formation of many impurities which co-eluted with the product. This made it difficult to isolate the product (or the starting material) in a pure form. The presence of product was confirmed by proton NMR, where all the desired peaks were observed. The sequence of elution for the products of 4-nitrobenzyl bromide reaction was not the same as observed for the first four electrophiles. Therefore, it was not possible to conclude if the product was the racemate or the *meso*-compound. The racemate:*meso* ratio also decreased for propargyl bromide while a higher ratio is observed for the first three electrophiles. For all the electrophiles, the racemate was the major product.

3.2.2 Enolate formation and stability

The conversion of ester to enolate was confirmed by NMR. After adding the starting material to the LDA- THF mixture, the reaction was stirred for 4 h during which the aliquots of reaction mixture were quenched with D_2O and extracted with EtOAc. The organic layer containing the deuterated starting material was collected, solvent was removed and the residue was dried under vacuum. If the ester was converted to enolate then quenching with D_2O would result in replacement of α- hydrogen with deuterium, resulting in a diminished proton peak at δ 4.31.
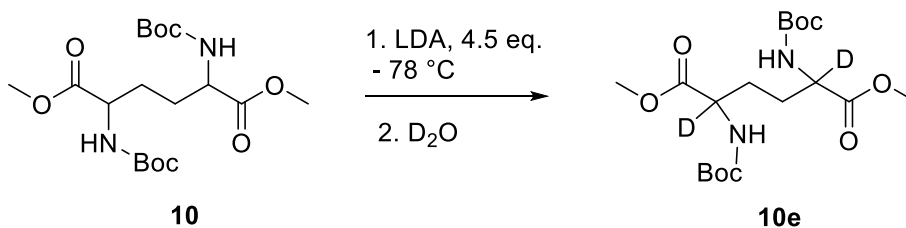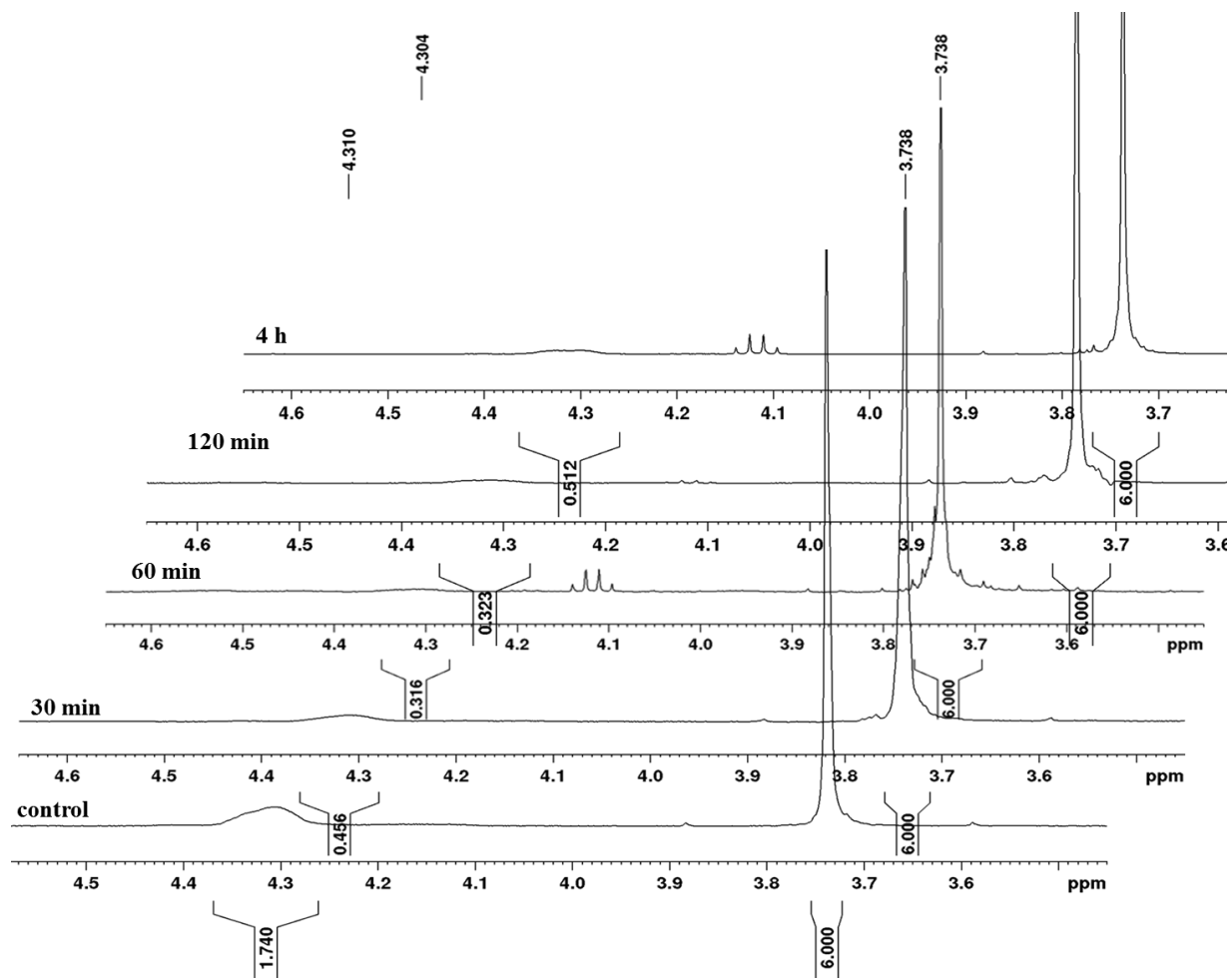
Figure 3.1. Overlay of ¹H NMR of fractions 10e, quenched at time intervals as shown in the figure. 'Control' represents the fraction quenched with H₂O.

The integration of the six methyl ester hydrogens (δ 3.74) was used as internal standard to observe the loss of proton signal of the α-hydrogens (δ 4.31) after quenching with D₂O (Figure 3.1). The loss of signal (from ~1.7 to ~0.5) after only 30 minutes indicated that enolate was certainly generated within 1 hour of adding LDA. Although the conversion was not 100%, the reaction yield remained unchanged when the enolate generation time was extended to 10 h (Table 3.4, entry 2 and 5).
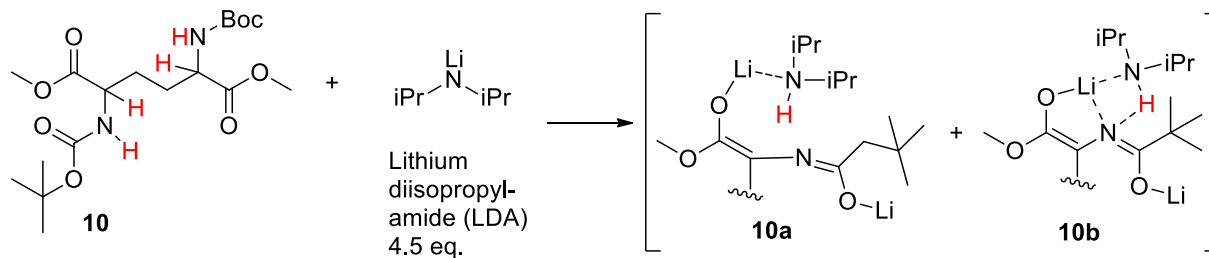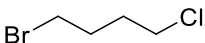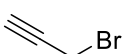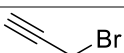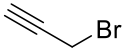
Figure 3.2. Enolate formation by LDA can result in complexes (10a and 10b) in which the internal proton is retained, and returned to the substrate after quenching. The acidic hydrogens are shown in red.

The enolates formed by amide bases like LDA have been known to revert back to the protonated state by the process called "internal proton return" (Figure 3.2).[61,63] After the deprotonation of the starting material, diisopropylamine is regenerated which is believed to coordinate with the lithium enolate. This amine-lithium enolate complex brings the amine proton close enough to the π-electrons of the enolate to reprotonate it. Any electrophile or a deuterated quenching agent added at this point does not result in alkylation or deuterated product; simply because the rate of "proton return" is faster. Hence, a complete disappearance of the α- proton was not observed in the above experiment. This phenomenon also explains the high recovery of starting material and low bisalkylation yield. Seebach[61] has successfully demonstrated that the internal proton return can be avoided by adding an extra equivalent of nBuLi after the enolate formation. The additional nBuLi reacts with the regenerated diisopropylamine to form more LDA. This procedure was successfully used previously in our laboratory[59] for the bislysine synthesis. However, adding extra nBuLi results in a mixture of LDA and enolate. The remaining LDA may react with electrophile or the product and result in a completely different product or a mixture of products at the end of the reaction. This is perhaps the reason why the method did not work well in the above reactions with electrophiles such as propargyl bromide.

33

Table 3.4. Effect of longer enolate- generation time on bisalkylation yields

Entry	Reaction condition	Enolate time	electrophile	Bisalkylation yield
1	4.5 + 2 eq. LDA, −78 ℃, 2 h	1 h	Br~~~Cl	10%
2	4.5 + 2 eq. LDA, -78 ℃	10 h	Br~~~Cl	10%
3	4.5 eq. LDA, -78 ℃, 2 h	1 h	≡~Br	32%
4	4.5 eq. LDA −78 ℃,	10 h	≡~Br	28%
5	4.5 + 2 eq. LDA −78 ℃	10 h	≡~Br	30%

3.2.3   Solvent and additives effect

Although all the reported procedures for the formation of amino ester enolates used THF as a solvent, the bisalkylation was also carried out in other less polar solvents (Table 3.5). The electrophile chosen for this study was propargyl bromide, since it gave maximum yield for bisalkylation with the standard conditions. The starting material was insoluble in diethyl ether, dimethoxyethane (DME) and toluene at −78 °C. The solubility was also checked at elevated temperature by slowly raising it up to –20 °C. When HMPA was added, the precipitate dissolved giving a clear yellow solution. However, for all the three solvents, the reaction proceeded in < 20% yield, the lowest yield being 10% with toluene (entry 4). The aggregated states of enolate formed with THF are seemingly aiding in the alkylation.

Table 3.5. Effect of varying solvents on bisalkylation yield
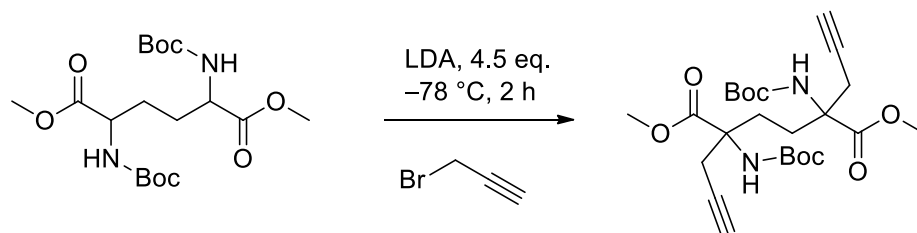
Entry	additive	solvent	Bisalkylation yield (%)
1	HMPA	THF	23
2	HMPA	Diethyl ether	15
3	HMPA	DME	14
4	HMPA	1:1 THF: DME	15
5	HMPA	Toluene	10

Table 3.6. Effect of lithium chloride on the bisalkylation yield

Entry	Electrophile	additive	Bisalkylation yield (%)	Racemate:*meso*
1	Br⌇	-	32	2.5:1.0
2	Br⌇	LiCl (6 eq.)	29	2.3:1.0
4	Br⌇Cl	-	12	4.6:1.0
5	Br⌇Cl	LiCl (6 eq.)	11	5.5:1.0

As described in section 3.1, using lithium chloride in alkylation reactions of amino acids increased the yield of reaction by 30%. Expecting a similar effect, 6 eq. of lithium chloride (1M in THF) solution was added to the LDA solution along with the starting material (Table 3.6). After one hour of enolate formation, the reaction mixture was stirred at −78 ℃ for 10 hours and then quenched with ammonium chloride solution. During the reaction, TLC was recorded at the intervals of 2, 4 and 8 hours for a parallel reaction which did not show any change over the course

35

of the reaction. Indeed, the isolated yield was 29% for the reaction with propargyl bromide (entry 2) and 11% with 1-bromo-4-chlorobutane (entry 4).

In conclusion, the bisalkylation reaction proceeded in low yields for all the electrophiles. The only factor affecting the yield was the reactivity of the electrophiles used. The effect of the additives HMPA and LiCl on either yield or stereochemistry was not very significant in the experiments described above. Therefore, it was difficult to make any conclusions about the plausible factors in the reaction procedure which could affect the yield. For synthesizing the dimer-analogues, the modified procedure, without HMPA and excess LDA was used.

3.3 Design and synthesis of allosteric inhibitors

As described in Section 1.6, there have been many attempts to design inhibitors targeting the active site of DHDPS. Compounds which were substrate analogues (1.1-1.3) or transition state analogues (1.16 and 1.19) proved to be only moderate to weak inhibitors. The synthesis of allosteric inhibitor (*R,R*)-bislysine put a spotlight on previously overlooked allosteric site of DHDPS and opened the door to a new class of inhibitors which would mimic the 'lysine dimer-like' framework. Analogous compounds of lysine and bislysine were synthesized by keeping the amino acid backbone intact and replacing the lysine side chain with different moieties.

3.3.1 Lysine analogues

Novel lysine analogues were synthesized as shown in Scheme 3.4 and Scheme 3.5 using diethyl acetamidomalonate (DEAM) as starting material. DEAM has been used to synthesize α-amino acids previously.[64,65] Two electrophiles, (2*E*)-1,4-dibromo-2-butene and propargyl bromide were used for *C*-alkylation of DEAM, leading to two different lysine analogues. For the synthesis of **16**, the enolate was generated using 10% NaOH as base, following the procedure by Roduit and Wyler.[66] (2*E*)-1,4-dibromo-2-butene was used as electrophile to obtain *C*-alkylated compound **14** in 44% yield. The amino group was introduced by nucleophilic displacement of the remaining allylic bromide with phthalimide in 45% yield using the procedure described previously for bislysine synthesis.[59] The phthalimide was then hydrolyzed to the amine in refluxing aqueous HCl for 3 days, which also removed the ester and amide protecting groups and resulted in decarboxylation to give the desired amino acid 89% yield after ion exchange chromatography.

For the synthesis of triazole **20**, cesium carbonate was used to generate the enolate from DEAM in acetonitrile, which was then reacted with propargyl bromide as the electrophile[67] with mild heating for 16 h, resulting in **17** in 88% yield. Apart from an increase in the yield, the $CsCO_3$ procedure was advantageous because of the simplified reaction procedure and workup, compared to the procedure described for synthesizing **14**. However with allylic electrophiles, the reaction has been shown to proceed with < 50% yield.[68] With (2*E*)-1,4-dibromo-2-butene, the reaction did not show much progress in my hands even after refluxing for 24 h and 70% of starting material was recovered. The alkyne was then converted to a 1,2,3-triazole using a procedure described previously with some modifications.[69] This so-called "Click" reaction, a copper catalyzed azide-alkyne cycloaddition using benzyl azide, afforded the corresponding 1-benzyl-1*H*-1,2,3-triazole

18 in moderate yield. Hydrogenolysis of the benzyl group using H_2 and palladium hydroxide proceeded smoothly to generate **19**, the 1*H*-1,2,3-triazole. The last step was the acid hydrolysis of amide and ester groups accompanied by decarboxylation to the monocarboxylic acid as above.
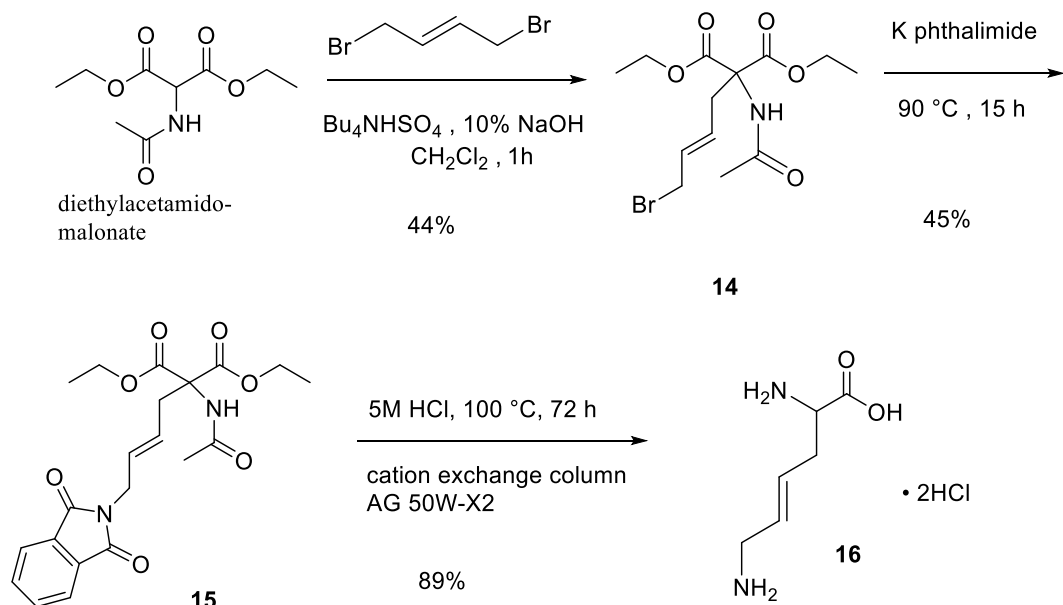
Scheme 3.4
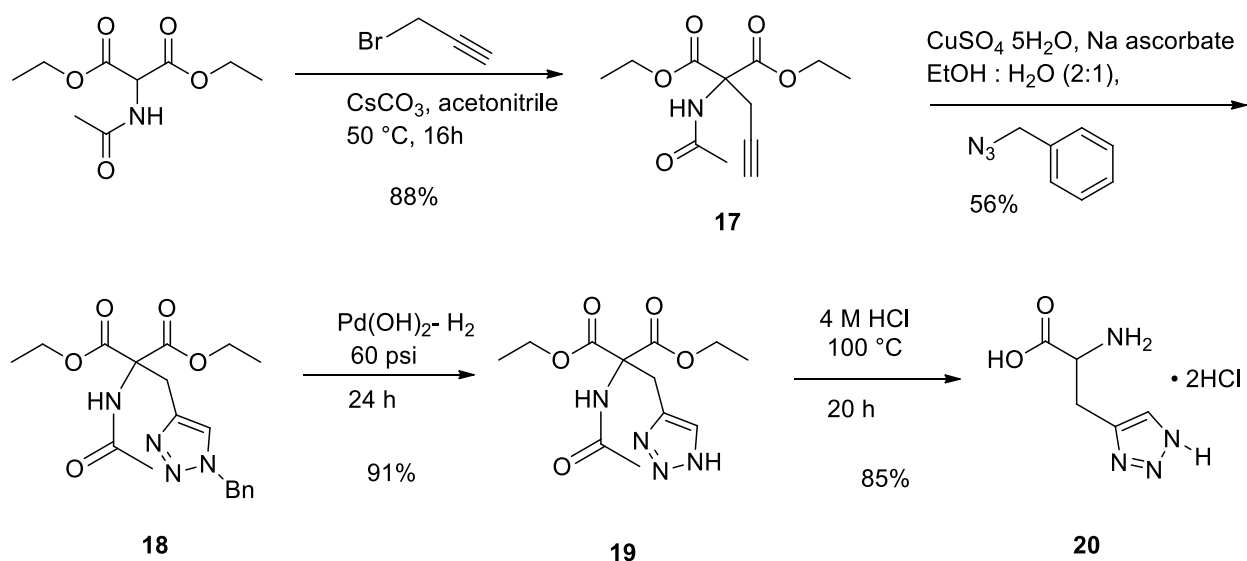
Scheme 3.5

3.3.2   Bislysine analogues

The bislysine analogues were synthesized using a similar procedure to that described previously.[59] The BOC-protected dimethyl ester of 2,5-diaminoadipate (**10**), synthesized as described in Scheme 1.1was used as the starting material to carry out bis-alkylation reactions. LDA (4.2 eq.) was used to generate enolate after which the desired electrophiles were added to obtain the bisalkylated product. The alkylation products were obtained as mixture of diastereomers which could be separated by flash column chromatography into a *meso* compound and a racemate. Intriguingly, both isolated products showed similar ^{1}H and ^{13}C NMR; but for all the bisalkylations, including the one in the bislysine synthesis, the minor isomer easily crystallized on standing at room temperature in the elution solvent (15% EtOAC in hexanes). The major product in all cases was isolated as an oil which foamed up under vacuum. For bislysine synthesis, both the compounds were carried forward and transformed into corresponding phthalimides. The deprotected phthalimide derivatives were then analyzed by HPLC where the racemate and *meso* isomers were identified. The major product was found to be the racemic mixture. For enzyme kinetics the (*R,R*) isomer was separated by semi-preparative HPLC at the phthalimide stage to obtain pure (*R,R*)-bislysine. Primary enzyme inhibition studies with racemic and *meso*-bislysine showed that even though the desired stereoisomer is (*R,R*)- bislysine, it was possible to carry out preliminary experiments using the racemate. For all the reactions, monoalkylated products were also isolated and unreacted starting material was recovered back.

The synthesis of **23** (Scheme 3.6) was achieved by using (2*E*)-1,4-dibromo-2-butene as the electrophile and following the exact route of bislysine synthesis. The alkylation proceeded in a similarly low yield, but nucleophilic displacement with phthalimide was more efficient (71% vs. 50%). Hydrolysis of all protecting groups gave the desired compound after ion exchange chromatography.

The synthesis of **26** is shown in (Scheme 3.7). 4-Nitrobenzyl bromide was used for the bisalkylation of **10**, although this reaction proceeded with extremely low yield (1.5%) and the product was difficult to isolate because of the associated impurities. The product, in its impure form was subjected to hydrogenation to form **25**, which could be isolated by column chromatography. The last step involved removal of *tert*-butoxycarbonyl protecting group and hydrolysis of methyl esters by refluxing in 5 M HCl to obtain **26** in very low overall yield.

Synthesis of the triazole analogue **31** was attempted using the synthetic route of the simple lysine analog **20** described above, however, the procedure needed to be modified as shown in Figure 3.10. Propargyl bromide was used as the electrophile for bisalkylation, which proceeded in 32% yield. Copper-catalyzed cycloaddition between benzyl azide and the acetylene **27** was performed at room temperature to obtain **28**, however the debenzylation followed by acidic hydrolysis led to the decomposition of reaction mixture. Therefore, hydrolysis of the methyl ester groups was first performed using lithium hydroxide under mild conditions, followed by hydrogenolysis using H_2 and palladium hydroxide as catalyst and lastly, the *tert*-butoxycarbonyl groups were removed using trifluoroacetic acid to obtain **31**. All three of these steps proceeded in moderate to good yield (72 – 89%). The final compound was purified using ion-exchange column and eluted in 4M HCl. The resulting product was thus isolated starting from **10** in 10% yield over four steps. This compares with the yields over three steps from **10** of 17% for **23**, ~ 0.2% for **26**, and the previously reported 5% for bislysine.
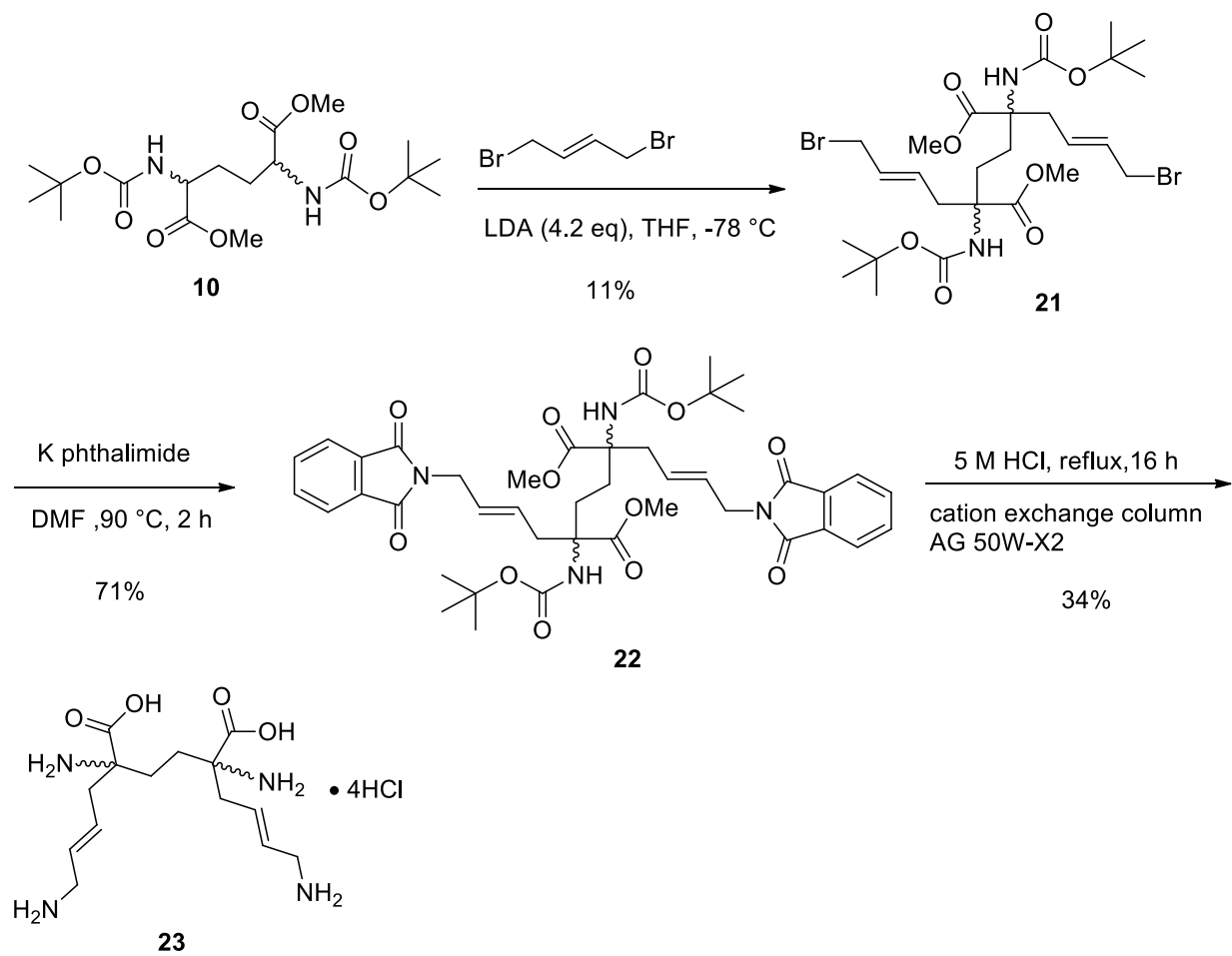
Scheme 3.6
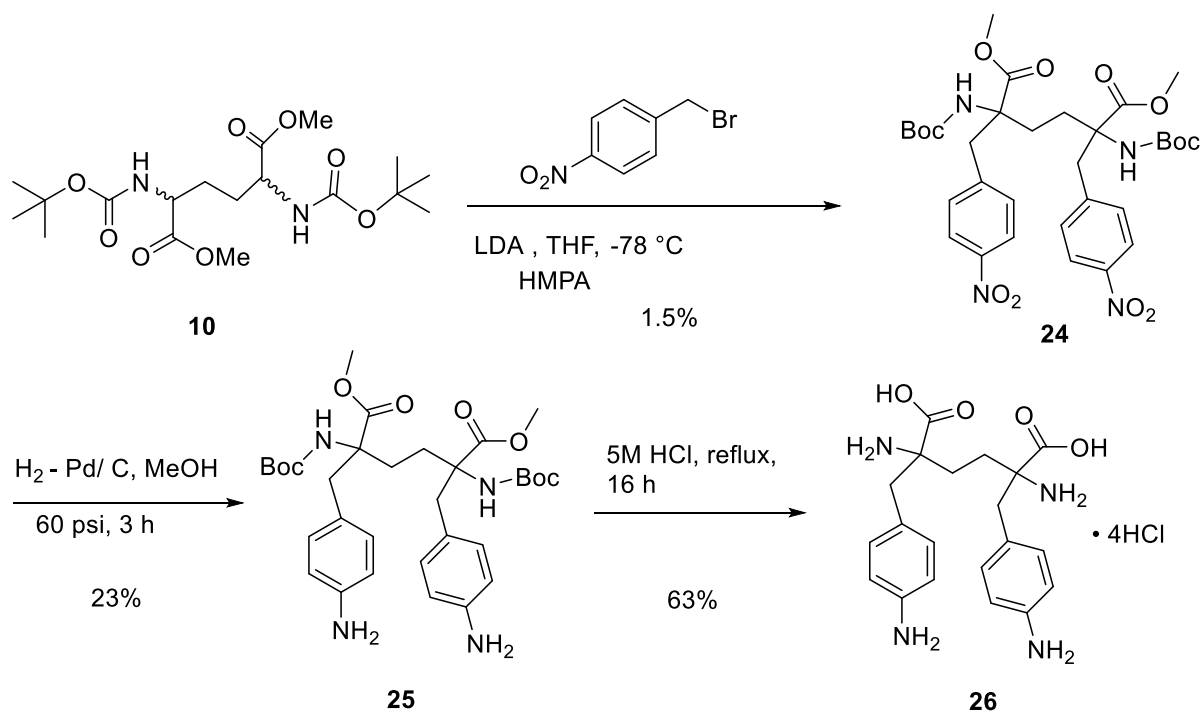
Scheme 3.7
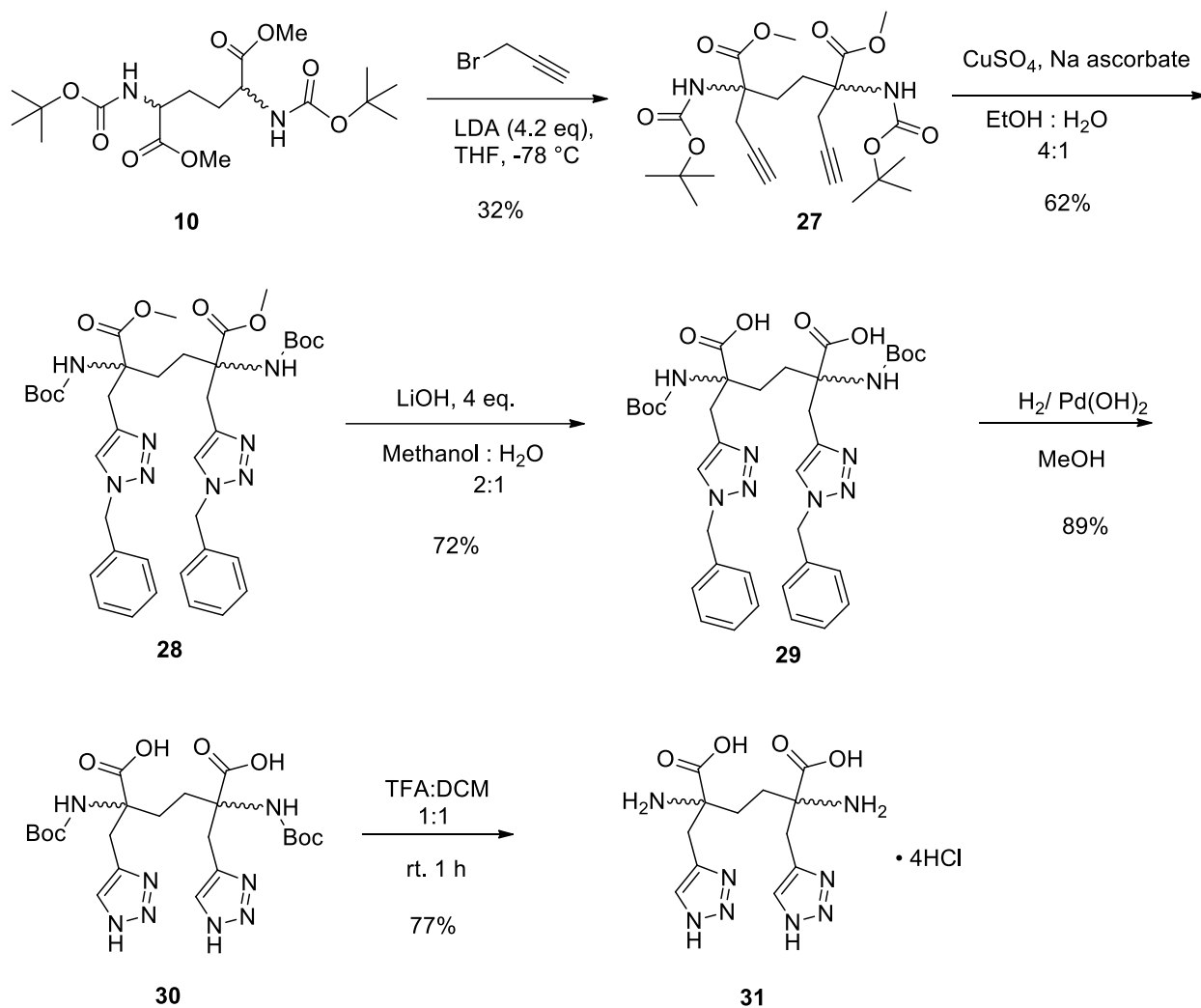
Scheme 3.8

3.4 Enzyme Inhibition Studies

3.4.1 *The DHDPS-DHDPR coupled assay*

A coupled assay refers to a method of measurement of enzymatic activity in which the enzyme under study is coupled with a second enzymatic reaction, which utilizes the product of the first reaction as its substrate. When the second enzyme is used in sufficient concentration, the first enzymatic reaction becomes the rate determining step. The DHDPS-DHDPR coupled assay was first described by Yugari and Gilvarg[29] in 1965, where DHDPR was used to as the second enzyme (Figure 3.3). DHDPR is a NADH-dependent enzyme in the lysine biosynthesis pathway which reduces dihydrodipicolinate, the product of DHDPS-catalyzed reaction to tetrahydrodipicolinate.

During the course of the second reaction, NADH is oxidized to NAD$^+$ which results in a decrease in the absorbance which can be monitored using a spectrophotometer. NADH absorbs strongly at 340 nm (e = 6.22 M^{-1}cm^{-1}) while neither NAD$^+$ or the product has absorbance in this range. In the presence of an excess of DHDPR, the decrease in the absorbance of NADH becomes the measure of the DHDPS-catalyzed reaction. For all the enzymatic studies described in this thesis, the coupled assay was used, the details of which are described in Section 5.2.
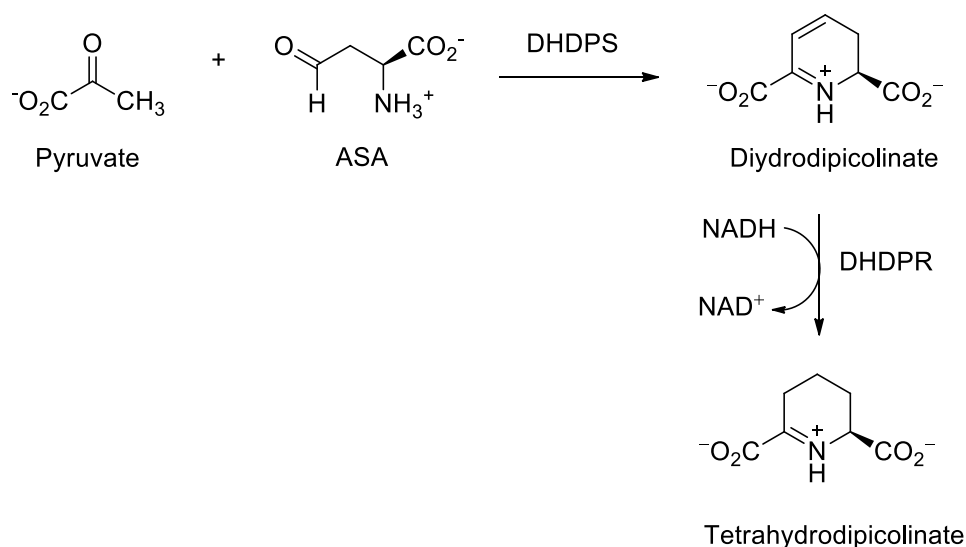
Figure 3.3. The DHDPS-DHDPR coupled assay

3.4.2   Measurement of enzyme activity

The kinetic parameters of DHDPS were obtained using the coupled assay with respect to both the substrates, ASA and pyruvate. This was done to ensure that the new batch of the enzyme was active and kinetic parameters were comparable to those obtained previously in our lab. The experiment was performed by varying the concentration of one substrate at different fixed concentrations of the other substrate. The obtained kinetic data was fitted to ping pong rate equation using Sigmaplot 12.0$^®$ and kinetic parameters were obtained,

$$v = V_{max}AB / (K_{M(B)}A + K_{M(A)}B + AB) ....3.1$$

where v is the initial velocity, V_{max} is the maximum velocity and $K_{M(A)}$ and $K_{M(B)}$ are the Michaelis-Menten constants for the substrates A and B. As shown in Table 3.7. Kinetic parameters of DHDPS catalyzed reaction, DHDPS showed behavior similar to that previously reported.[48] The double

44

reciprocal plots of Figure 3.4 A and B show parallel lines, which is diagnostic of a ping pong kinetic mechanism.[70] This is consistent with the established reaction as described in Figure 1.11.

Table 3.7. Kinetic parameters of DHDPS catalyzed reaction

	Observed	Reported[48]
$K_{M(ASA)}$	0.16 ± 0.01 mM	0.12 ± 0.01 mM
$K_{M(pyruvate)}$	0.35 ± 0.02 mM	0.27 ± 0.01 mM
k_{cat}	84 ± 1 s^{-1}	76 ± 1 s^{-1}

(A)

(B)
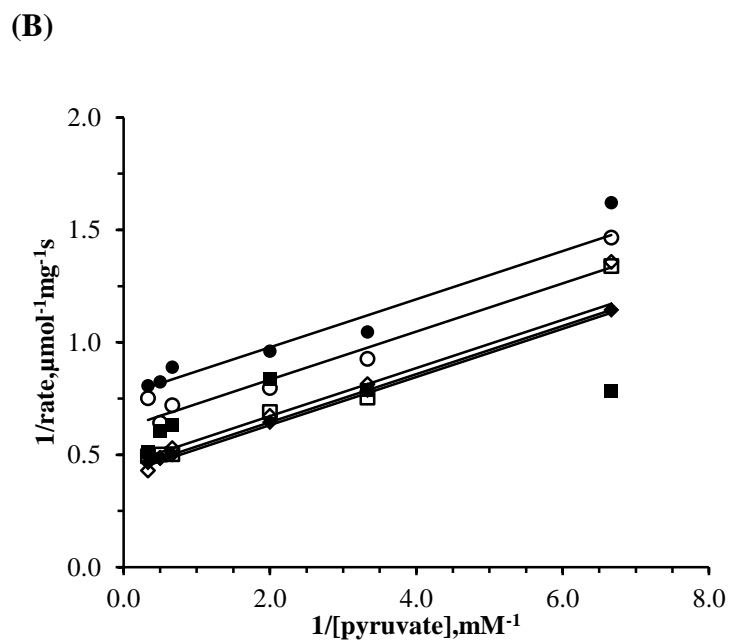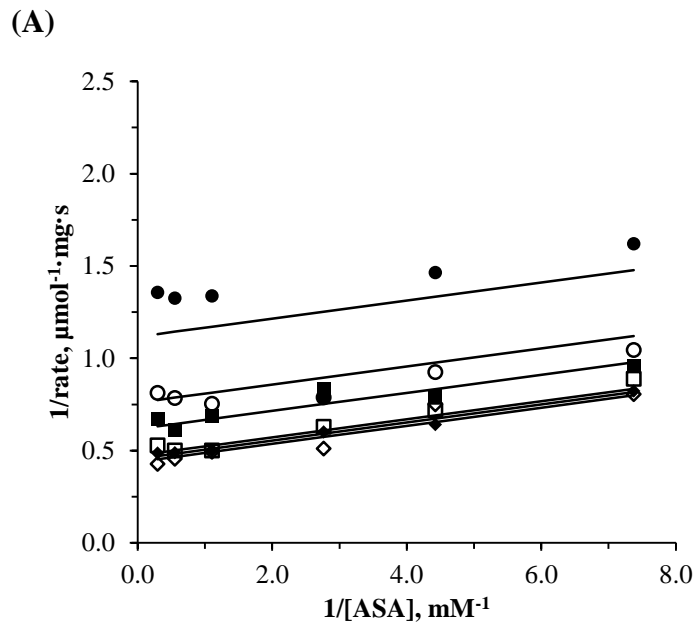
Figure 3.4. Double Reciprocal plot of the DHDPS-catalyzed reaction. Solid lines represent global fit of the data to Equation 3.1. (A) Concentration of pyruvate is varied (●) 0.15 mM (○) 0.30 mM (■) 0.50 mM (□) 1.5 mM (♦) 2.0 mM (◊) 3.0 mM. (B) Concentration of ASA is varied -(●) 0.13 mM, (○) 0.23 mM (■) 0.36 mM (□) 0.90 mM (♦) 1.81 mM (◊) 3.39 mM.

3.4.3 *Screening of inhibitors*

For enzyme inhibition studies, the DHDPS-DHDPR coupled assay was used with a fixed concentration of ASA (0.14 mM) and pyruvate (3 mM). The near-saturating concentration of pyruvate was chosen because it has been previously established by Skovpen and Palmer[48] that allosteric inhibitor binding is enhanced by the presence of pyruvate. The near-K_M concentration of ASA was chosen as a standard for comparison of each inhibitor. The inhibitor concentrations were selected in such a way that maximum number of data points could be recorded with the amount of inhibitor available. DHDPS activity was measured by recording the decrease in absorbance of NADH at 340 nm. The percent activity vs. inhibitor concentration plots were used to estimate the IC_{50}, which is the concentration of inhibitor which causes 50% inhibition of the enzyme activity. IC_{50} values of compounds are indicative of their effectiveness as enzyme inhibitors. Since the assay is performed only with fixed concentrations of the substrate, the plot of relative activity vs. inhibitor concentration can be used as convenient way to evaluate the strength of the inhibitor. For example, the IC_{50} of (*R,R*)-bislysine was found to be ~ 0.3 μM. The steady state kinetic experiments revealed the K_i value to be 0.2 μM, which is similar in magnitude to the IC_{50} value.

Synthesized inhibitors were tested using the DHDPS-DHDPR coupled assay described above, and the results are shown in Figure 3.4 and 3.5. It has previously been shown that the lysine L-thialysine (*S*-aminoethyl L-cysteine) is an allosteric inhibitor of DHDPS from *C. jejuni*, with an IC_{50} of be 2.2 mM.[49] The 10-fold decrease in efficacy was very drastic since the only difference in thialysine structure is the presence of sulfur instead of carbon. However, it has been demonstrated that the pK_a of thialysine is lower than that of lysine.[71] Therefore, it was speculated that the pK_a of the ε-amino group affects the activity of inhibitors. Apart from thialysine, α-methyl-D,L-lysine was shown to be a very poor allosteric inhibitor[49], indicating that the allosteric site is very specific in terms of accommodating a compound. The analogues described in sections 3.3.1 and 3.3.2 were tested for inhibition against DHDPS and the percent activity curves were plotted to determine their potency.
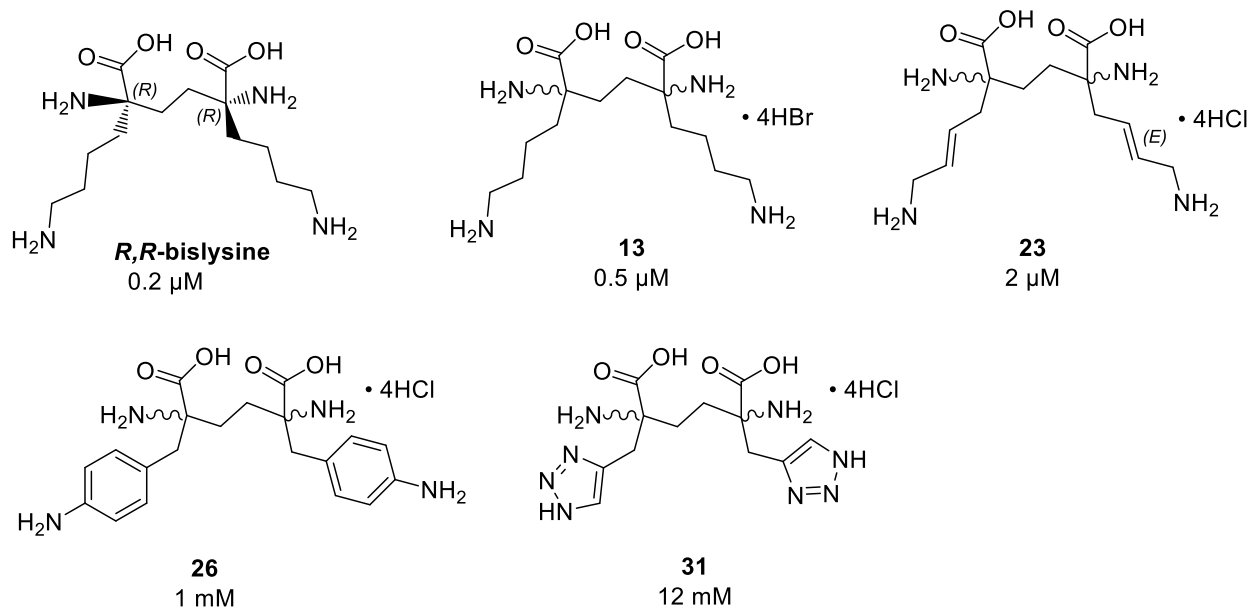
Figure 3.5. Dimeric allosteric inhibitors of DHDPS and their IC$_{50}$ values
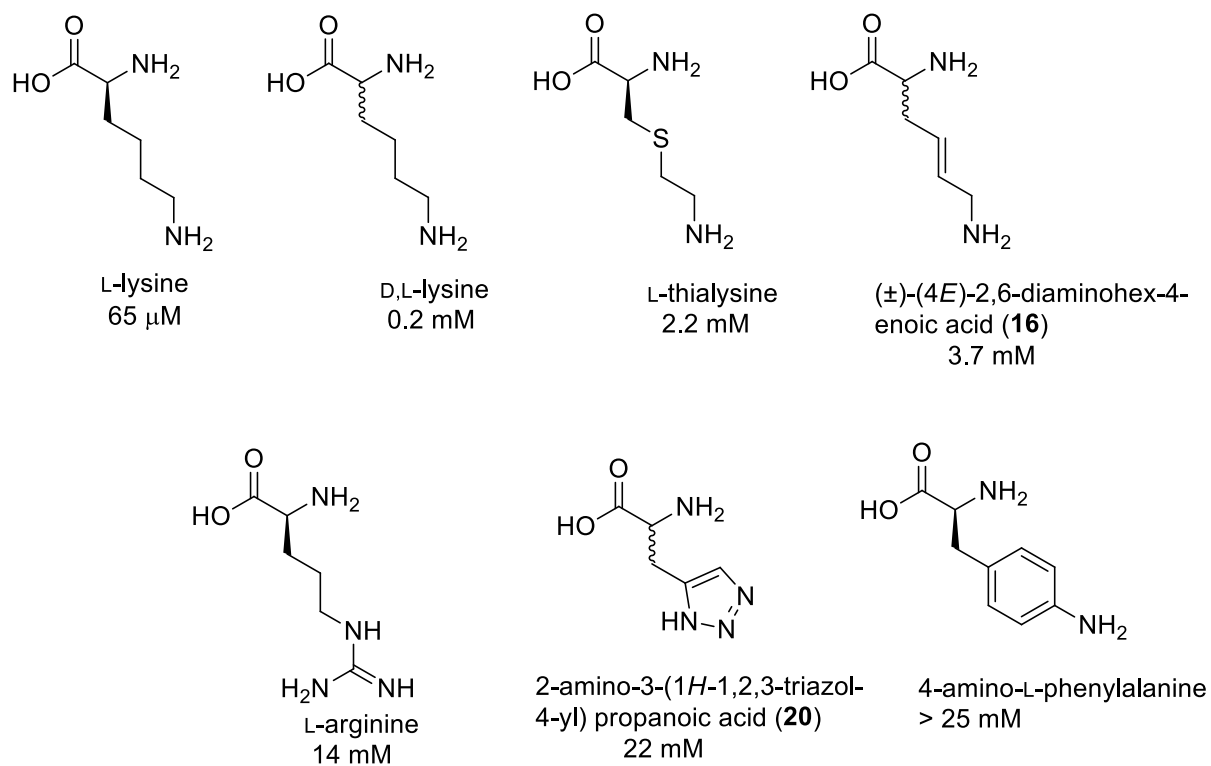
Figure 3.6. Monomeric allosteric inhibitors of DHDPS.

3.4.4 Amino acids as weak allosteric inhibitors

(A)

L-Histidine

4-Amino-L-phenylalanine

(B)

L-Thialysine

2-Amino-3-(1*H*-1,2,3-triazol-4-yl) propanoic acid (20)
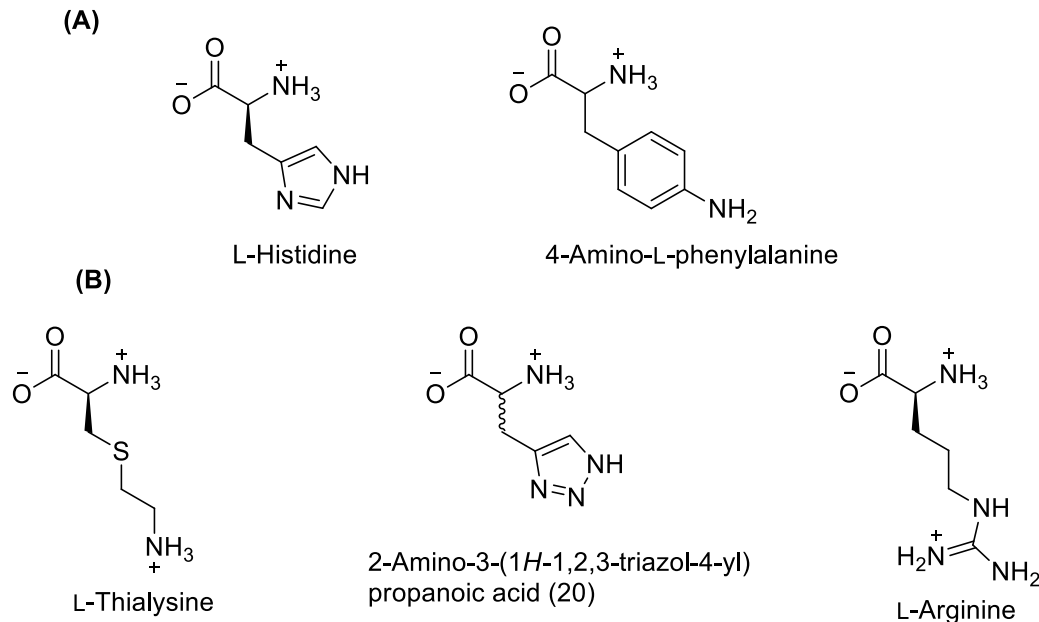
L-Arginine

Figure 3.7. (A) Amino acids showing no inhibitory effect on DHDPS and (B) weak allosteric inhibitors of DHDPS at pH 8.

Naturally occurring amino acids histidine and arginine, which possess amino groups in their side chains, were tested for inhibition. Arginine showed a maximum of 55% inhibition at 14 mM concentration. Increase in inhibitor concentration did not inhibit the enzyme any further. The weak inhibition was as expected and it can be attributed to the structurally dissimilar side chain of arginine compared to lysine, with pK_a 12.5. Because of these factors, even the presence of a hydrogen-bond donor did not make arginine a good inhibitor.

Histidine did not inhibit the enzyme activity. The imidazolylmethyl side chain is shorter than the aminobutyl group of lysine and perhaps places the terminal N-H of the imidazole ring further away from His59, making it difficult to form a hydrogen bond between the two groups. However, 2-amino-3-(1*H*-1,2,3-triazol-4-yl) propanoic acid **20**, which is structurally similar to histidine, did show weak inhibition, with $IC_{50} = 22$ mM. The difference in these compounds is again, the pK_a, which is near 7 for an imidazole side chain of histidine and near 9.5 for **20**, closer to the pK_a of lysine. This suggests that a pK_a near 10 may be an important feature of any inhibitor.

To further examine the importance of pK_a, 4-amino-L-phenylalanine (4ALP) was tested for inhibition. The amino group at the para-position of the phenyl ring might be close to His59 when bound to the allosteric site, but the pK_a is much lower (close to 5). It was expected that this

compound could behave as a weak inhibitor but even at 25 mM concentration there was no inhibition observed. The inhibition curves for weak inhibitors are shown in Figure 3.8.
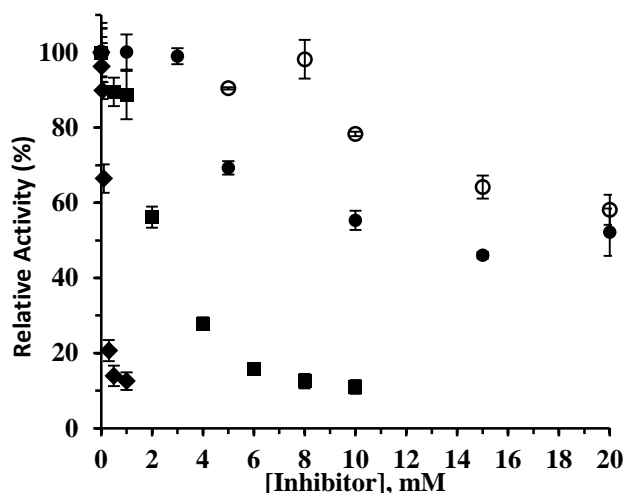
Figure 3.8. Inhibition of DHDPS by (±) lysine (♦), L-thialysine (■), (20) (○) and arginine (●).

3.4.5 *Enzyme inhibition by (±)-2,5-diamino-2,5-bis[(2E)-4-aminobut-2-en-1-yl] hexanedioic acid tetrahydrochloride (23) and (±)-(4E)-2,6-diaminohex-4-enoic acid (16)*

16   **23**
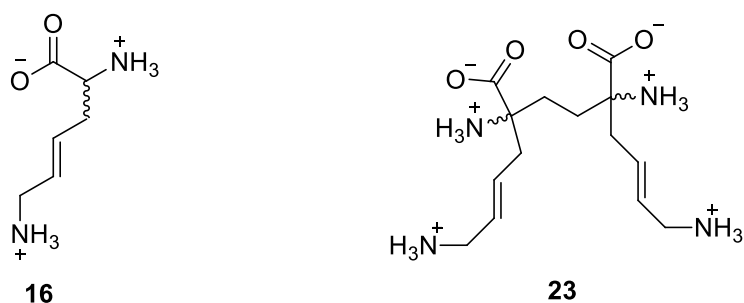
Figure 3.9. Moderate inhibitors of DHDPS at pH 8.

The simplest modification introduced in the bislysine scaffold was addition of a double bond at carbon-4 of the side chain (Figure 3.9). The double bond provides more rigidity to the side chain by restricting bond rotation but the structure still has the 4-carbon side chain like lysine. It was observed that introduction of this double bond into lysine and bislysine raises the IC_{50} value 4-fold for **23** (Figure 3.11) and 20-fold for **16** (Figure 3.12). This decrease in inhibitory activity may also be explained by a change in the pK_a of the ε-amino group, which is lowered by the

50

presence of the double bond. It is well known that pK_a values of allylic amines are about 1 unit lower than similar alkyl amines, as shown in Figure 3.10.[72]

n-propylamine   *n*-butylamine   allylamine

pK_a 10.53   10.59   9.49
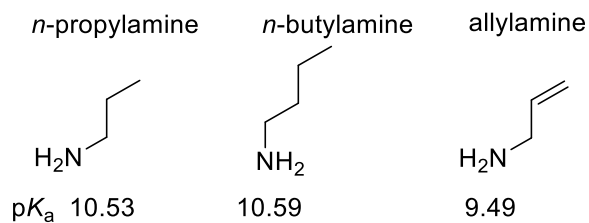
Figure 3.10. Comparison of pK_a of aliphatic amines
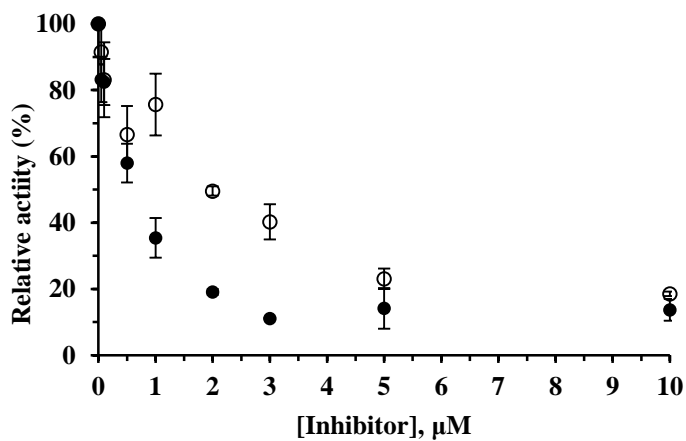
Figure 3.11. Inhibition of DHDPS by (±)-bislysine (●) and (23) (○).
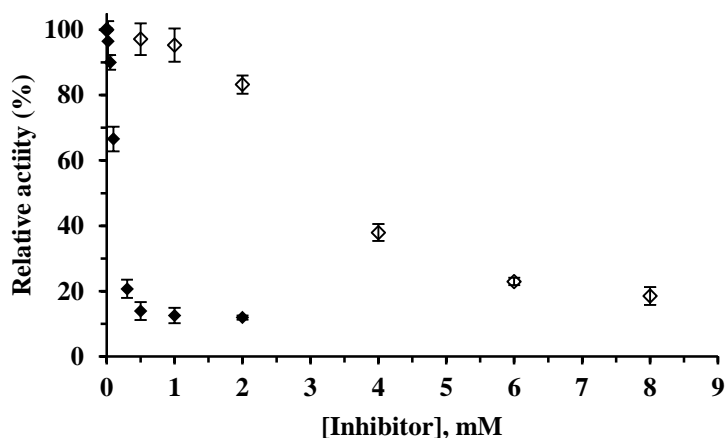
Figure 3.12. Inhibition of DHDPS by (±)-lysine (♦) and (16)(◊)

3.4.6   Enzyme   inhibition   using   (±)-2,5-diamino-2,5-bis[(1H-1,2,3-triazol-4-yl)methyl]
hexanedioic   acid   tetrahydrochloride   (31)   and   2,5-diamino-2,5-bis[(4-
aminophenyl)methyl] hexanedioic acid tetrahydrochloride (26).

26   31
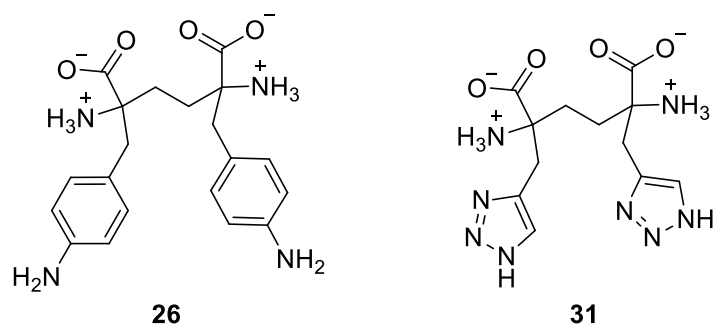
Figure 3.13. Bislysine analogues as weak inhibitors of DHDPS at pH 8.

Although there were many difficulties faced while synthesizing the bis-*para*-aminophenylalanine analog **26**, it was important to test it as an inhibitor to see if the pK_a effect was similar to that observed with **16** and **23**. The introduction of an aromatic ring in a compound comes with advantages, such as more rigidity in the structure and increased molecular interactions. In the case of DHDPS it was important to explore the space available in the allosteric cavity and see if a large moiety can be accommodated as a part of the side chain. Both the analogues were assayed for inhibition. Interestingly, **26** showed 50% inhibition at 1 mM concentration which proved that the bulky aromatic ring did not prevent inhibitory activity (Figure 3.14). The higher IC_{50} value compared to other analogues can be a result of a drastic change in pK_a of the side chain

52

amino group, or poor fit of the substrate in the allosteric site. The result with **26** was very encouraging for introducing aromatic rings in the side chains of inhibitor. Due to the poor yield of this synthesis, the activity curve could not be completed to get an estimate of the residual activity.

(A)
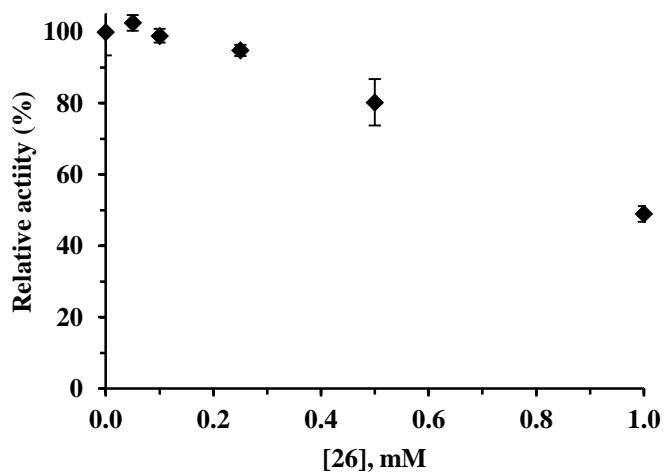
(B)
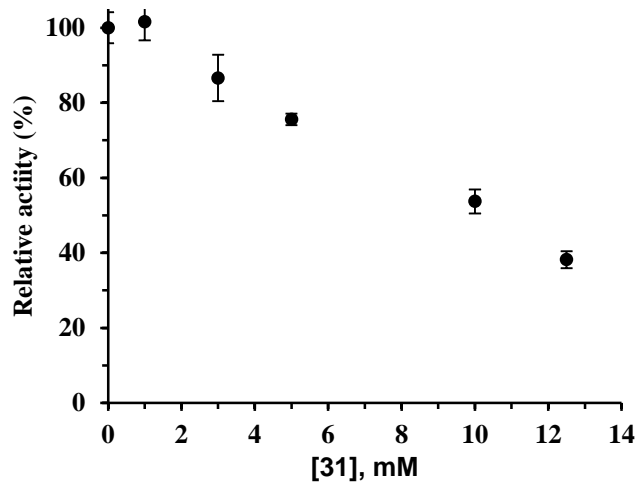
Figure 3.14. Inhibition of DHDPS by (26) and (31).

The dimeric analogs bislysine and **23** were more than 200-fold better inhibitors than the corresponding monomers. Therefore, it was expected that bis-triazolyl derivative **31** would have an IC_{50} value in micromolar range. The synthesis of **31** was comparatively easier than that of **26**

53

and bislysine. The first alkylation step with propargyl bromide as well as the click reaction worked in moderate yield and large scale synthesis for further studies such as crystallization, binding experiments and cell based assays would be possible. The final compound also has only four charged groups at pH 8, which make it less polar and possibly more cell-permeable. Therefore, even high micromolar-range inhibition would have been an encouraging result. But surprisingly, **31** showed only 20% inhibition below 5 mM, with an estimated IC_{50} of 12 mM (Figure 3.14). The available quantity of inhibitor only allowed measurements up to 12.5 mM concentration, which showed 62% inhibition. Even though **31** is better than its amino acid analogue, it is better by only 2 fold, unlike other bislysine analogues. This result suggests that it is very important that the inhibitor can hydrogen bond with His59, and the length of the side chain of **31** may not allow that. Whether the pK_a of the donor group is equally important needs to be examined further. Arginine and **23** are good examples of compounds with varying pK_a but these compounds also have altered chain lengths which might be responsible for the lowered inhibition.

4 CONCLUSIONS

- Significant improvement was not achieved in the bisalkylation of the protected diaminoadipate, suggesting that a different synthetic approach may be necessary to make this synthesis efficient.

- Lysine analogues (α-amino acids) were synthesized in much higher yield compared to the bislysine analogues and all of them were poorer inhibitors than the bislysine analogues. The results obtained from lysine analogues can be used to estimate the activity of their dimeric counterparts, although the relationship between their activities is not linear. The lysine analogues thus offer an advantage because of the ease in their synthesis.

- The bislysine analogue **23** is a weaker inhibitor than bislysine, despite being a close structural analog. The *trans* double bond of the side chain of **23** would allow it to adapt a similar configuration with fewer degrees of freedom (Figure 4.1). This supports the hypothesis that the pK_a of the side chain ε-amino group is an important determinant of inhibition.
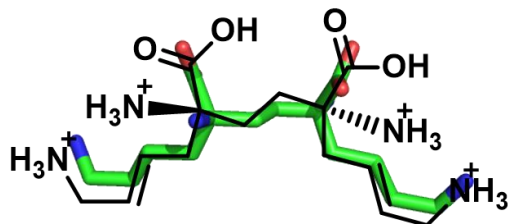
Figure 4.1. The overlay of crystal structure of *R,R*-bislysine and its analogue 23. Bislysine is shown as green sticks and compound 23 in in black.

- Lysine analog **20** is a weaker inhibitor than lysine, despite having a predicted pK_a value closer to lysine. Both **26,** with an aniline substituent and **31,** with a triazole substituent were found to be less effective than bislysine. A possible explanation is that the inhibitors, which had their terminal amino groups farther away from His59, failed to make a strong hydrogen bond. The weak inhibition observed with these compounds could mean that they still bind in the allosteric site; but the binding is not as tight as other inhibitors This supports the hypothesis that the side chain hydrogen bonding interaction with His59 is sensitive to chain length.

20   **26**   **31**
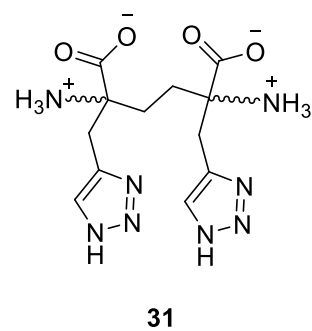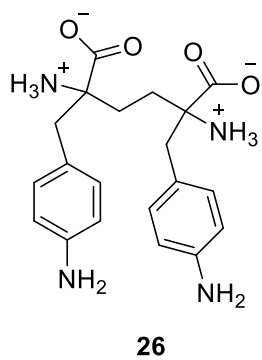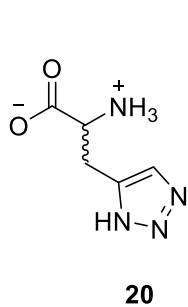
Overall, this work highlights some important structural features of allosteric inhibitors which affect their activity. This knowledge can help to develop new class of antibacterial agents targeting the cell wall synthesis. The results obtained by this study can be used to synthesize more drug-like and potent inhibitors of DHDPS and extend the knowledge towards DHDPS from other bacterial species.

5 EXPERIMENTAL PROCEDURES

5.1 Protein overexpression and purification

Making cell stock: LB media (5 mL) containing 50 µg/mL ampicillin was inoculated from a single colony of *E. coli* XL1Blue transformed with recombinant plasmid pQE80L containing the *C. jejuni dap*A gene[48]. The cells were grown overnight at 310 K by shaking at 250 rpm. The cell suspension was then pelleted in 1.5 mL Eppendorf tubes by centrifugation. The cell pellets were suspended in a fresh media containing 0.5 mL LB broth with ampicillin (50 µg/mL) and 0.7 mL of 80% glycerol. These cell stocks were stored in –80 °C.

Overexpression of protein: LB broth (500 mL) containing 50 µg/mL ampicillin was inoculated with 1 mL of cell stock and incubated at 310 K in a shaker at 250 rpm until it reached an optical density of 0.45. Isopropyl β-D-1-thiogalactopyranoside (IPTG) was added to a final concentration of 0.5 mM to induce overexpression of protein. The incubation was continued for another 15 h at 288 K, before centrifugation at $5,180 \times$ g for 30 min. The resulting cell pellet was suspended in 10 mL binding buffer (20 mM Tris –HCl, 5 mM imidazole, 500 mM NaCl, 12.5% glycerol, pH 7.9), chilled in an ice bath, and sonicated using a Virsonic 600 Ultrasonic Cell Disrupter. The resulting crude lysate was centrifuged at $27,000 \times$ g for 30 min at 4 °C to separate the cell debris from the protein. The supernatant containing DHDPS was filtered through a 0.45 µM syringe filter and loaded onto a 1-mL HiTrap^{TM} IMAC FF column (GE Healthcare), prepared according to the manufacturer's procedure and equilibrated with 5 mL binding buffer, which facilitates the binding of the His-tagged protein to the column. The column was then washed with 5 mL binding buffer, 5 mL 1:1 mixture of wash buffer (20 mM Tris –HCl, 100 mM EDTA, 500 mM NaCl, 12.5% glycerol, pH 7.9) and binding buffer, 15 mL 1:1 mixture of strip buffer (20 mM Tris –HCl, 5 mM imidazole, 500 mM NaCl, 12.5% glycerol, pH 7.9) and binding buffer and then 15 mL stripping buffer which results in the elution of the protein. Fractions were analyzed by SDS-PAGE and the purest fractions were pooled and dialyzed at 4 °C for 24 h against 1 L storage buffer (20 mM Tris –HCl, 100 mM NaCl, 40% glycerol, pH 7.9). The resulting protein was concentrated to 0.59 mg/mL using an Amicon Ultra-15 Centrifugal Filter (30 kDa MWCO, EMD Millipore). Enzyme concentrations were determined by Nanodrop ND-1000 using calculated parameters (ProtParam) for DHDPS (MW 34069 Da, $\varepsilon_{280} = 18068$ M^{-1} cm^{-1}).[73]

5.2   Enzyme assay

The activity of DHDPS was measured using a coupled assay in which dihydropicolinate reductase (DHDPR) is present in sufficient quantity to oxidize NADH at a rate equal to the DHDPS catalyzed reaction.[29] The ping pong kinetics experiments were performed to compare the kinetic parameters of DHDPS with the reported values in order to ensure that the enzyme was active. The second substrate of the enzymatic reaction, ASA was synthesized according to the reported procedure.[74] The kinetic measurements were performed on Beckman DU640 spectrophotometer at 25 ºC. A typical assay contained 100 mM HEPES buffer, 0.16 mM NADH, 0.45 μg DHDPS, 9.03 μg DHDPR and varying concentrations of ASA (0.13-3.39 mM) and pyruvate (0.15-3.00 mM). The initial velocity of DHDPS was determined using the decrease in absorbance of NADH ($\varepsilon_{340} = 6220$ $M^{-1}cm^{-1}$) due to its oxidation. The experiment was performed by varying the concentration of one substrate at different fixed concentrations of the other substrate. For all the experiments, the reaction was initiated by the addition of the enzyme DHDPS.

5.3   Organic synthesis of inhibitors

All moisture- and air-sensitive reactions were performed under an inert atmosphere of nitrogen. The syringes, needles, magnetic stirring bars and glassware (flasks etc.) were dried at 120 °C overnight and cooled in desiccators. All chemicals were purchased from Sigma-Aldrich Canada, Ltd (Oakville, ON) or Alfa Aesar (Ward Hill, MA) unless stated otherwise. Dry DCM and THF were obtained using a MB- solvent purification system (University of Saskatchewan). Diisopropylamine was freshly distilled from CaH_2. Flash chromatography was performed using Merck silica gel 60 (230-400 mesh). Thin layer chromatography (TLC) was performed on precoated glass plates (Merck, silica gel 60, F 254) or aluminum plates. The spots were detected using UV light (254 nm) and by charring after treatment with cerium phosphomolybdate. Proton magnetic resonance (^{1}H NMR) and carbon magnetic resonance (^{13}C NMR) spectra were recorded on the Bruker 500 MHz spectrometer. Multiplicity is indicated by: s (singlet), d (doublet), t (triplet), q (quartet), m (multiplet) and br (broad). Mass spectra were recorded on a Q-star XL MS/MS System. Electron impact (EI) ionization was accomplished at 70 eV and chemical ionization (CI) at 50 eV.

(±)-Diethyl 2-[(2*E*)-4-bromobut-2-en-1-yl)]-2-acetamidopropanedioate

14
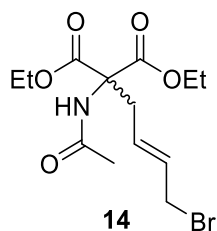
The reaction was carried out according to the procedure described by Roduit and Wyler.[66] To a stirring solution of DEAM (4.00 g, 18.4 mmol) in dichloromethane (60 mL), tetrabutylammonium bisulfate (6.25 g, 18.4 mmol) was added in one portion followed by (2*E*)-1,4-dibromo-2-butene (5.91 g, 27.6 mmol). A 20% aqueous sodium hydroxide solution (7.36 g, 184 mmol) was then added dropwise over a period of 10 min. The resulting biphasic reaction mixture was stirred vigorously at room temperature. After 1 hour, the aqueous and organic layers were separated and the organic layer was concentrated by rotary evaporation. The resulting oil was partitioned between water (50 mL) and diethyl ether (50 mL). The layers were separated and the aqueous layer was washed with diethyl ether (2 × 20 mL). The combined Et$_2$O layer was washed with brine and then evaporated under reduced pressure to get crude product which was purified by flash column chromatography (25% EtOAc in hexanes) to afford the product as white solid. (2.72 g, 42%). m.p. 72-74 °C. **^{1}H NMR** (500 MHz, CDCl$_3$) δ 6.73 (s, 1H), 5.76 (dt *J* = 15.2, 7.6 Hz, 2H), 5.53 (dt *J* = 15.2, 7.6 Hz, 2H), 4.25 (qd *J* = 7.2, 1.1 Hz, 4H), 3.87 (d, *J* = 7.5 Hz, 2H), 3.09 (d, *J* = 7.5 Hz. 2H), 2.03 (s, 3H), 1.26 (t, *J* = 7.1 Hz, 3H). Spectral data matched the literature data.

(±)-Diethyl 2-acetamido-2-[(2*E*)-4-(1,3-dioxo-2,3-dihydro-1*H*-isoindol-2-yl)but-2-en-1-yl]- propanedioate

15
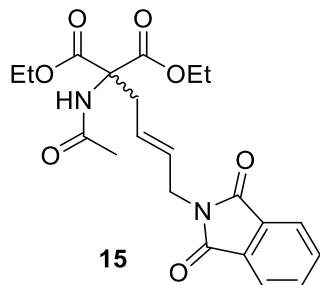
To a solution of **14** (2.72 g, 7.77 mmol) in dry DMF (15 mL), potassium phthalimide (4.31 g, 23.3 mmol) was added in one portion. The resulting mixture was vigorously stirred for 16 h at 90 °C. The reaction mixture was cooled to room temperature and DMF was removed under

reduced pressure. The residue was suspended in water (50 mL) and extracted with EtOAc (3×20 mL). The combined organic layers were washed with water, brine and dried over Na_2SO_4. The solvent was removed under reduced pressure to yield crude product which was purified by flash column chromatography (50% EtOAc in hexanes) to obtain the pure compound as white solid (1.52 g, 47% yield). m.p. 130-132 °C. **^{1}H NMR** (500 MHz, CDCl$_3$) δ 7.82 (dd, J = 5.4, 3Hz, 4H), 7.70 (dd, J = 5.4, 3Hz, 4H), 6.72 (s, 2H), 5.59-5.44 (m, 2H), 3.02 (d, J = 6.7 Hz, 2H), 4.19 (q, J = 7.1 Hz. 6H), 1.98 (s, 3H), 1.20 (t, J = 7.1 Hz). **^{13}C NMR** (125 MHz, CDCl$_3$) δ 169.1, 167.8, 167.5, 134.1, 132.1, 128.7, 127.7, 123.3, 66.1, 62.6, 39.3, 35.4, 23.0. HRMS m/z calcd [M+Na]$^+$ calcd C$_{21}$H$_{24}$N$_2$O$_7$Na 439.1481 observed 439.1472.

(±)-(*4E*)-2,6-diaminohex-4-enoic acid

16
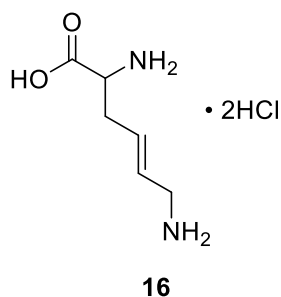
Aqueous HCl (5 M, 10 mL) was added to solid compound **15 (**1.5 g, 3.60 mmol). The resulting mixture was stirred and refluxed for 24 h. The reaction mixture was cooled to room temperature and evaporated under reduced pressure to yield crude solid product which was purified by ion exchange chromatography using Dowex AG 50W X2 (acidic form). The crude was loaded on the column as an aqueous solution. The column was washed with water (5 mL) followed by elution with 3 mL each of 1, 2, 3, and 4M HCl solution. The compound was eluted in 2M HCl and obtained as a pale yellow solid after evaporation. (0.69 g, 89%). **^{1}H NMR** (500 MHz, D$_2$O) δ 5.91-5.82 (m, 2H), 4.17 (t, J = 6.5 Hz, 1H), 2.83-2.71 (m, 2H), 5.91-5.82 (m, 2H). **^{13}C NMR** (125 MHz, CDCl$_3$) δ 171.4, 129.7, 127.2, 52.3, 40.6, 32.6. HRMS m/z calcd for C$_6$H$_{13}$N$_2$O$_2$ [M+H]$^+$ calcd 145.0972, observed 145.0977.

(±)-Diethyl 2-acetamido-2-(prop-2-yn-1-yl) propanedioate
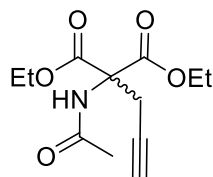
17

The reaction was carried out using the procedure described previously,[67,75] with some modifications. To a stirring solution of DEAM (500 mg, 2.30 mmol) in dry acetonitrile (20 mL), cesium carbonate (1.50 g, 4.60 mmol) was added in one portion. The resulting slurry was stirred at room temperature for 30 min. Propargyl bromide (80% solution in toluene, 0.51 mL, 3.4 mmol) was then added and the mixture was stirred at 50 °C for 16 h. The reaction mixture was cooled and the acetonitrile was evaporated under reduced pressure. The residue was suspended in water, and extracted with ethyl acetate (3 × 20 mL). The combined organic layer was washed with water, brine and then dried over Na_2SO_4. Solvent was removed under vacuum to obtain the crude which was purified by FCC (40% EtOAc in hexanes). The pure product was obtained as white solid compound (0.52 g, 88%). m.p. 92-94 °C. **^{1}H NMR** (500 MHz, CDCl$_3$) δ 6.94 (s, 1H), 4.27-4.20 (m, 4H), 3.24 (d, J = 2.5Hz, 2H), 2.04 (s, 3H), 1.95 (t, J = 3 Hz, 1H), 1.23 (t, J = 7.1 Hz, 6H). **^{13}C NMR** (125 MHz, CDCl$_3$) δ169.3, 166.7, 78.3, 71.4, 65.3, 63.02, 23.8, 22.9, 14.0.

## (±)-Diethyl -2-acetamido-2-[(1-benzyl-1*H*-1,2,3-triazol-4-yl)methyl]- propanedioate
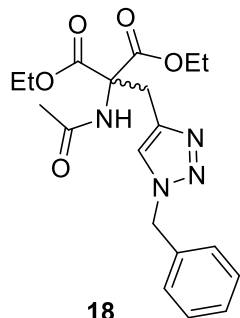
18

To a solution of **17** (0.52 g, 2.0 mmol) in EtOH (5.0 mL), a 2.5 M aqueous solution of CuSO$_4$ (0.046 mL, 0.115 mmol), followed by sodium ascorbate (0.23 g, 1.1 mmol) solution (2.5 mL) was added so that the ethanol:water ratio was 2:1. Benzyl azide (0.52 mL, 4.1 mmol) was then added and the resulting biphasic reaction mixture was stirred vigorously for 24 h. EtOH was then removed under reduced pressure. The residue was diluted with water and extracted with ethyl acetate (3 × 20 mL). The organic extracts were combined, washed with brine and dried over

Na$_2$SO$_4$. Solvent was removed by rotary evaporation to give a crude oily product which was purified by FCC (60% EtOAc in hexanes) to obtain pure compound as white solid. (0.44 g, 56%). m.p. 74-76 °C. **^{1}H NMR** (500 MHz, CDCl$_3$) δ 7.37-7.30 (m, 3H), 7.22-7.16 (m, 3H), 6.69 (s, 1H), 5.45 (2H, s) 4.23 (q, *J* = 7.1 Hz, 4H), 3.72 (s, 2H), 1.90 (s, 3H), 1.22 (t, *J* = 7 Hz, 6H).**^{13}C NMR** (125 MHz, CDCl$_3$) 169.2, 167.4, 142.4, 134.8, 129.2, 128.8, 128.0, 122.9, 66.1, 62.9, 54.1, 29.1, 23.0, 14.0. HRMS m/z calcd for C$_{19}$H$_{25}$N$_4$O$_5$ [M+H]$^+$ calcd 389.1780, observed 389.1810.

1,3-Diethyl 2-acetamido-2-(1*H*-1,2,3-triazol-4-ylmethyl) propanedioate
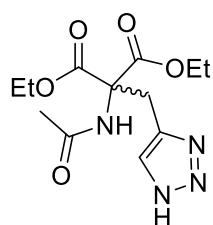
19

To a solution of **18** (440 mg, 1.13 mmol) in ethyl acetate (2.0 mL) in a hydrogenation flask, 10% Pd/C (44 mg, 10% by wt. of **18**) was added followed by methanol (5.0 mL). After two vacuum/H$_2$ cycles to replace air inside the flask with H$_2$, the reaction mixture was vigorously stirred at room temperature under 60 psi for 24 h. The reaction mixture was then filtered through a bed of Celite®. The filtrate was collected and solvent was removed under reduced pressure to obtain **23** as colorless solid, (0.31 g, 92 %). **^{1}H NMR** (500 MHz, MeOD) δ 7.54 (s, 1H), 4.23 (m, 4H), 3.72 (s, 2H), 2.02 (s, 3H), 1.24 (t, *J* = 7.1 Hz, 6H). **^{13}C NMR** (125 MHz, MeOD) δ 172.8, 168.3, 67.8, 63.70, 29.6, 22.30, 14.3. HRMS m/z calcd for C$_{12}$H$_{18}$N$_4$O$_5$ [M+H]$^+$ calcd 289.1277, observed 299.1362.

2-amino-3-(1*H*-1,2,3-triazol-4-yl) propanoic acid
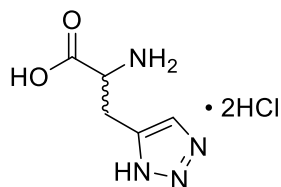
20

Aqueous HCl (5 M, 5 mL) was added to solid compound **19** (80 mg, 0.27 mmol). The resulting mixture was stirred and refluxed for 24 h. The reaction mixture was cooled to room

temperature and evaporated under reduced pressure to yield crude solid product which was purified by ion exchange chromatography using Dowex AG 50W X2 (acidic form). The crude was loaded on the column as an aqueous solution. The column was washed with water (5 mL) followed by elution with 2 mL each of 1, 2, 3, and 4M HCl solution. The compound was eluted in 2M HCl and obtained as a pale yellow solid after evaporation. (45 mg, 89%). **^{1}H NMR** (500 MHz, D_2O) δ 7.91 (s, 1H), 4.30 (t, J = 6 Hz, 1H), 3.35 (dd, J = 6, 2.5 Hz, 2H).**^{13}C NMR** (125 MHz, D_2O) δ 170.5, 138.8, 127.0, 52.2, 24.9. HRMS m/z calcd for $C_5H_9N_4O_2$ [M+H]$^+$ calcd 157.0720, observed 157.0718.

Dimethyl 2,5-dibromohexanedioate

6

Compound **6** was obtained using the procedure reported by Skovpen and Palmer.[59] Neat thionyl chloride was added to adipic acid (20.0 g, 137 mmol) and refluxed under an inert atmosphere at 80 °C for 3 h. Excess thionyl chloride (25 mL, 342 mmol) was removed under reduced pressure to obtain adipoyl chloride (25.0 g, 137 mmol) as a colorless oil. For bromination, the r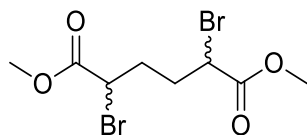eaction set up consisted of a 2-neck 1 L round bottom flask equipped with a reflux condenser and a dropping funnel. The assembly was placed in an oil bath on an electronic stirrer and charged with adipoyl chloride. Effluent from the condenser was vented into a beaker with 250 mL 10% sodium thiosulphate solution to trap the bromine gas. Additionally, a 500W lamp was placed close to the reaction flask. The lamp was turned on and the assembly was heated to 80 °C. To the adipoyl chloride, neat bromine (17.6 mL, 342 mmol) was added using the dropping funnel very slowly, over a period of 3 hours. The bromination reaction was monitored by NMR and additional bromine was added if required. After the reaction was complete (7-8 h) the excess bromine was removed by purging with a stream of nitrogen into the flask, and the crude product was added dropwise to cold methanol (140 mL) on ice. The resulting suspension was left stirring for 14 h at room temperature. The product was then filtered. The filtrate was concentrated under reduced pressure and purified by FCC (15% ethyl acetate in hexanes) to give more product. Yield 43.03 g 46%. **^{1}H**

NMR (500 MHz, CDCl$_3$) δ 4.24 (s, 1H), 3.78 (s, 3H), 2.34-1.95 (m, 2H). Spectral data matched with the literature data.

Dimethyl 2,5-bis(1,3-dioxo-2,3-dihydro-1*H*-isoindol-2-yl)hexanedioate

7
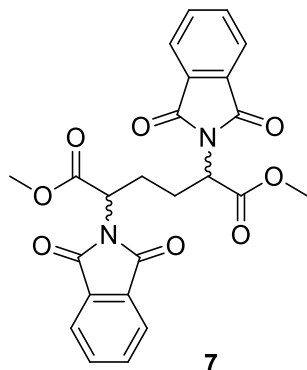
The mixture of stereoisomers of **7** was obtained using a reported method.[58] To a stirring solution of **6** (43.03 g, 129.6 mmol), in dry DMF (150 mL), potassium phthalimide (120 g, 648 mmol) was added in one portion. The mixture was heated to 90 °C and the reaction continued for 2h. The cooled reaction mixture was then diluted with chloroform and the resulting solution was poured into water. The chloroform layers were combined, and the solvent was removed *in vacuo* to the point of crystallization followed by addition of diethyl ether to promote rapid crystallization. The solid product was filtered, washed with diethyl ether and dried to obtain white solid. FCC (30% ethyl acetate in hexanes) afforded the title compound as white solid, (45g, 53%). **¹H NMR** (500 MHz, CDCl$_3$) δ 7.91-7.85 (m, 4H), 7.89-7.74 (m, 4H), 4.81(t, *J* = 5.0 Hz, 2H), 3.66 (s, 6H), 2.39-2.29 (m, 2H), 2.29-2.19 (m, 2H). Spectral data matched with the literature data.

2,5-Diaminohexanedioic acid
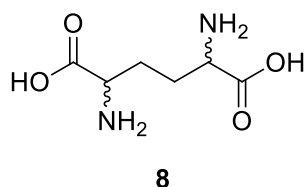
8

The reaction was performed according to the procedure reported by Skovpen and Palmer.[59] To the mixture of stereoisomers of **7** (20.0 g, 43.1 mmol), a 1:1 mixture (100 mL) of 48% aqueous HBr and glacial acetic acid was added and the mixture was refluxed at 115 °C while stirring. The

hydrolysis was complete after 25 days. (The reaction mixture becomes clear). The reaction mixture was cooled and filtered to remove phthalic acid and filtrate was evaporated *in vacuo*. The residue was dissolved in water, filtered and neutralized with saturated ammonium hydroxide solution. The resulting white precipitate was filtered and dried. The product was isolated as a mixture of stereoisomers (7.66 g, 89% yield). **^{1}H NMR** (500 MHz, CD$_3$OD) δ 4.06 (d, J = 2.2Hz, 2H), 2.30-2.00 (m, 4H). Spectral data matched with the literature data.

Dimethyl 2,5-diaminohexanedioate dihydrochloride

9
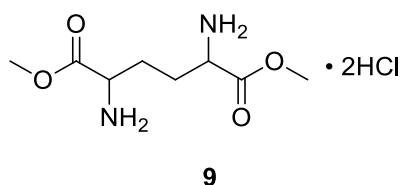
The reaction was performed according to the procedure reported by Skovpen and Palmer.[59] A round bottom flask was charged with methanol (120 mL) and cooled on ice under nitrogen. Acetyl chloride (15.4 mL, 216 mmol) was added dropwise over a period of 10 min. The solid compound **8** (6.35 g, 36.0 mmol) was added rapidly and the resulting suspension was heated to reflux. After 2 h, the mixture was cooled and the solvent was evaporated *in vacuo* to obtain a white crystalline product as the dihydrochloride salt (9.89 g, 99%) The product was used without further purification. **^{1}H NMR** (500 MHz, CD$_3$OD) δ 4.18-4.15 (m, 2H), 3.87 s, 6H, 2.23-1.96 (m, 4H). Spectral data matched the literature data.

Dimethyl 2,5 bis([(tertbutoxy)carbonyl]amino)hexanedioate

10
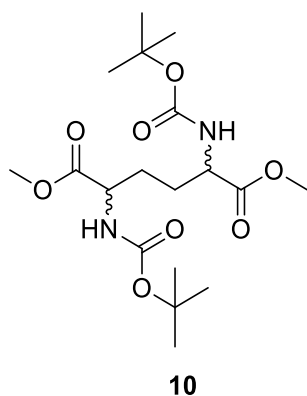
The protection of the amino groups was carried out using the reported procedure by Skovpen and Palmer.[59] To a suspension of **9** (4.82 g, 17.4 mmol) in THF (50 mL) placed an in ice

bath, trimethylamine (7.33 mL, 52.2 mmol), was added dropwise under N_2 atmosphere. A solution of di-*tert*-butyl dicarbonate (11.4 g, 52.2 mmol) in THF (20 mL) was then added to the reaction mixture over a period of 1 h. The reaction was warmed to room temperature and stirred for 16 h after which the temperature was raised to 50 ºC and maintained for 3 hours. The reaction mixture was then allowed to cool and the solvent was removed under reduced pressure. The resulting suspension was partitioned between ethyl acetate (30 mL) and saturated sodium bicarbonate (60 mL) solution. The organic layer collected and the extraction was repeated twice with ethyl acetate (30 mL). The combined organic layers dried over sodium sulfate and concentrated *in vacuo*. The resulting sticky residue was stirred in diethyl ether (50 mL) for 1 h in ice-water bath to induce crystallization. The white solid obtained was filtered under vacuum and dried. The filtrate was collected and after concentrating *in vacuo*, was subjected to flash column chromatography (30% ethyl acetate in hexanes) to obtain the remaining compound. The total yield was 5.31g, 75%. **¹H NMR** (500 MHz, CDCl₃) δ 5.08 (br s, 2H), 4.30 (br m, 2H), 3.73 (s, 6H), 1.92-1.82 (m, 2H), 1.73-1.65 (m, 2H), 1.44 (s, 18H). Spectral data matched the literature data.
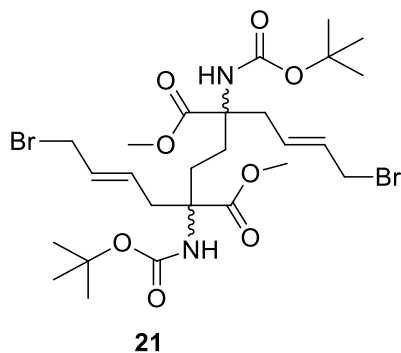
(±)-Dimethyl 2,5 bis([(tertbutoxy)carbonyl]amino)-2,5-bis[(2*E*)-4-bromobut-2-en-1-yl]-hexanedioate

21

To a dry round bottom flask charged with THF (20 mL), freshly distilled diisopropylamine (1.50 mL, 10.7 mmol) was added under nitrogen atmosphere. The solution was cooled to –78 °C and *n*-butyllithium, 2.35 M solution in hexanes (4.3 mL, 10.0 mmol) was added dropwise. The reaction was warmed to 0 °C and stirred at the same temperature for 20 min. The reaction mixture was again cooled to –78 °C and a solution of **10** (0.900 g, 2.22 mmol) in THF (5 mL) was added dropwise over a period of 15 min under nitrogen atmosphere and stirred at the same temperature for 1 h. A solution of (2*E*)-1,4-dibromo-2-butene (2.37 g, 11.1 mmol) in THF was then added

dropwise to the reaction and it was stirred for 2 h maintaining the temperature at –78 °C. The cooling was then removed and the reaction was quenched by adding saturated ammonium chloride solution (20 mL). The aqueous layer was extracted with ethyl acetate (4 × 20 mL). The combined organic layers were washed with water, then brine and dried over solid Na_2SO_4. The solvent was then removed under reduced pressure to get crude product which was purified by FCC (15% ethyl acetate in hexane) and two diastereomers **21A** (22 mg, 1.5% yield) and **21B** (0.15 g, 9.3% yield) were isolated as white crystalline solid (**21A**) and sticky solid (**21B**). Compound **21B** was obtained as a crystalline solid after standing in hexanes for 3 days. It was carried forward for the next step and later confirmed as a racemic mixture by HPLC. The formation of racemic mixture as the major product was in agreement with the previously reported reaction in the synthesis of bislysine.[59] **(A)** m.p. 125-126 °C. **^{1}H NMR** (500 MHz, CDCl$_3$) 5.59-5.48 (m, 3H), 5.70 (dt, J = 15, 7.5 Hz, 2H), 3.91-3.83 (m, 4H), 3.75 (s, 6H), 3.13-2.99 (m, 2H), 2.43 (dd, J = 13.6, 7.4 Hz, 2H), 1.70 (d, J = 8.75 Hz, 2H), 1.44 (s, 18H). **^{13}C NMR** (125 MHz, CDCl$_3$) δ 173.1, 153.6, 130.6, 129.5, 63.3, 52.9, 38.1, 32.4, 30.0, 28.3. **(B)** m.p. 132-134 °C. **^{1}H NMR** (500 MHz, CDCl$_3$) δ 5.73 (dt, J = 15, 7.5 Hz, 2H), 5.54 (dt, J = 15, 7.5 Hz, 2H), 5.39 (br s, 2H), 3.87 (d, J = 5 Hz, 4H) 3.75 (s, 6H), 2.94 (br s, 2H), 2.51 (dd, J = 10, 5 Hz, 2H), 2.21 (s, 2H), 1.55-1.50 (m, 2H), 1.43 (s, 18H). **^{13}C NMR** (125 MHz, CDCl$_3$) δ 173.3, 154.0, 130.9, 129.4, 79.6, 62.86, 52.8, 38.0, 32.4, 29.6, 28.4. HRMS m/z calcd for $C_{26}H_{42}Br_2N_2O_8Na$ [M+Na]$^+$ 693.1185 observed 693.1144

 (±)-Dimethyl ({[(*tert*-butoxy)carbonyl]amino})-2,5-bis[(2E)-4-(1,3-dioxo-2,3-dihydro-1H-isoindol-2-yl)but-2-en-1-yl]hexanedioate
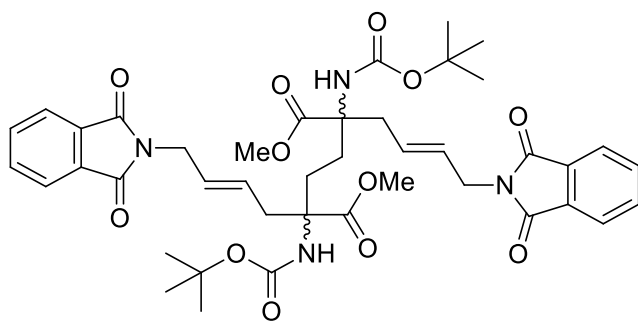
22

To a solution of racemic **21B** (0.060 g, 0.074 mmol) in dry DMF (5 mL), solid potassium phthalimide (0.033 g 0.22 mmol) was added in one portion at room temperature. The reaction

mixture was heated to 100 °C and stirred for 3 h. It was then cooled to room temperature and DMF was evaporated under reduced pressure. The residue was suspended in water (10 mL) and extracted with ethyl acetate (5 mL × 3). The combined organic layers were washed with water, then brine, and then dried over Na_2SO_4. The solvent was then removed under vacuum to yield crude product which was purified by FCC (60% ethyl acetate in hexanes) to get a colorless sticky solid (0.042 mg, 70% yield). **^{1}H NMR** (500 MHz, $CDCl_3$) δ 7.82 (dd, $J = 5.5$, 3Hz, 4H), 7.69 (dd $J = 5.5$, 3Hz, 4H), 5.58- 5.46 (m, 4H), 5.31 (br s, 2H), 2.50-2.39 (m, 2H), 2.13 (br s, 2H), 1.54-1.44 (m, 2H), 1.35 (m, 18H) **^{13}C NMR** (125 MHz, $CDCl_3$) δ 173.5, 168.0, 154.1, 134.1, 132.3, 128.9, 128.1, 123.4, 79.5, 62.8, 52.8, 39.6, 38.1, 29.9, 28.4. HRMS m/z calcd for $C_{42}H_{51}N_4O_{12}$ $[M+H]^+$ 803.3497, found 803.3503.

(±)-2,5-Diamino-2,5-bis[(2*E*)-4-aminobut-2-en-1-yl]hexanedioic acid tetrahydrochloride
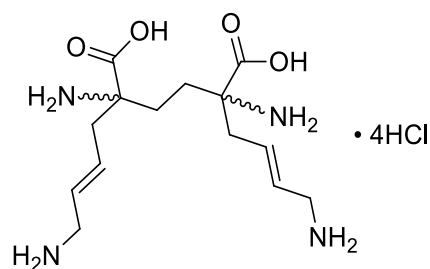
23

To compound **22** (0.030 g, 0.037 mmol) in a round bottom flask, 5M HCl (2 mL) was added and the resulting mixture was stirred and refluxed for 24 h. The reaction mixture was cooled to room temperature and evaporated to dryness under reduced pressure to yield a brownish residue which was purified by ion exchange chromatography using Dowex AG 50W X2. The product was eluted in 4 M HCl and obtained as a colorless solid after evaporation of the fractions (6 mg, 35% yield). **^{1}H NMR** (500 MHz, D_2O) δ 5.90- 5.80 (m, 4H), 3.63 (d, $J = 5.0$ Hz, 4H), 2.81 (dd, $J = 14$, 6 Hz, 2H), 2.67 (dd, $J = 14$, 6 Hz, 2H), 2.13-2.04 (m, 2H), 2.02-1.92 (m, 2H). **^{13}C NMR** (500 MHz, D_2O) δ 172.8, 128.8, 128.4, 63.1, 40.64, 38.0, 29.6. HRMS m/z calcd for $C_{14}H_{26}N_4O_4$ $[M+H]^+$ 315.1988, found 315.2026.

Dimethyl 2,5-bis({[(*tert*-butoxy)carbonyl]amino})-2,5-bis[(4-nitrophenyl)methyl] hexanedioate
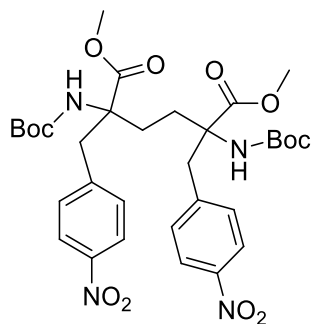
24

      To a dry round bottom flask charged with THF (10 mL), freshly distilled diisopropylamine (0.41 mL, 2.97 mmol) was added under nitrogen atmosphere. The solution was cooled to –78 °C and a freshly titrated *n*-butyllithium solution in hexanes (1.18 mL, 2.78 mmol) was added dropwise over a period of 10 min. The reaction was warmed to 0 °C and stirred at the same temperature for 20 min. The reaction mixture was again cooled to –78 °C and a solution of **10** (0.25 g, 0.62 mmol) in THF (3 mL) was added dropwise over a period of 10 min under nitrogen atmosphere. A solution of 4-nitrobenzyl bromide in THF was then added dropwise to the reaction and it was stirred for 2 hours maintaining the temperature at –78 °C. The cooling was then removed and the reaction was quenched by adding saturated NH₄Cl solution (10 mL) and extracted with ethyl acetate (10 mL × 3). The combined organic layers were washed with water, brine and dried over solid Na₂SO₄. The solvent was then removed under reduced pressure to get crude product which was purified by FCC (15% EtOAc in hexanes) twice to obtain product with ~70% purity as estimated by NMR (25 mg, 1.5%). This product was carried forward without further characterization.

Dimethyl 2,5-bis[(4-nitrophenyl)methyl]-2,5-bis({[(*tert*-butoxy)carbonyl]amino}) hexanedioate
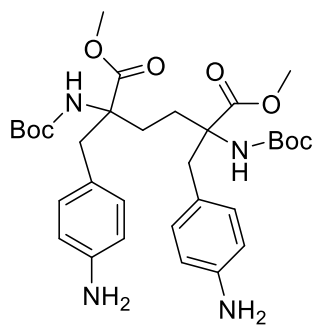
25

To a solution of **24** (0.025 g, 0.037 mmol) in ethyl acetate (2 mL) in a hydrogenation flask, 10% Pd/C (0.003 g, 10% by wt. of **24**) was added followed by methanol (2 mL). After two vacuum/H_2 cycles to replace air inside the flask with H_2, the reaction mixture was vigorously stirred at room temperature under 60 psi for 3 h. The reaction mixture was then filtered through a bed of Celite®. The filtrate was collected and solvent was removed under reduced pressure to obtain **25** as sticky yellowish solid (5 mg, 32%).**^{1}H NMR** (500 MHz, MeOD) δ 6.78 (d, J = 8 Hz, 4H), 6.56 (d, J = 8.5 Hz, 4H), 5.42 (s, 2H), 3.77 (s, 6H), 3.59 (br s, 3H), 3.46 (d, J = 14.1 Hz, 2H), 2.91 (d, J = 13.8 Hz, 2H), 2.74 (s, 1H), 2.12-2.16 (m, 2H), 1.87-1.80 (m, 2H), 1.48 (s, 18H). **^{13}C NMR** (125 MHz, MeOD) δ 173.43, 153.83, 145.13, 130.5, 129.4, 126.5, 79.0, 65.1, 40.4, 37.6, 30.5, 28.6. HRMS m/z calcd for $C_{32}H_{46}N_4O_8Na$ [M+Na]$^+$ 615.3349, found 615.3391.

2,5-diamino-2,5-bis[(4-aminophenyl)methyl] hexanedioic acid tetrahydrochloride
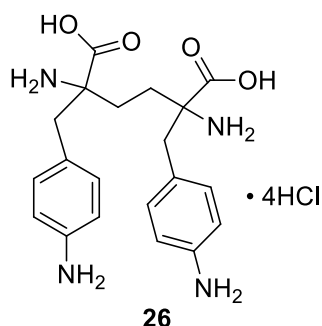
To compound **25** (0.005 mg, 0.008 mmol) in a round bottom flask, 5M HCl (2 mL) was added and the resulting mixture was stirred and refluxed for 24 h. The reaction mixture was cooled to room temperature and evaporated to dryness under reduced pressure to yield crude solid product which was purified by ion exchange chromatography using Dowex AG 50W X2 (acid form). The column was eluted with one mL each of 1, 2, 3, 4 and 5M HCl solution. Each fraction (0.50 mL) was evaporated to dryness to record ^{1}H NMR. The product was detected in 4 M HCl. The fractions containing the product were combined and evaporated to dryness to obtain a colorless solid. (2.7 mg, 63% yield). **^{1}H NMR** (500 MHz, D_2O) δ 7.34 (s, 8H), 3.81(d, J = 3.05, 1H), 3.41 (d, 2H, J = 14.5 Hz), 3.11(d, J = 14.5 Hz, 2H), 2.31(m, 2H), 1.88-1.83(m, 2H).**^{13}C NMR** (125 MHz, D_2O) δ 173.2, 134.2, 131.64, 129.6, 123.5, 64.8, 41.4, 30.3. HRMS m/z calcd for $C_{20}H_{27}N_4O_4$ [M+H]$^+$ 387.1998, found 387.2024.

70

(±)-Dimethyl ({[(*tert*-butoxy)carbonyl]amino})-2,5-bis[(prop-2-yn-1-yl]hexanedioate
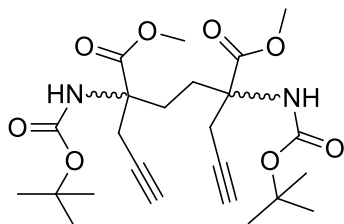
27

To a dry round bottom flask charged with THF (15 mL), freshly distilled diisopropylamine (1.00 mL, 7.12 mmol) was added under nitrogen atmosphere. The solution was cooled to –78 °C and *n*-butyllithium, 2.25 M solution in hexanes (2.96 mL, 6.673 mmol) was added dropwise. The reaction was warmed to 0 °C and stirred at the same temperature for 20 min. The reaction mixture was again cooled to –78 °C and a solution of **10** (0.600 g, 1.48 mmol) in THF (4 mL) was added dropwise over a period of 10 min under nitrogen atmosphere and stirred at the same temperature for 45 min. Propargyl bromide solution (5.9 mmol, 0.88 mL, 80% in toluene) was then added dropwise to the reaction and it was stirred for 2 hours maintaining the temperature at –78 °C. The cooling was then removed and the reaction was quenched by adding saturated NH$_4$Cl solution (15 mL). THF was then removed under vacuum and the aqueous layer was extracted thrice with ethyl acetate (15 mL × 4). The combined organic layers were washed with water, then brine, and dried over solid Na$_2$SO$_4$. The solvent was then removed under reduced pressure to obtain crude product which was purified by FCC (15% EtOAc in hexanes). Two diastereomers were isolated as white solids **27A,** (67 mg, 9%). **m.p.** 171-173 °C and **27B** (0.161 g, 23%). **m.p.** 139-140 °C. **^{1}H NMR** (500 MHz, CDCl$_3$) δ 5.60 (br s, 2H), 3.76 (s, 6H), 3.16 (d, *J* = 16.3 Hz, 2H), 2.69 (d, 16.8 Hz, 2H), 2.12-2.01 (m, 2H), 1.95 (s, 2H), 1.74 (d, *J* = 9.1 Hz, 2H), 1.49 (s, 18H). **(B)**. **^{1}H NMR** (500 MHz, CDCl$_3$) δ 5.49 (s, 2H), 3.76 (s, 6H), 3.03 (br d, *J* = 15.5 Hz, 2H), 2.82 (d, *J* = 17 Hz), 2.18 (br s, 2H), 1.96 (s, 2H), 1.63-1.55 (m, 2H), 1.43 (s, 18H). **^{13}C NMR** (125 MHz, CDCl$_3$) δ 172.5, 154.2, 80.0, 79.2, 71.1, 61.7, 53.1, 29.1, 28.4, 25.9. HRMS m/z calcd for C$_{24}$H$_{37}$N$_2$O$_8$ [M+H]$^+$ 481.2544, observed 481.2553.

(±)-Dimethyl ({[(*tert*-butoxy)carbonyl]amino})-2,5-bis[(1benzyl-1*H*-1,2,3-triazol-4-yl)methyl]hexanedioate
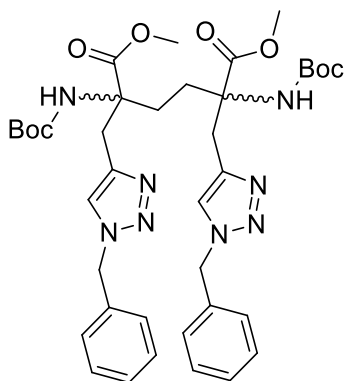
28

To a solution of **27B** (0.140 g, 0.291 mmol) in EtOH (5 mL), a 0.25 M aqueous solution of CuSO$_4$ (0.058 mL, 0.014 mmol) followed by sodium ascorbate (0.29 g, 0.14 mmol) solution (2.5 mL) was added. Neat benzyl azide (0.12 mL, 0.87 mmol) was then added and the resulting biphasic reaction mixture was stirred vigorously for 36 h at room temperature. EtOH was then removed under reduced pressure. The residue was diluted with water and extracted with ethyl acetate (3 × 20 mL). The organic extracts were combined, washed with brine, and dried over Na$_2$SO$_4$. Solvent was removed to get crude oily product which was purified by FCC (60% EtOAc in hexanes) to obtain pure compound as a colorless solid (0.13 g, 62%). **m.p.** 150-151°C. **^{1}H NMR** (500 MHz, CDCl$_3$) 7.39-7.30 (m, 6H), 7.25-7.20 (m, 4H), 7.13 (s, 2H), 5.49-5.40 (m, 6H), 3.75 (s, 6H), 3.55 (d, *J* = 15 Hz, 2H), 3.24 (d, *J* = 15 Hz, 2H), 2.30-2.19 (m, 2H), 1.30 (s, 18H).**^{13}C NMR** (125 MHz, CDCl$_3$) δ 173.0, 153.8, 143.0, 134.6, 129.0, 128.6, 128.0, 122.6, 79.2, 62.6, 53.9, 52.8, 31.3, 30.1, 28.2. HRMS m/z calcd for C$_{38}$H$_{50}$N$_8$O$_8$Na [M+ Na]$^+$ 769.3649, observed 769.3643.
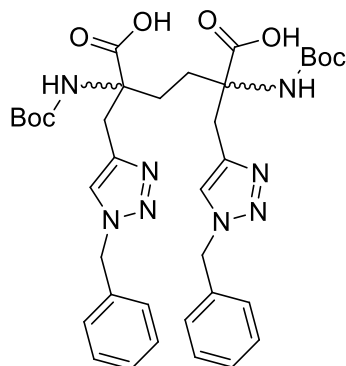
(±)-({[(*tert*-Butoxy)carbonyl]amino})-2,5-bis[(1benzyl-1*H*-1,2,3-triazol-4-yl)methyl]hexanedioic acid

29

To a solution of **28** (0.125 g, 0.167 mmol), in methanol (5 mL), solid LiOH·H$_2$O (0.028 g, 0.67 mmol) was added in one portion at room temperature. The reaction was warmed to 40 °C and stirred for 4 h, after which methanol was removed under vacuum. The residue was diluted with water, acidified with 5% citric acid solution and extracted with EtOAc (10 mL × 3). The organic extracts were combined, washed with brine and dried over Na$_2$SO$_4$. Solvent was removed to get crude oily product which was purified by FCC (4% MeOH/DCM) to obtain pure compound as colorless solid (0.13 g, 62%). The resulting white solid was used for the next step without further purification (0.092 g, 0.128 mmol, 72%). **^{1}H NMR** (500 MHz, CDCl$_3$) δ 7.37-7.28 (m, 6H), 7.23-7.12 (m, 6H), 5.66 (br s, 1H), 5.49-5.37 (m, 4H), 3.74 (br s, 1H), 3.68-3.56 (m, 2H), 3.79-3.25 (m, 2H), 2.49- 2.26 (m, 2H), 1.80 (t, *J* = 12 Hz, 1H), 1.36-1.17 (m, 18H) HRMS m/z calcd for C$_{36}$H$_{45}$N$_8$O$_8$ [M-1]$^-$ 717.3366, observed 717.3439.
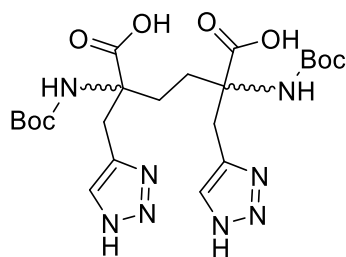
(±)-({[(*tert*-Butoxy)carbonyl]amino})-2,5-bis[(1*H*-1,2,3-triazol-4-yl)methyl]hexanedioic acid

30

To a solution of **29** (0.090 g, 0.12 mmol) in ethyl acetate (2.0 mL) in a hydrogenation flask, 10 % Pd(OH)$_2$ 0.009 g, 10% by wt. of **29**) was added followed by methanol (5.0 mL). After two vacuum/H$_2$ cycles to replace air inside the flask with H$_2$, the reaction mixture was vigorously stirred at room temperature under 60 psi for 8 hours. The reaction mixture was then filtered through a bed of Celite®. The filtrate was collected and solvent was removed under reduced pressure to obtain pale white amorphous solid (0.060 g, 89%).The compound was used for the next step without further purification. **^{1}H NMR** (500 MHz, MeOD) δ 7.47 (s, 2H), 3.49 (d, J = 14.9 Hz, 2H), 3.39 (d, J =14.9 Hz, 2H), 2.19-2.07 (m, 2H), 1.44 (s, 18H). HRMS m/z calcd for C$_{22}$H$_{33}$N$_8$O$_8$ [M-1]$^-$ 537.2426 observed 537.2427

(±)-2,5-Diamino-2,5-bis[(1H-1,2,3-triazol-4-yl)methyl] hexanedioic acid tetrahydrochloride
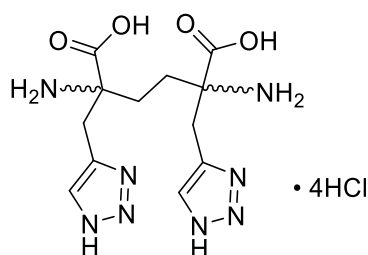
31

A mixture of compound **30** (0.060 g, 0.11 mmol) in DCM (2.0 mL) was cooled to 0 °C. Trifluoroacetic acid (2.0 mL) was then added dropwise and the resulting solution was warmed to room temperature. After 15 min, the reaction mixture was evaporated to dryness under reduced pressure to yield crude solid product which was purified by ion exchange chromatography using Dowex AG 50W X2 and eluting in 4 M HCl. The fractions containing the product were evaporated to dryness to get a colorless solid (0.027 g, 77% yield). **^{1}H NMR** (500 MHz, D$_2$O) δ 7.81 (d, J = 12 Hz, 1H), 3.75 (s, 1H), 3.48-3.43 (m, 2H), 3.35-3.30 (m, 2H), 2.18-1.95 (m, 4H). **^{13}C NMR** (125 MHz, D$_2$O) δ 171.3, 169.9, 138.1, 127.4, 62.5, 62.3, 54.1, 30.3, 29.1. HRMS m/z calcd for C$_{12}$H$_{17}$N$_8$O$_4$ [M-1]$^-$ 337.1378, observed 336.1363.

6 REFERENCES

(1) Stanton, T. B. (2013) A call for antibiotic alternatives research. *Trends Microbiol. 21*, 111–113.

(2) Walsh, C. (2000) Molecular mechanisms that confer antibacterial drug resistance. *Nature 406*, 775–781.

(3) World Health Organization. (2014) *Antimicrobial resistance: global report on surveillance.*Geneva, Switzerland.

(4) Lewis, K. (2013) Platforms for antibiotic discovery. *Nat. Rev. Drug Discov. 12*, 371–387.

(5) Kohanski, M. A., Dwyer, D. J., and Collins, J. J. (2010) How antibiotics kill bacteria: from targets to networks. *Nat. Rev. Microbiol. 8*, 423–435.

(6) Hutton, C. A., Southwood, T. J., and Turner, J. J. (2003) Inhibitors of lysine biosynthesis as antibacterial agents. *Mini Rev. Med. Chem. 3*, 115–127.

(7) Izaki, K., Matsuhashi, M., Strominger, J. (1968) Biosynthesis of the peptidoglycan of bacterial cell walls. *J. Biol. Chem. 243*, 3180–3196.

(8) Walsh, C. (2003) *Antibiotics: actions, origins, resistance* 1st ed. ASM Press, Washington D.C.

(9) Bugg, T. D., and Walsh, C. T. (1992) Intracellular steps of bacterial cell wall peptidoglycan biosynthesis: enzymology, antibiotics, and antibiotic resistance. *Nat. Prod. Rep. 9*, 199–215.

(10) Heijenoort, J. van. (2001) Formation of the glycan chains in the synthesis of bacterial peptidoglycan. *Glycobiology 11*, 25R–36R.

(11) Bouhss, A., Trunkfield, A. E., Bugg, T. D. H., and Mengin-Lecreulx, D. (2008) The biosynthesis of peptidoglycan lipid-linked intermediates. *FEMS Microbiol. Rev. 32*, 208–233.

(12) Bugg, T. D., and Brandish, P. E. (1994) From peptidoglycan to glycoproteins: common features of lipid-linked oligosaccharide biosynthesis. *FEMS Microbiol. Lett. 119*, 255–62.

(13) Jordan, S., Hutchings, M. I., and Mascher, T. (2008) Cell envelope stress response in Gram-positive bacteria. *FEMS Microbiol. Rev. 32*, 107–146.

(14) Waxman, D. J., and Strominger, J. L. (1983) Penicillin-binding proteins and the mechanism of action of beta-lactams antibiotics. *Annu Rev Biochem 52*, 825–869.

(15) Strynadka, N. C. J., Adachi, H., Jensen, S. E., Johns, K., Sielecki, A., Betzel, C., Sutoh, K., and James, M. N. G. (1992) Molecular structure of the acyl-enzyme intermediate in beta-lactam hydrolysis at 1.7 A resolution. *Nature 359*, 700–705.

(16) Bayles, K. W. (2000) The bactericidal action of penicillin: new clues to an unsolved mystery. *Trends Microbiol. 8*, 274–8.

(17) Reynolds, P. E. (1989) Structure, biochemistry and mechanism of action of glycopeptide antibiotics. *Eur. J. Clin. Microbiol. Infect. Dis. 8*, 943–950.

(18) Williams, D. H., and Bardsley, B. (1999) The vancomycin group of antibiotics and the fight against resistant bacteria. *Angew. Chem. Int. Ed. 38*, 1172–1193.

(19) Deresinski, S. (2007) Counterpoint: Vancomycin and *Staphylococcus aureus*--an antibiotic enters obsolescence. *Clin. Infect. Dis. 44*, 1543–8.

(20) Nikolaidis, I., Favini-Stabile, S., and Dessen, A. (2014) Resistance to antibiotics targeted to the bacterial cell wall. *Protein Sci. 23*, 243–259.

(21) Skarzynski, T., Mistry, A., Wonacott, A., Hutchinson, S. E., Kelly, V. A., and Duncan, K. (1996) Structure of UDP-*N*-acetylglucosamine enolpyruvyl transferase, an enzyme essential for the synthesis of bacterial peptidoglycan, complexed with substrate UDP-*N*-acetylglucosamine and the drug fosfomycin. *Structure 4*, 1465–74.

(22) Frère, J. M. (1995) Beta-lactamases and bacterial resistance to antibiotics. *Mol. Microbiol. 16*, 385–395.

(23) Karageorgopoulos, D. E., Wang, R., Yu, X.-H., and Falagas, M. E. (2012) Fosfomycin: evaluation of the published evidence on the emergence of antimicrobial resistance in Gram-negative pathogens. *J. Antimicrob. Chemother. 67*, 255–68.

(24) Takahata, S., Ida, T., Hiraishi, T., Sakakibara, S., Maebashi, K., Terada, S., Muratani, T., Matsumoto, T., Nakahama, C., and Tomono, K. (2010) Molecular mechanisms of fosfomycin resistance in clinical isolates of *Escherichia coli. Int. J. Antimicrob. Agents 35*, 333–7.

(25) Reynolds, P. E., and Courvalin, P. (2005) Vancomycin resistance in enterococci due to synthesis of precursors terminating in D -Alanyl- D -Serine *49*, 20–25.

(26) Cox, R. J., Sutherland, A., and Vederas, J. C. (2000) Bacterial diaminopimelate metabolism as a target for antibiotic design. *Bioorganic Med. Chem. 8*, 843–871.

(27) Yoshida, N.; Izumi, Y.; Tani, I.; Tanaka, S.; Takaishi, K.; Hashimoto, T.; Fukui, K. (1957) Studies on the bacterial cell wall. XII. Studies on the chemical composition of bacterial cell walls and spore membranes. *J. Bacteriol. 74*, 94–100.

(28) Viola, R. E. (2001) The central enzymes of the aspartate family of amino acid biosynthesis. *Acc. Chem. Res. 34*, 339–349.

(29) Yugari, Y., and Gilvarg, C. (1965) The condensation step in diaminopimelate synthesis. *J. Biol. Chem. 240*, 4710–4716.

(30) Farkas, W., and Gilvarg, C. (1965) The reduction step in diaminopimelic acid biosynthesis. *J. Biol. Chem. 240*, 4717–4722.

(31) Fan, C., Clay, M. D., Deyholos, M. K., and Vederas, J. C. (2010) Exploration of inhibitors for diaminopimelate aminotransferase. *Bioorg. Med. Chem. 18*, 2141–51.

(32) Sutherland, A., Caplan, J. F., and Vederas, J. C. (1999) Unsaturated α-aminopimelic acids as potent inhibitors of *meso*-diaminopimelic acid (DAP) D-dehydrogenase. *Chem. Commun.* 555–556.

(33) Bukhari, A., and Taylor, A. (1971) Genetic analysis of diaminopimelic acid-and lysine-requiring mutants of *Escherichia coli*. *J. Bacteriol. 105*, 844–854.

(34) Pavelka, M. S., and Jacobs, W. R. (1996) Biosynthesis of diaminopimelate, the precursor of lysine and a component of peptidoglycan, is an essential function of *Mycobacterium smegmatis. J. Bacteriol. 178*, 6496–507.

(35) Fujimoto, S., and Amako, K. (1990) Guillain-Barré syndrome and *Campylobacter jejuni* infection. *Lancet 335*, 1350.

(36) Kumpaisal, R., Hashimoto, T., and Yamada, Y. (1987) Purification and characterization of dihydrodipicolinate synthase from wheat suspension cultures. *Plant Physiol. 85*, 145–51.

(37) Cornish-Bowden, A. (1979) *Fundamentals of enzyme kinetics.* Portland Press, London.

(38) Dobson, R. C. J., Valegård, K., and Gerrard, J. A. (2004) The crystal structure of three site-directed mutants of *Escherichia coli* dihydrodipicolinate synthase: further evidence for a catalytic triad. *J. Mol. Biol. 338*, 329–39.

(39) Karsten, W. E. (1997) Dihydrodipicolinate synthase from *Escherichia coli:* pH dependent changes in the kinetic mechanism and kinetic mechanism of allosteric inhibition by L-lysine. *Biochemistry 36*, 1730–9.

(40) Blickling, S., Renner, C., Laber, B., Pohlenz, H. D., Holak, T. A., and Huber, R. (1997) Reaction mechanism of *Escherichia coli* dihydrodipicolinate synthase investigated by X-ray crystallography and NMR spectroscopy. *Biochemistry 36*, 24–33.

(41) Conly, C. J. T., Skovpen, Y. V, Li, S., Palmer, D. R. J., and Sanders, D. A. R. (2014) Tyrosine 110 plays a critical role in regulating the allosteric inhibition of *Campylobacter jejuni* dihydrodipicolinate synthase by lysine. *Biochemistry 53*, 7396–7406.

(42) Girish, T. S., Sharma, E., and Gopal, B. (2008) Structural and functional characterization of *Staphylococcus aureus* dihydrodipicolinate synthase. *FEBS Lett. 582*, 2923–2930.

(43) Domigan, L. J., Scally, S. W., Fogg, M. J., Hutton, C. A., Perugini, M. A., Dobson, R. C. J., Muscroft-Taylor, A. C., Gerrard, J. A., and Devenish, S. R. A. (2009) Characterisation of dihydrodipicolinate synthase (DHDPS) from *Bacillus anthracis. Biochim. Biophys. Acta. 1794*, 1510–1516.

(44) Mirwaldt, C., Korndörfer, I., and Huber, R. (1995) The crystal structure of dihydrodipicolinate synthase from *Escherichia coli* at 2.5 A resolution. *J. Mol. Biol. 246*, 227–239.

(45) Evans, G., Schuldt, L., Griffin, M. D. W., Devenish, S. R. A., Grant Pearce, F., Perugini, M. A., Dobson, R. C. J., Jameson, G. B., Weiss, M. S., and Gerrard, J. A. (2011) A tetrameric structure is not essential for activity in dihydrodipicolinate synthase (DHDPS) from *Mycobacterium tuberculosis. Arch. Biochem. Biophys. 512*, 154–159.

(46) Griffin, M. D. W., Dobson, R. C. J., Pearce, F. G., Antonio, L., Whitten, A. E., Liew, C. K., Mackay, J. P., Trewhella, J., Jameson, G. B., Perugini, M. A., and Gerrard, J. A. (2008) Evolution of quaternary structure in a homotetrameric enzyme. *J. Mol. Biol. 380*, 691–703.

(47) Pearce, F. G., Dobson, R. C. J., Weber, A., Lane, L. A., McCammon, M. G., Squire, M. A., Perugini, M. A., Jameson, G. B., Robinson, C. V., and Gerrard, J. A. (2008) Mutating the tight-dimer interface of dihydrodipicolinate synthase disrupts the enzyme quaternary structure: Toward a monomeric enzyme. *Biochemistry 47*, 12108–12117.

(48) Skovpen, Y. V., and Palmer, D. R. J. (2013) Dihydrodipicolinate synthase from *Campylobacter jejuni*: Kinetic mechanism of cooperative allosteric inhibition and inhibitor-induced substrate cooperativity. *Biochemistry 52*, 5454–5462.

(49) Skovpen, Y. (2014) *Novel inhibitors of dihydrodipicolinate synthase.* PhD dissertation,

University of Saskatchewan, SK.

(50) Atkinson, S. C., Dogovski, C., Downton, M. T., Czabotar, P. E., Dobson, R. C. J., Gerrard, J. A., Wagner, J., and Perugini, M. A. (2013) Structural, kinetic and computational investigation of *Vitis vinifera* DHDPS reveals new insight into the mechanism of lysine-mediated allosteric inhibition. *Plant Mol. Biol. 81*, 431–446.

(51) Phenix, C. P., and Palmer, D. R. J. (2008) Isothermal titration microcalorimetry reveals the cooperative and noncompetitive nature of inhibition of *Sinorhizobium meliloti* L5-30 dihydrodipicolinate synthase by (*S*)-lysine. *Biochemistry 47*, 7779–7781.

(52) Coulter, C. V., Gerrard, J. A., Kraunsoe, J. A. E., Moore, D. J., and Pratt, A. J. (1996) (*S*)-Aspartate semi-aldehyde : synthetic and structural studies. *Tetrahedron 52*, 7127–7136.

(53) Coulter, C. V, Gerrard, J. A., Kraunsoe, J. A. E., and Pratt, A. J. (1999) *Escherichia coli* dihydrodipicolinate synthase and dihydrodipicolinate reductase : kinetic and inhibition studies of two putative herbicide targets. *Pestic. Sci. 55*, 887–895.

(54) Turner, J. J., Gerrard, J. A., and Hutton, C. A. (2005) Heterocyclic inhibitors of dihydrodipicolinate synthase are not competitive. *Bioorganic Med. Chem. 13*, 2133–2140.

(55) Mitsakos, V., Dobson, R. C. J., Pearce, F. G., Devenish, S. R., Evans, G. L., Burgess, B. R., Perugini, M. A., Gerrard, J. A., and Hutton, C. A. (2008) Inhibiting dihydrodipicolinate synthase across species: Towards specificity for pathogens? *Bioorg. Med. Chem. Lett. 18*, 842–844.

(56) Boughton, B. A., Griffin, M. D. W., O'Donnell, P. A., Dobson, R. C. J., Perugini, M. A., Gerrard, J. A., and Hutton, C. A. (2008) Irreversible inhibition of dihydrodipicolinate synthase by 4-oxo-heptenedioic acid analogues. *Bioorganic Med. Chem. 16*, 9975–9983.

(57) Boughton, B. A., Dobson, R. C. J., Gerrard, J. A., and Hutton, C. A. (2008) Conformationally constrained diketopimelic acid analogues as inhibitors of dihydrodipicolinate synthase. *Bioorganic Med. Chem. Lett. 18*, 460–463.

(58) Sheehan, J. C., and Bolhofer, W. A. (1950) An improved procedure for the condensation of potassium phthalimides with organic halides. *J. Am. Chem. Soc. 72*, 2786–2788.

(59) Skovpen, Y. V, Conly, C. J. T., Sanders, D. A. R., and Palmer, D. R. J. (2016) Biomimetic design results in a potent allosteric inhibitor of dihydrodipicolinate synthase from *Campylobacter jejuni*. *J. Am. Chem. Soc. 138*, 2014–2020.

(60) Bartlett, P. A., and Barstow, J. F. (1982) Ester-enolate Claisen rearrangement of α-amino acid derivatives. *J. Org. Chem. 47*, 3933–3941.

(61) Seebach, D. (1988) Structure and reactivity of lithium enolates. From pinacolone to selective *C*-alkylations of peptides. Difficulties and opportunities afforded by complex structures. *Angew. Chem. Int. Ed. English 27*, 1624–1654.

(62) Andrei, M., Efskind, J., and Undheim, K. (2007) A stereoselective synthesis of a spiro-bridged bis(α-amino acid) derivative based on Ru(II)-catalysed RCM reactions. *Tetrahedron 63*, 4347–4355.

(63) Vedejs, E., and Lee, N. (1995) Lewis acid-induced internal proton return in enolate complexes with chiral amines. *J. Am. Chem. Soc. 117*, 891–900.

(64) Coulter, A. W., and Talalay, P. (1968) Studies on the microbiological degradation of steroid ring A. *J. Biol. Chem. 243*, 3238–3247.

(65) Cocolas, G. H., and Hartung, W. H. (1957) Amino acids. XV. Michael addition reactions of diethyl acetamidomalonate. *J. Am. Chem. Soc. 79*, 5203–5204.

(66) Roduit, J.-P., and Wyler, H. (1985) Synthesis of 1,2-dihydropyridines, 2,3- dihydro-4-(1*H*)-pyridinone, and 1,2,3,4-tetrahydropyridines via *N*-acyl *N*,*O*-hemiacetal formation). *Helv. Chim. Acta 68*, 403–414.

(67) Kotha, S., Goyal, D., Thota, N., and Srinivas, V. (2012) Synthesis of modified phenylalanine peptides by cross enyne metathesis and a Diels-Alder reaction as key steps. *Eur. J. Org. Chem.* 1843–1850.

(68) Kotha, S., and Singh, K. (2004) *N*-Alkylation of diethyl acetamidomalonate: synthesis of constrained amino acid derivatives by ring-closing metathesis. *Tetrahedron Lett. 45*, 9607–9610.

(69) Ferreira, M. de L. G., Pinheiro, L. C. S., Santos-filho, O. A., Pecanha, M. D. S., Sacramento, C. Q., Machado, V., Ferreira, V. F., Souza, T. M. L., and Boechat, N. (2014) Design, synthesis, and antiviral activity of new 1*H* -1,2,3-triazole nucleoside ribavirin analogs. *Med. Chem. Res. 23*, 1501–1511.

(70) Segel, I. (1975) *Enzyme Kinetics: Behavior and analysis of rapid equilibriumand steady-state enzyme systems.* John Wiley and Sons, Inc., New York.

(71) Li, C., and Gershon, P. D. (2006) pK_a of the mRNA cap-specific 2'-O-methyltransferase catalytic lysine by HSQC NMR detection of a two-carbon probe. *Biochemistry 45*, 907–917.

(72) Hall, H. K. (1957) Correlation of the base strength of amines. *J. Am. Chem. Soc. 79*, 5441–5445.

(73) Walker, J. M. (2005) *The proteomics protocols handbook.* Humana Press, Totowa, N.J.

(74) Roberts, S. J., Morris, J. C., Dobson, R. C. J., Baxter, C. L., and Gerrard, J. A. (2004) Two complete syntheses of (*S*)-aspartate semi-aldehyde and demonstration that Δ^2-tetrahydroisophthalic acid is a non-competitive inhibitor of dihydrodipicolinate synthase. *Arkivoc x*, 166–177.

(75) Shchetnikov, G. T., Peregudov, A. S., and Osipov, S. N. (2007) Effective pathway to the α-CF$_3$-substituted azahistidine analogues. *Synlett* 136–140.